DYSTROGLYCAN STABILIZATION OF BASEMENT MEMBRANES REGULATES DEVELOPMENT OF THE VISUAL SYSTEM

By

Reena Clements

A DISSERTATION

Presented to the Neuroscience Graduate Program

Vollum Institute

and the Oregon Health & Science University School of

Medicine

in partial fulfillment of the requirements for the degree of

Doctor of Philosophy

March 2018

School of Medicine

Oregon Health & Science University

_____

CERTIFICATE OF APPROVAL

_____

This is to certify that the Ph.D. dissertation of

REENA CLEMENTS

has been approved on March 9, 2018

_____
Member & Chair, Anthony P. Barnes, PhD

_____
Advisor, Kevin Wright, PhD

_____
Member, Peter Barr-Gillespie, PhD

_____
Member, Catherine Morgans, PhD

_____
Member, Kelly Monk, PhD

Table of Contents

Chapter 1 Continued

Chapter 2   94

Conclusions and Future Directions   138

References   149

List of Abbreviations

Abbreviation	Expanded Name
CTB	Cholera Toxin Subunit B
DG	Dystroglycan
ECM	Extracellular Matrix
GCL	Ganglion Cell Layer
ILM	Inner Limiting Membrane
INL	Inner Nuclear Layer
IPL	Inner Plexiform Layer
ISPD	Isoprenoid Synthase Domain Containing
LGN	Lateral Geniculate Nucleus
MTN	Medial Terminal Nucleus
OFL	Optic Fiber Layer
ONL	Outer Nuclear Layer
OPL	Outer Plexiform Layer
RGC	Retinal Ganglion Cell
SC	Superior Colliculus
SCN	Suprachiasmatic Nucleus

Acknowledgements

Abstract

During development, specific combinations of molecular cues guide the proper formation of neural circuits. Neuronal migration, axon guidance, and synapse formation and pruning are among the developmental phenomenon that must occur with extreme precision to form a functional nervous system. Due to the complexity of the nervous system and the functional redundancy of many proteins, elucidating the precise nature of the molecular basis of development remains a challenge. Additionally, while the function of many proteins is well understood during embryonic development, their role in shaping the postnatal circuit remains poorly understood. The transmembrane glycoprotein dystroglycan has been implicated in neuronal migration and axon guidance in the developing sensory system. Dystroglycan regulates cell migration in the brain by stabilizing laminin in cortical basement membranes. However, its role in the developing visual system remains relatively unknown. In this thesis, I utilize the retina and developing visual system to further elucidate the role of dystroglycan in neuronal development. I utilize genetic models including $ISPD^{L79*/L79*}$ and $DG^{F/-}; Six3^{Cre}$ to answer two questions. First, I examine the role of dystroglycan in the retina, including developmental cell migration, postnatal cellular positioning and laminar targeting of synapses. Second, I investigate how dystroglycan regulates axons as they exit the retina and target retinorecipient brain regions. I show that dystroglycan stabilizes the inner limiting membrane, which is required for neuronal migration and axon guidance within the retina. As a consequence of

inner limiting membrane loss, the mature circuit contains cellular ectopias of multiple cell types. Inner retinal neurons are unable to target axons and dendrites into appropriate retinal lamina or mosaically space their cell bodies. Retinal ganglion cells, which are located adjacent to the inner limiting membrane, undergo increased programmed cell death, while other cell types are spared. Despite the profound inner retinal defects, retinal waves (spontaneous bursts of activity from amacrine cells) are grossly normal in the absence of dystroglycan. I next focus on the retinal ganglion cell axons as they target visual brain regions. At the optic chiasm early in development, axons stall and an early ipsilateral projection forms. I show that this is due to breakdown of the basement membrane, which normally acts as a growth substrate for incoming axons. Postnatally, axons exit the chiasm and correctly target retinorecipient brain regions. However, axons fail to laminate these targets appropriately, with ipsilateral axons invading regions that should be exclusively contralateral. Interestingly, despite being in the wrong location within their target region, ipsilateral axons still prune and stabilize. This work describes the profound defects that occur in the visual system due to loss of dystroglycan and characterizes basement membranes as a critical substrate for neuronal migration and axon growth.

Introduction

Sensory systems are the primary means through which organisms interact with their environment. Broadly, the peripheral nervous system receives sensory information and sends it to the central nervous system. This information is processed and used to output a behavior in response to the original sensory stimulus. The complex interactions in these systems are vital to the survival of any organism. The ability of mature circuits to process sensory information is attributed to the precise formation of sensory pathways during the embryonic and early postnatal stages of an organism's life. Without the foundation of a properly formed sensory circuit, neurodevelopmental sensory processing disorders may occur. Specific combinations of molecular cues guide neurons to form functional neural circuits; however, many molecular mechanisms that contribute to normal brain development remain unknown. The work presented in this thesis characterizes a novel molecular mechanism in the development of a functional visual system.

Novel Molecular Regulators of Development

Many molecular regulators of development, specifically, transcription factors and other proteins that direct the specific lamination of neuronal cell bodies and guidance of axons to their targets, are poorly understood. To determine new genes involved in neural circuit development, a forward genetic technique may be utilized. Forward genetic screens are conducted by causing random mutations in the genome, examining resulting progeny for a phenotype

of interest, and then mapping which genes cause the phenotype. Traditionally, forward genetic approaches have been used in model organisms such as *C. elegans*, *Drosophila*, or *Danio rerio* to determine molecular mechanisms of processes such as dendritic branching and morphogenesis (Dong et al., 2013). Genetic screens in mice may also be utilized, but are more complex to conduct than in other model organisms.

A previous forward genetic screen (Wright et al., 2012) discovered that mutations in genes that regulate the glycosylation of the protein dystroglycan impact axon guidance and cellular migration during nervous system development. Axons from neurons in the dorsal spinal cord exhibit crossing defects in the floorplate, and there is a breakdown of the cortical basement membrane. The phenotypes observed vary in severity depending on the level of glycosylation lost on dystroglycan. The work presented in this thesis utilizes one of the mutants found in this forward genetic screen, isoprenoid synthase domain-containing, or *ISPD*$^{L79*/L79*}$ (Figure 1), which models the most severe form of functional dystroglycan loss, and uses this mutation as model to study visual system development.

Biology of Dystroglycan

Dystroglycan, originally described as a laminin-binding component of the dystrophin glycoprotein complex (Ibraghimov-Beskrovnaya et al., 1992), is a transmembrane protein with extensive extracellular glycosylation and intracellular connections to the actin cytoskeleton (Figure 1) (Moore and Winder, 2010). The dystroglycan gene codes for a α and β subunits that are post-translationally

cleaved and non-covalently associate at the cell membrane (Ibraghimov-Beskrovnaya et al., 1992; Moore and Winder, 2010). Numerous reports linked muscular dystrophies in human patients to genetic dysfunctions impacting dystroglycan or the dystrophin glycoprotein complex (Lim and Campbell, 1998; Straub and Campbell, 1997). Early work on dystroglycan and dystrophin function suggested an important role in muscle stability (Ervasti et al., 1990; Winder, 1997). *In vitro* models demonstrated direct dystroglycan binding to laminin, and dystroglycan was thus hypothesized to be important in maintaining muscle cell architecture (Matsumura et al., 1997). Additional reports demonstrated that when dystroglycan-laminin binding was lost, muscle cell death was induced via the PI3K/AKT pathway (Langenbach and Rando, 2002). These early data point to an important role for dystroglycan as a crucial transmembrane connector between the extracellular matrix (ECM) and intracellular signaling components.

The extracellular α subunit of dystroglycan is heavily glycosylated and is the portion of the protein that binds directly to ECM components such as laminin-1, laminin-2, agrin, and perlecan (Henry and Campbell, 1999; Sunada et al., 1994; Winder, 2001; Yamada et al., 1994). While only predicted to have a molecular weight of 40 kDa, α–dystroglycan detected by immunoblot shows a molecular mass closer to 120 kDa, demonstrating the extensive post-translational glycosylation (Barresi and Campbell, 2006; Ibraghimov-Beskrovnaya et al., 1992). Glycosylation of dystroglycan is essential for its ligand-binding capabilities. Studies in which α–dystroglycan is normally expressed but hypoglycosylated demonstrate that full glycosylation of

dystroglycn is required for ligand-binding to laminin, agrin, and neurexin (Michele et al., 2002). Only one mutation on dystroglycan itself has been shown to recapitulate muscular dystrophy phenotypes (Hara et al., 2011). Mutations in proteins that are both involved in the glycosylation of dystroglycan and associated with muscular dystrophy phenotypes include POMGnT1, POMT1, POMT2, Fukutin, FKRP, LARGE, B3gnt1and ISPD (Beltran-Valero de Bernabe et al., 2002; Brockington et al., 2001; Kobayashi et al., 1998; Roscioli et al., 2012; Toda, 1999; van Reeuwijk et al., 2007; van Reeuwijk et al., 2005; Wright et al., 2012; Yoshida et al., 2001). The abundance of mutations associated with dystroglycan glycosylation further solidifies that post-translational glycosylation is essential for dystroglycan function. When dystroglycan stabilization of laminin is lost, processes normally carried out by laminin fail to function. Laminin concentrations at the neuromuscular junction are important for concentrating acetylcholine receptors, and in the absence of glycosylated dystroglycan to stabilize laminin, acetylcholine receptors fail to cluster (Montanaro et al., 1998).

The transmembrane and intracellular β subunit of dystroglycan transduces extracellular signals to intracellular signaling cascades and connects directly with the actin cytoskeleton. When laminin or other adhesion proteins bind to dystroglycan extracellularly, β dystroglycan is phosphorylated at a tyrosine in its WW binding domain, leading to interactions with utrophin and dystrophin (Ilsley et al., 2001; James et al., 2000) and SH2 domain containing proteins including c-Src (Sotgia et al., 2001). Additionally, dystroglycan interacts with Grb2 through its SH3 domain (Russo et al., 2000; Yang et al., 1995) and directly interacts with the

ERK-MAP kinase pathway (Spence et al., 2004b). The intracellular subunit of dystroglycan also has an important role in regulating the actin cytoskeleton. Previous reports demonstrate direct interaction of dystroglycan and F-actin and a function in bundling actin filaments (Chen et al., 2003). Additionally, dystroglycan plays a role in filopodial formation that is mediated by ezrin binding and interaction with Cdc-42 (Batchelor et al., 2007; Spence et al., 2004a). Integrins also bind laminin, and the downstream ERK signaling pathway is influenced by dystroglycan activity (Ferletta et al., 2003; Yoshida et al., 1998). Dystroglycan intracellular signaling activates numerous downstream signaling pathways involving the actin cytoskeleton, thereby providing an important role in stabilization and strength in muscle cells.

Dystroglycan and the Extracellular Matrix

The extracellular matrix (ECM) provides environmental and structural support to cells. Specifically, ECM molecules can form into an organized basement membrane, consisting of laminins, nidogens, perlecans, and type IV collagens (Timpl and Brown, 1996). Proteins that compose basement membranes do not necessarily have the ability to cluster on their own; rather, basement membranes require additional laminin receptors such as dystroglycan or β1-Integrin for proper assembly and organization (Schwarzbauer, 1999). Dystroglycan organizes laminin in the basement membrane and this initial interaction is necessary for the recruitment of additional basement membrane components (Henry and Campbell, 1998). Dystroglycan is expressed in numerous tissues in mice, including skeletal muscle, where it was originally

identified, kidney, and brain (Durbeej et al., 1998; Moore et al., 2002). Work on dystroglycan outside skeletal muscle reveals that it is essential for the formation of an extra-embryonic, laminin-rich, Reichart's membrane (Williamson et al., 1997). Additionally, perturbing dystroglycan glycosylation in the brain by removing its laminin-binding capabilities recapitulates phenotypes seen in patients with muscular dystrophies (Moore et al., 2002). Early reviews on dystroglycan raised the possibility that it may be required in the general organization of basement membranes across all tissue, especially basement membranes with high concentrations of laminin (Henry and Campbell, 1999).

Basement membranes provide positional and adhesive cues for cells, including neurons. Without a basement membrane, cellular positioning becomes extremely disorganized. The ECM or basement membrane may also play a role in axon growth and guidance *in vivo*. In the grasshopper, research suggests that some growth cones have selective affinity for the non-neuronal basement membrane (Bastiani et al., 1985). In *C. elegans*, nidogen, a basement membrane component, is required for longitudinal nerve axon guidance (Clay and Sherwood, 2015; Kim and Wadsworth, 2000). Recently, work on dystroglycan showed that it plays a role in axon guidance in the spinal cord due to its ability to localize Slit in basement membranes (Wright et al., 2012). Dystroglycan provides a good model studying the role of the ECM and basement membranes in axon guidance due to its extensive extracellular connections with basement membrane components. The work presented in this thesis discusses a role for dystroglycan in maintaining the basement membrane as a growth substrate for axons. Of note,

the work presented in Chapter 1 discusses the role of the basement membrane of the retina, the inner limiting membrane, which has been shown to express high levels of laminin and perlecan during development (Halfter et al., 2005a).

Mechanisms of Cortical Circuit Development

During development, combinations of molecular cues specify differentiation of neurons, direct the migration of somas, instruct axon guidance, and promote synapse formation at specific locations within a circuit. In the developing cortex, multipotent progenitor cells in the ventricular zone divide asymmetrically into neurons and new radial glial progenitor cells and migrate to form the layers of the cortex in an inside-out manner, with the youngest neurons found in the most superficial layers (Bystron et al., 2008; Tamamaki et al., 2001). Once radial glia are specified due to expression of brain-lipid binding protein (Feng et al., 1994), they anchor one process apically to the pia and the other to the surface of the ventricular zone that forms the scaffold on which migrating neurons will travel to form the layers of the cortex (Rakic, 1972). Generally, postmitotic neurons extend a leading process along the radial glial scaffold and migrate towards the pial surface (Rakic, 1972). In an inside-out manner, these neurons form the intermediate zone and the preplate. The preplate splits into the marginal zone (most superficial) and cortical plate, the region in which the layers of the cortex are found (Hatten, 1999). Within the cortical plate, neuronal lineages can be traced. Neurons that are found in the same radial column are the result of continuous asymmetric divisions of a progenitor cell to produce multiple daughter neurons, whereas neurons in the same horizontal lamina are the result

of symmetric divisions of progenitor cells that go on to divide asymmetrically to produce daughter neurons (Kornack and Rakic, 1995).

Recent work has further elucidated the specific movements that migrating neurons undergo, generally characterized into four steps. First, a neuron must be generated asymmetrically from a radial precursor cell division. Second, neurons migrate out of the ventricular zone into the subventricular zone. Third, they undergo a multipolar phase, detached from the radial glial scaffold. Finally, neurons regain bipolar morphology and travel apically on the radial glial scaffold (Kriegstein and Noctor, 2004; Tabata and Nakajima, 2003). Additionally, while on the radial glial scaffold, neurons can exhibit different kinds of migratory behavior (Nadarajah et al., 2001). For example, in somal translocation, the leading process of the cell extends superficially towards the pia, followed by upward motion of the soma (Berry and Rogers, 1965). In contrast, locomotion occurs when the entire cell moves at once along the radial scaffold (Rakic, 1972).

Mutations that impact radial migration and cortical layering can result in failures to produce enough neurons or to form cortical layers correctly (also called lissencephaly, or "smooth brain"). In *Reelin* mutants, neurons remain attached to the radial glial scaffold and do not split from the preplate into the cortical plate, resulting in an inverted migration pattern, where later-born neurons are located basally instead of apically to the pial surface (Caviness and Sidman, 1973; Kandel, 2013; Olson and Walsh, 2002). *Lis1* and *Doublecortin*, two microtubule-associated mutations, cause neurons to have defects in nuclear movements. In these mutants, neurons do split from the preplate, but eventually

form a thicker cortex with abnormal layering (Gleeson et al., 1998; Kandel, 2013; Olson and Walsh, 2002; Ross et al., 1997). *Reelin* encodes an extracellular protein that has been suggested to link the extracellular environment with the intracellular microtubule dynamics, interacting with components of the extracellular environment such as integrins (Olson and Walsh, 2002). These extracellular, laminin-binding proteins, including integrins and dystroglycan, may also be crucial in regulating the extracellular environment to ensure proper neuronal migration, as their deletion causes phenotypes that mimic lissencephaly (Olson and Walsh, 2002).

The developing brain is highly plastic and uses mechanisms such as synapse pruning and developmental cell death to ensure that the appropriate number of neurons and synaptic connections will be present in the mature circuit (Cowan et al., 1984; Jessell and Sanes, 2000; Tau and Peterson, 2010). Many neurodevelopmental sensory processing disorders result from improper circuit formation. Irrespective of the specifics of the sensory disorder, any errors in the wiring of a developmental circuit will lead to deficits in the adult circuit, whether this be structurally or in the ability of the circuit to process sensory information. While defects in cortical development have been extensively studied, the elaborate complexity of the cortex often makes it a non-ideal model to study the molecular mechanisms of neurodevelopmental defects.

One way to study the precise mechanisms in which various molecular cues contribute to the wiring of a circuit during development is to utilize a highly stereotyped circuit. The retina makes an ideal model system to study the

9

molecular basis of circuit development due to its accessibility and the discrete number of cell types that exist within specific locations in the mature circuit. While still complex, the retina provides a more accessible model of study than the cortex.

Next, I will detail general nervous system phenotypes seen in patients with dystroglycan disorders and establish the retina and visual system as a model for studying dystroglycan function.

The Role of Dystroglycan in Nervous System Development

Mutations in the function of α-dystroglycan cause a range of congenital muscular dystrophies, whichrange in phenotypic severity. On the most severe end, patients with Walker-Warburg Syndrome, Muscle-Eye Brain Disease, and Fukuyama congenital muscular dystrophy present with neurodevelopmental abnormalities in addition to muscular dystrophy (Godfrey et al., 2011). One brain abnormality that patients with dystroglycan mutations develop is cobblestone lissencephaly, which occurs when there are defects in proper neuronal migration. In multiple mouse models of dystroglycan deletion, dystroglycan stabilization of laminin in the cortical basement membrane is lost, causing detachment of radial glial endfeet and neuronal migration defects. Additionally, mice present with enlarged ventricles and hydrocephalus (Booler et al., 2016; Satz et al., 2010a; Wright et al., 2012). Neuronal migration defects are also present in the cerebellum and hippocampus (Michele et al., 2002; Qu and Smith, 2005). These defects are specifically due to the decrease in glycosylation of dystroglycan.

Conversely, when the intracellular signaling domain of dystroglycan is deleted, mice appear grossly normal (Satz et al., 2010a).

Some patients with dystroglycanopathies exhibit mental retardation, including intellectual disabilities (Godfrey et al., 2011). Dystroglycan has also been shown to play a role at synapses. In the hippocampus, dystroglycan is associated with the dendrites of pyramidal neurons, and in the olfactory bulb has been linked to inhibitory synapses (Zaccaria et al., 2001). Several studies show that hippocampal long-term potentiation, a form of synaptic plasticity, induced by high frequency stimulation, does not occur in dystroglycan null mice (Moore et al., 2002; Satz et al., 2010b). At inhibitory hippocampal synapses, dystroglycan clusters with $GABA_A$ receptors at the synapse (Lévi et al., 2002), and loss of dystroglycan prevents homeostatic inhibitory plasticity (Pribiag et al., 2014). Most recently, dystroglycan has been shown to play a specific role in CCK basket cell terminals in the hippocampus, elucidating a role for dystroglycan in particular inhibitory interneurons (Früh et al., 2016). Work on dystroglycan at the synapse may elucidate the molecular basis behind the non-anatomical defects seen in patients with dystroglycan-related disorders.

The role of dystroglycan outside of muscle, specifically in the nervous system, is still poorly understood. Neurodevelopmental abnormalities seen in patients with dystroglycanopathies also commonly include retinal dysplasias or other visual impairments; mouse models of this particular aspect of the phenotype have been poorly studied. Here, I aim to determine the molecular mechanisms of dystroglycan function in the developing visual system, and to

determine if dystroglycan plays a similar role in regulating cell migration in the retina as it does in the developing cortex.

Development of the Retina

During development, the eye field is specified by expression of transcription factors such as Rx, Pax6, Six3, and Otx2 (Fuhrmann, 2008). During neural tube formation, the eye first forms during invagination of the optic vesicles in the ventral forebrain to form the retina, retinal pigment epithelium, and optic stalk (Fuhrmann, 2008, 2010). The early embryonic retina consists of a pool of retinal progenitor cells whose radial processes are connected to the apical and basal side of the retina, with cell bodies eventually differentiating on the apical side (Centanin and Wittbrodt, 2014). In the mature retina, there are six types of neurons (Figure 2) and one type of glial cell (Harris, 1997; Young, 1985). These neurons and glia differentiate from the progenitor pool in a stereotyped order: first ganglion cells, followed by horizontal cells and cones, then amacrine cells and rods, and finally bipolar cells and Muller glia (Bassett and Wallace, 2012; Cepko et al., 1996; Livesey and Cepko, 2001; Reese, 2011).

Retinal ganglion cells (RGCs) are located on basal side of the retina and are the only cell type to project an axon out of the retina and into the brain (Austin et al., 1995). Inhibition of Notch signaling (Austin et al., 1995; Cepko et al., 1996) and activation of transcription factors including Shh, Math5, and Brn3-b promote RGC fate (Gan et al., 1996; Wang et al., 2001; Zhang and Yang, 2001). Over the course of development, RGC differentiation proceeds in an "inside-out"

fashion: the earliest-born cells differentiate in central retina and later-born cells are located in the periphery (Centanin and Wittbrodt, 2014).

Horizontal cells and amacrine cells, retinal interneurons, are specified by many overlapping transcription factors (Poche and Reese, 2009). Cells are initially specified from the progenitor pool by the expression of Foxn4 and Ptf1a. At this point, transcription factor expression diverges, and the horizontal and amacrine cells begin to become distinct interneuron populations. Prox1 directs horizontal cell fate, and Lim1 directs the final migration of these cells. Math3 and NeuroD1 promote amacrine cell fate. Downstream transcription factors, including Barhl2, Bhlhb5, and Isl1, distinguish individual classes of amacrine cells, such as glycinergic, GABAergic, and cholinergic (Poche and Reese, 2009). Deleting these transcription factors individually or in combination leads to the promotion of mostly horizontal cells, mostly amacrine cells, or in some cases, rod photoreceptors (Inoue et al., 2002; Ohsawa and Kageyama, 2008). The combinations of transcription factors that lead to differing cell fates remain an open area of research.

Cone and rod photoreceptors, found on the apical surface of the retina and adjacent to the retinal pigment epithelium, are light sensing cells and, along with intrinsically photosensitive RGCs, the first cell types in the retinal circuit to receive light information. The transcription factor Otx2 signals to the Crx homeobox gene to direct the differentiation of photoreceptors (Furukawa et al., 1997; Nishida et al., 2003). Nrl signaling through Nr2e3 further specifies rod and cone photoreceptors (Mears et al., 2001).

Bipolar cells are important for transmitting information from photoreceptors to RGCs. During bipolar cell differentiation, Mash1 and Math3 promote cellular differentiation of progenitors to neuronal fate, and Chx10 then specifies the neurons to become bipolar cells (Hatakeyama et al., 2001). Subtypes of bipolar cells are specified by later expression of factors such as Vsx1 and Bhlhb4 (Bramblett et al., 2004; Chow et al., 2004).

The bHLH transcription factor Hes5 is involved in both maintaining the proliferating progenitor cells and promoting Muller glial cell fate (Hojo et al., 2000; Ohsawa and Kageyama, 2008).

After specification of the six neuronal and one glial cell type in the retina, the cells continue to mature during postnatal development. Cells adapt discrete functions as well as make specific connections within the mature circuit based on their particular transcriptome.

Cells and Connections in the Mature Retina

Retinal progenitor cells differentiate into six discrete neurons, and there is significant diversity within RGCs, amacrine cells, and bipolar cells. Around thirty discrete kinds of RGCs have been characterized based on morphology, physiology, and genetics (Field and Chichilnisky, 2007; Sanes and Masland, 2015). The various functions of RGCs include detection of motion, color, direction of movement, and even photosensitivity (Freedman et al., 1999; Gollisch and Meister, 2010; Vaney et al., 2012), further contributing to the wide array of diversity within each cell type. Several research groups labeled specific subtypes of RGCs using *cre* or transgenic lines and characterized the different stratification

patterns and projections within the retina and visual brain targets (Kim et al., 2010b; Osterhout et al., 2014). There are at least 25 different classes of amacrine cell in mammals, classified using Golgi stain and dendritic stratification, including mono-stratified narrow-field cells, diffuse-stratified narrow-field cells, medium-field cells, and wide-field cells (MacNeil et al., 1999; MacNeil and Masland, 1998). Bipolar cell diversity has been classified using molecular markers, axon stratification within the IPL, dendritic fields, and cone contacts (Ghosh et al., 2004; Masland, 2012; Wassle et al., 2009).

Each retinal neuron type positions its cell body into a specific lamina of the retina (Figure 2). Rod and cone photoreceptors stratify into the outer nuclear layer (ONL); horizontal cells, bipolar cells, and amacrine cells stratify into the inner nuclear layer (INL); and RGCs and displaced amacrine cells stratify into the ganglion cell layer (GCL) (Bassett and Wallace, 2012). Additionally, each neuron makes highly specific synaptic connections with other neurons in the circuit. The outer plexiform layer (OPL) contains a specialized ribbon synapse, in which dendritic tips of bipolar cells and horizontal cells insert into invaginations of the photoreceptor synaptic terminal. Cones typically contain many ribbon synapse regions to connect with multiple ON-bipolar cell dendrites, whereas rods contain one synaptic ribbon site to connect with one OFF-bipolar cell dendrite (Sterling and Matthews, 2005). The inner plexiform layer (IPL) contains synapses between bipolar cells, amacrine cells, and RGCs (Bassett and Wallace, 2012). The optic or nerve fiber layer, which grows along the inner limiting membrane (ILM) contains the axons of RGCs that exit the retina and synapse with targets in the

15

brain (Bassett and Wallace, 2012). In the mature circuit, photoreceptors transduce photon information to RGCs via the bipolar cells. Horizontal cells and amacrine cells provide inhibitory input that help encode complex information and create center-surround receptive fields (Diamond, 2017).

During postnatal development, after a cell's soma has migrated to its appropriate lamina, its axonal and dendritic processes begin to stabilize to form the synaptic lamina. Initially, neurons extend complex dendritic arbors that may go beyond a normal laminar targeting region. Over the course of developmental time, neurons prune back their dendritic arbors to target appropriate lamina or sublamina (Kim et al., 2010c; Reese, 2011). Cadherins play a role in regulating dendritic size of horizontal cells and self-avoidance between dendritic branches in starburst amacrine cells (Lefebvre et al., 2012; Tanabe et al., 2006). Additionally, there are many subdivisions within the IPL that dendrites target. Generally, dendrites of ganglion cells and amacrine cells that reside in the outer layers of the IPL are "OFF" cells, meaning that they hyperpolarize in response to light, whereas dendrites that reside in the inner layers of the IPL are "ON" type cells and depolarize in response to light (Famiglietti and Kolb, 1976). Sema5A, Sema5B, and DSCAM have been implicated in directing neurites to laminate within the IPL (Li et al., 2015; Matsuoka et al., 2011). Downstream of traditional cues, intracellular signaling molecules including PTEN have been implicated in the formation of the IPL (Sakagami et al., 2012), suggesting that our understanding of the molecular basis of retinal layer development is still extremely limited.

In addition to highly specific cell body, axonal, and dendritic lamination, somas in the horizontal plane of the retina are tiled into mosaics. Cell bodies of RGCs, photoreceptors, horizontal cells, and amacrine cells tile such that the dendritic fields provide full coverage of the entire retina and visual space (Nguyen-Ba-Charvet and Chedotal, 2014; Wassle and Boycott, 1991). Retinal mosaics form by one or a combination of four methods: cell fate determination, tangential migration of cells, apoptosis, or homotypic interactions that cause dendritic repulsion (Nguyen-Ba-Charvet and Chedotal, 2014). MEGF10 and MEGF11 have recently shown to be involved in homotypic repulsive interactions of horizontal cells and amacrine cells (Kay et al., 2012). RGC and amacrine cell repulsive dendritic interactions are mediated by DSCAM (Fuerst et al., 2009; Fuerst et al., 2008).

Ongoing research continues to elucidate molecular cues that govern cell type specification, laminar targeting of axons and dendrites, and cell body spacing. Understanding these molecular cues contributes to our broad understanding of neural circuit development. Neurod6 was recently described to specify a new kind of amacrine cell subtype (Kay et al., 2011). Different type II cadherins specify Type 2 OFF and Type 5 ON bipolar cells and are important for targeting these cells to their appropriate lamina (Duan et al., 2014). Sema-Plexin signaling has been implicated in starburst amacrine cell dendritic targeting (Sun et al., 2013). DSCAM is necessary for stabilization of dendrites to the IPL (Li et al., 2015). Satb1 and Contactin 5 regulate the dendritic development and stratification of an on-off direction selective RGC (Peng et al., 2017). Elucidating

17

the molecular mechanisms of cell body and synapse targeting, spacing, and refinement remains an ongoing and open area of research. The work presented in this thesis describes a new dystroglycan phenotype in which cellular and dendritic targeting and mosaic spacing are disrupted in the retina.

Axon Guidance of the Retina and Visual System

Axons of RGCs must travel towards the center of the retina and exit at the optic disc to leave the eye. From here, they extend through the optic chiasm and synapse at specific image-forming and non-image forming regions in the brain. Early work by Roger Sperry in the visual system suggested that neurons in the retina are able to connect to their appropriate target region due to the presence of a chemoattractant (Sperry, 1943). Later investigations using genetic screens at the *Drosophila* ventral nerve cord midline implicated two genes, *Robo* and *Comm*, as important factors in directing growth cones to cross the midline during development (Seeger et al., 1993). Slit was later found to be the repulsive ligand that binds Robo at the midline, preventing axons from crossing (Kidd et al., 1999). The function of Comm is to prevent Robo from being trafficked to the cell membrane, removing the sensitivity to the Slit repulsive cue and allowing axons to cross the midline (Keleman et al., 2005). Similar attractive and repulsive cues are responsible for RGC axon guidance out of the retina and through the visual system.

The first step in RGC axon guidance is growth towards the optic disc. RGC axons are initially polarized towards the optic disc by CSPGs (Brittis et al., 1992; Brittis and Silver, 1995). As in the spinal cord, Robos are expressed by

18

RGCs and play a role in intraretinal axon guidance. In Robo1 deficient retinas, this polarity is lost in later-born RGCs, and the axons take aberrant trajectories (Thompson et al., 2009). After the axon forms and begins to grow, it extends in the optic fiber layer, the inner most part of the retina. In Robo2 deficient retinas, axons are no longer restricted to the optic fiber layer and instead grow in the outer layers of the retina. While Robo2-deficient retinas still extend in fasciculated bundles towards the optic disc, they do so in inappropriate retinal layers (Thompson et al., 2009). These results corroborate results from Slit knockout mice, where *Slit2* and *Slit1/2* deficient retinas show both polarity defects and mislocalization of axons away from the optic fiber layer (Thompson et al., 2006b). Once at the optic disc, netrin-1 signals locally through DCC receptors on the axons to allow exit from the retina (Deiner et al., 1997). EphB2 and EphB3 also mediate axon guidance at the optic disc from the dorsal retina, with axons in EphB-deficient retinas exhibiting pathfinding errors and sometimes growing to the opposite side of the eye (Birgbauer et al., 2000). These errors are similar to, but less severe than, the phenotypes observed in the Netrin-1/DCC pathway. In the ventral retina, Bmpr1b-deficient axons also show similar pathfinding errors at the optic disc (Liu et al., 2003).

Once RGC axons have successfully exited the retina, they proceed to target visual centers in the brain with a subset of the axons crossing at the optic chiasm to innervate the contralateral brain. The extent of the ipsilateral projection depends on the organism, where the position of the eyes dictate how much overlap the left and right eyes have in their visual fields. Organisms such as fish

and birds have only crossed projections, whereas humans have up to a 40%
uncrossed projection (Petros et al., 2008). In the mouse, approximately 3-5% of
the axons are uncrossed; these axons originate in the ventrotemporal retina from
a population of cells that are specified by Zic2 and EphB1 expression (Herrera et
al., 2003; Petros et al., 2008). At the chiasm, EphrinB2, a repulsive cue, is
expressed by radial glia. Axons expressing EphB1 are repulsed and turn into the
ipsilateral optic tract, forming the uncrossed projection (Williams et al., 2003).
The remainder of the axons form the crossed projection, which is specified by
neuropilin-1 expressing RGCs that respond to the attractive ligand VEGF at the
chiasm (Erskine et al., 2011). The crossed, contralateral projection forms first,
prior to embryonic day 14 (e14), continuing through RGC genesis at P0, and the
uncrossed ipsilateral projections forms between e14-e17 (Guillery et al., 1995;
Sretavan and Reichardt, 1993). Additional molecular cues play a role in normal
patterning and positioning at the chiasm. In Slit1/2 double knockouts, an ectopic
projection of fibers appears anterior to the normal chiasm, suggesting a role for
Slits in keeping RGC axons confined to the appropriate location of the chiasm
(Plump et al., 2002). Deletion of Secreted Frizzled-Related Proteins show a
similar ectopic growth phenotype (Marcos et al., 2015). Nr-CAM knockouts
present with an increase in size of the ipsilateral projection (Williams et al.,
2006), and Semaphorin3D is responsible for helping form the contralateral
projection (Sakai and Halloran, 2006). However, little is known about the
molecular cues that mediate axon crossing at the chiasm. Most mutations cause
enlargement of and ectopic projections around the chiasm, and one report of a

Gap43 mutation (Strittmatter et al., 1995b) describes a stalling of axons at the chiasm. The work presented in this thesis will describe the dystroglycan model in which axons initially stall at the chiasm and the resulting consequences when axons begin innervating the brain.

After exiting the chiasm, axons of RGCs synapse in visual-forming brain regions, such as the lateral geniculate nucleus and superior colliculus, as well as non-image-forming brain regions, such as the suprachiasmatic nucleus, medial terminal nucleus, and nucleus of the optic tract. Not surprisingly, Robos are also involved in regulating axon guidance post-chiasm. *Robo2* knockout mice show ectopic projections to the internal capsule and diencephalon, and *Robo1* knockout mice show aberrant projections into the cortex (Plachez et al., 2008). Similarly, when the function of the ECM-interacting protein β1-Integrin is reduced, there are various pathfinding errors of axons along the visual projection (Stone and Sakaguchi, 1996). In the lateral geniculate nucleus, the crossed projection forms an outer shell, and the uncrossed projection forms an inner shell. Initially, neurons make broad projections that are eventually refined and pruned to create the final circuit (Stevens et al., 2007). Generally, mutations impacting axon guidance or synaptic pruning within the lateral geniculate nucleus, such as in β2 knockouts, which lack a subunit of the nicotinic acetylcholine receptor, show increased overlap in the crossed and uncrossed projections (Torborg and Feller, 2004). Numerous reports have studied topographic mapping within the tectum and superior colliculus. EphBs and Ephrins have been described to mediate the innervation pattern of both the medial-lateral and anterior-posterior axes in the

tectum or superior colliculus (Feldheim et al., 2000; Frisen et al., 1998; Hindges et al., 2002; Mann et al., 2002). Semaphorin3D is highly expressed in the ventral tectum (Liu et al., 2004), and Wnt3 is expressed medially in both tectum and colliculus (Schmitt et al., 2006). Perturbations in these gradients cause defects in retinotopic map formation. Contactin4 and Sema6a are responsible for directing subsets of RGC axons to non-image forming centers in the accessory optic system (Osterhout et al., 2015; Sun et al., 2015). The work described in this thesis unveils a new phenotype in which axons inappropriately cross at the chiasm, proceed to mislaminate the brain visual centers, and binocularly innervate target areas which normally only receive monocular input.

Dystroglycan Function in the Retina and Visual System

Loss of functional dystroglycan or other laminin receptors such as β1-Integrin have profound impacts on the development of the retina. Many mutations that impact the glycosylation of dystroglycan have retinal phenotypes that recapitulate phenotypes seen in patients with muscular dystrophy. In POMGnT1 deficient retinas, used as a model of Muscle-Eye-Brain Disease, retinas are thinner with fewer RGCs and display abnormal electroretinograms (Liu et al., 2006). Additionally, the ILM is discontinuous and ectopias of Muller glial endfeet and RGCs are observed (Hu et al., 2010). Retinal detachments in older mice have also been reported (Takahashi et al., 2011). Fukutin, a gene responsible for Fukuyama-type congenital muscular dystrophy, also causes disorganized retinal laminar structure, loss of electroretinogram b wave, retinal detachment, and lens abnormalities (Takeda et al., 2003). FKRP models revealed thinner retinas and

disorganization of the GCL and ILM (Chan et al., 2010). Myodystrophy, modeled with mutations in Large, shows thinning of the retina, ectopically located cells, a broken ILM, and defects in the electroretinogram (Lee et al., 2005). A mutation in ISPD has been described in human patients with Muscle-Eye-Brain Disease or Walker-Warburg Syndrome (Czeschik et al., 2013; Roscioli et al., 2012). ISPD is involved in the glycosylation of dystroglycan, so patients with ISPD mutations do not have functional dystroglycan (Kanagawa and Toda, 2017). Until recently, no mouse model using ISPD had been described (Wright et al., 2012), and the implications in the retina remain unknown.

Additional genes that are associated with dystroglycan or laminin but not with dystroglycanopathies also cause defects in retinal development. Patients with mutations in the laminin β2 gene show abnormal eye phenotypes. The laminin β2 mouse model shows grossly normal development, but has abnormalities in photoreceptor morphology, electroretinograms, synapse formation, and a higher instance of apoptosis (Libby et al., 1999; Zenker et al., 2004). Knockout mice lacking both the laminin β2 and γ3 genes lose ILM-related proteins, including β-dystroglycan and nidogen, and have thinner retinal layers, ectopically located cells, and abnormal electroretinograms (Pinzon-Duarte et al., 2010). Loss of the laminin receptor β1-integrin or its downstream signaling adaptors also show ectopic aggregates of cells and ILM disruptions (Riccomagno et al., 2014). At the synaptic level, Pikachurin, an extracellular-matrix like protein, interacts with dystroglycan presynaptically at the photoreceptor-bipolar cell ribbon synapse. In the absence of Pikachurin or dystroglycan, bipolar cell

dendritic tips fail to invaginate into photoreceptor synapses, and mice exhibit altered electroretinograms (Omori et al., 2012; Sato et al., 2008). Selective loss of β-dystroglycan or dystrophin did not alter laminar structure but did alter the clustering of a potassium channel in Muller glial endfeet and impacted visual transmission (Satz et al., 2009).

Previous work modeling dystroglycanopathies in the retina documented gross anatomical and functional changes but did not thoroughly characterize the effects on each cell type or the mechanisms of the phenotype. Additionally, previous studies have described mutations that cause structural abnormalities in the retina but exhibit normal axon guidance in the retina and throughout visual targets in the brain (Riccomagno et al., 2014). The work presented in this thesis fills two gaps in the field. The first study (Chapter 1) reveals a role of the ILM for maintaining cellular lamination and survival in the inner retina, and characterizes the impacts on each cell type. The second study examines the visual targets in the brain (Chapter 2) and demonstrates that the basement membrane at the optic chiasm is an essential substrate for growth and organization of ipsilateral and contralateral RGC axon projections. Loss of the basement membrane at the chiasm creates an interesting phenotype where RGC axons are misrouted to the wrong side of the brain, but target the correct brain regions and maintain stable connections throughout adulthood that are inappropriately located within correct brain regions.

Figure 1
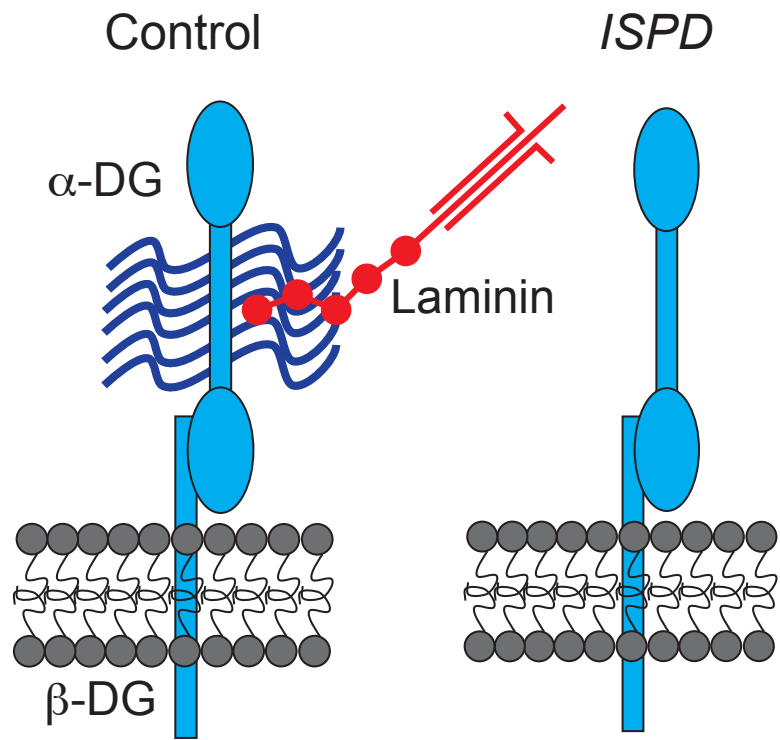
Figure 1: Schematic of dystroglycan. Control: Dystroglycan consists of two subunits, an extracellular α and transmembrane and intracellular β subunit. The α subunit undergoes extensive glycosylation (dark blue) in a mucin-like region. Glycosylation allows dystroglycan to bind to proteins in the extracellular matrix such as laminin, which contains an α, β, and γ chain (cross shape), as well as a dystroglycan binding region (ball on string). The intracellular subunit of dystroglycan connects directly to the actin cytoskeleton. *ISPD*: When mutations are present that impact the glycosylation of dystroglycan, the dystroglycan protein is present, but ligand-binding function is lost.

Figure 2

ILM

GCL

IPL

INL

OPL

ONL
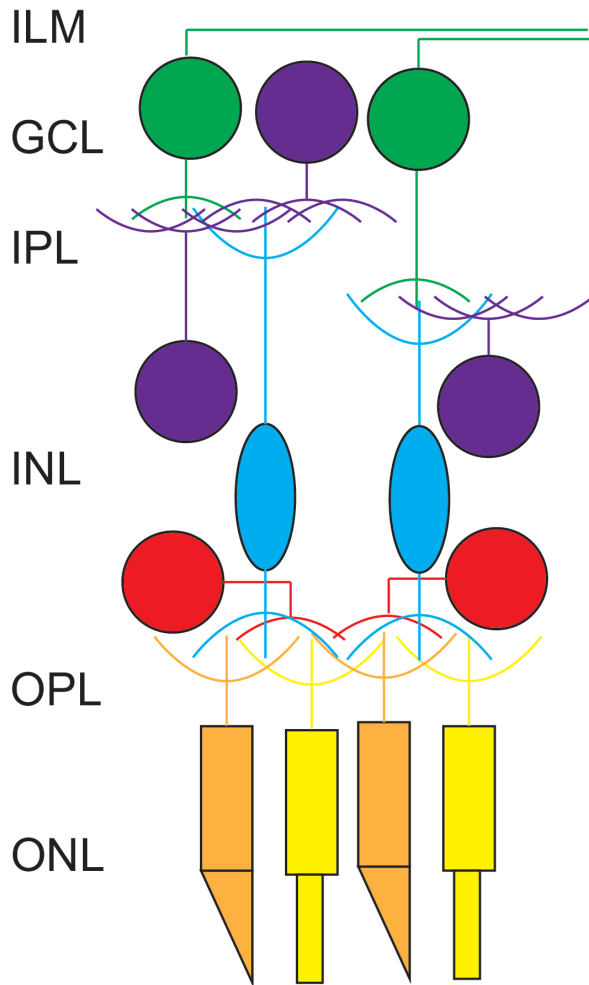
Figure 2: The mature retina. Neurons present in the mature retina are photoreceptors, including rods (yellow) and cones (orange), bipolar cells (blue), RGCs (green), horizontal cells (red), and amacrine cells (purple). Photoreceptor cell bodies are found in the outer nuclear layer (ONL), bipolar, horizontal, and amacrine cell bodies are found in the inner nuclear layer (INL), and ganglion cell bodies and displaced amacrine cell bodies are found in the ganglion cell layer (GCL). Synapses between photoceptors, bipolar cells, and horizontal cells are found in the outer plexiform layer (OPL), and synapses between bipolar cells, amacrine cells, and ganglion cells are found in the inner plexiform layer (IPL). Ganglion cells extend axons along the inner limiting membrane (ILM), a laminin-rich retinal basement membrane.

Chapter 1

Dystroglycan Maintains Inner Limiting Membrane Integrity to Coordinate Retinal Development

Reena Clements[1], Rolf Turk[3], Kevin P. Campbell[3], and Kevin M. Wright[1, 2]

1) Neuroscience Graduate Program, 2) Vollum Institute, Oregon Health & Science University, Portland, OR 97239, USA, 3) Howard Hughes Medical Institute, Department of Molecular Physiology and Biophysics, Department of Neurology, Department of Internal Medicine, The University of Iowa Roy J. and Lucille A. Carver College of Medicine, Iowa City, IA 52242, USA.

Supplemental Figures were not submitted for peer review

Abstract

Proper neural circuit formation requires the precise regulation of neuronal migration, axon guidance and dendritic arborization. Mutations affecting the function of the transmembrane glycoprotein dystroglycan cause a form of congenital muscular dystrophy that is frequently associated with neurodevelopmental abnormalities. Despite its importance in brain development, the role for dystroglycan in regulating retinal development remains poorly understood. Using a mouse model of dystroglycanopathy (*ISPD*^{L79*}) and conditional *dystroglycan* mutants of both sexes, we show that dystroglycan is critical for the proper migration, axon guidance and dendritic stratification of neurons in the inner retina. Using genetic approaches, we show that dystroglycan functions in neuroepithelial cells as an extracellular scaffold to maintain the integrity of the retinal inner limiting membrane (ILM). Surprisingly, despite the profound disruptions in inner retinal circuit formation, spontaneous retinal activity is preserved. These results highlight the importance of dystroglycan in coordinating multiple aspects of retinal development.

Significance Statement

The extracellular environment plays a critical role in coordinating neuronal migration and neurite outgrowth during neural circuit development. The transmembrane glycoprotein dystroglycan functions as a receptor for multiple extracellular matrix proteins, and its dysfunction leads to a form of muscular dystrophy frequently associated with neurodevelopmental defects. Our results demonstrate that dystroglycan is required for maintaining the structural integrity

of the inner limiting membrane (ILM) in the developing retina. In the absence of functional dystroglycan, ILM degeneration leads to defective migration, axon guidance and mosaic spacing of neurons, and a loss of multiple neuron types during retinal development. These results demonstrate that disorganization of retinal circuit development is a likely contributor to visual dysfunction in patients with dystroglycanopathy.

Introduction

The precise lamination of neurons is critical for establishing proper connectivity in the developing nervous system. The retina is organized in three cellular layers: the outer nuclear layer (ONL) comprised of rod and cone photoreceptors; the inner nuclear layer (INL) containing horizontal cells, bipolar cells and amacrine cells; and the ganglion cell layer containing RGCs and displaced amacrine cells (Bassett and Wallace, 2012). Two synaptic lamina form postnatally: the outer plexiform layer (OPL), which contains synapses between photoreceptors, bipolar cells and horizontal cells; and the inner plexiform layer (IPL), which contains synapses between bipolar cells, amacrine cells and RGCs. The molecular cues that direct the laminar positioning of neurons and the stratification of their processes within the synaptic layers remain poorly understood.

Unlike the cerebral cortex, where many neurons migrate along the radial glia scaffold, retinal migration does not require contact between neurons and neuroepithelial cells (Reese, 2011). RGCs, bipolar cells, and photoreceptors migrate by nuclear translocation through a basally-directed process. Basal

process contact with the inner limiting membrane (ILM) is critical for the polarization and migration of RGCs (Randlett et al., 2011). The ILM is enriched with extracellular matrix (ECM) proteins including laminins, Collagen IV, and perlecan (Taylor et al., 2015; Varshney et al., 2015). Mutations in specific laminins (Lamα1, Lamβ2 and Lamγ3) or the laminin receptor β1-Integrin disrupt formation of the ILM and organization of the ganglion cell layer (GCL) (Edwards et al., 2010; Gnanaguru et al., 2013; Pinzon-Duarte et al., 2010; Riccomagno et al., 2014). How laminins and other ECM proteins are initially organized in the ILM and how the ILM directs the organization of the retina remains unclear.

In addition to β1-Integrin, the transmembrane glycoprotein dystroglycan functions as a receptor for laminins and other ECM proteins through its extracellular α-subunit. Dystroglycan connects to the actin cytoskeleton through the intracellular domain of its transmembrane β-subunit, which is part of the dystrophin glycoprotein complex (Moore and Winder, 2010). Mutations disrupting the glycosylation of dystroglycan affect its binding to Laminin G (LG)-domain containing ECM proteins and lead to a form of congenital muscular dystrophy termed dystroglycanopathy (Taniguchi-Ikeda et al., 2016). The most severe forms, Muscle-Eye-Brain disease (MEB) and Walker Warburg Syndrome (WWS), are accompanied by cortical malformation (type II lissencephaly), cerebellar abnormalities, and retinal dysplasias (Dobyns et al., 1989).

Brain malformations in dystroglycanopathies reflect the critical role that dystroglycan plays in maintaining the architecture of the neuroepithelial scaffold (Moore et al., 2002; Myshrall et al., 2012). Focal regions of retinal dysplasia have

also been observed in mouse models of dystroglycanopathy, with ectopic cells protruding through the ILM (Chan et al., 2010; Lee et al., 2005; Satz et al., 2008; Takahashi et al., 2011; Takeda et al., 2003). In *Xenopus*, morpholino depletion of *dystroglycan* results in micropthalmia, degeneration of the ILM, and abnormal positioning of photoreceptors, bipolar cells, and retinal ganglion cells (Lunardi et al., 2006). However, several important questions regarding the role of dystroglycan in mammalian retinal development remain unaddressed. First, what is the underlying cause of retinal dysplasia in dystroglycanopathy? Second, is dystroglycan required for the proper migration and lamination of specific subtypes of retinal neurons? Third, how does the loss of dystroglycan affect axon guidance, dendritic stratification and mosaic spacing in the retina? Finally, how do retinal dysplasias in models of dystroglycanopathy affect the function of the retina?

Here, using multiple genetic models, we identify a critical role for dystroglycan in multiple aspects of retinal development. We show that dystroglycan within the neuroepithelium is critical for maintaining the structural integrity of the ILM. We provide *in vivo* evidence that dystroglycan's maintenance of the ILM is required for proper neuronal migration, axon guidance, formation of synaptic lamina, and the survival of multiple retinal neuron subtypes. Surprisingly, spontaneous retinal activity appears unperturbed, despite the dramatic disruption in inner retinal development. Together, these results provide critical insight into how dystroglycan directs the proper functional assembly of retinal circuits.

Materials and Methods

Experimental Design and Statistical Analysis

Mice were maintained on mixed genetic backgrounds and were used irrespective of sex. All phenotypic analysis was conducted with $n \geq 3$ animals obtained from at least two different litters of mice. Statistical analysis was performed using JMP Pro 13.0 software (SAS Institute). Comparison between two groups was analyzed using a Student's t-test. Comparison between two or more groups was analyzed using a Two-Way ANOVA and Tukey post-hoc test. Comparison of retinal wave parameters was analyzed using a Wilcoxon Rank Sums test. The significance threshold was set at 0.05 for all statistical tests. * indicates $p<0.05$; ** indicates $p<0.01$; *** indicates $p<0.001$.

Animals

Animal procedures were approved by OHSU Institutional Animal Care and Use Committee and conformed to the National Institutes of Health *Guide for the care and use of laboratory animals*. Animals were euthanized by administration of CO_2. The day of vaginal plug observation was designated as embryonic day 0 (e0) and the day of birth in this study was designated as postnatal day 0 (P0). The generation and genotyping protocols for $ISPD^{L79*/L79*}$ (Wright et al., 2012), $DG^{F/F}$ (Moore et al., 2002) and $DG^{\beta cyt}$ (Satz et al., 2009) mice have been described previously. The presence of the cre allele in $Sox2^{Cre}$ (Hayashi et al., 2002), $Six3^{Cre}$ (Furuta et al., 2000), $Isl1^{Cre}$ (Yang et al., 2006) and $Nestin^{Cre}$ mice (Tronche et al., 1999) was detected by generic cre primers. $ISPD^{+/L79*}$, $DG^{\beta cyt/+}$, and $DG^{F/+}$; $Six3^{Cre}$ or $DG^{F/+}$ age matched littermates were used as controls.

Tissue Preparation and Immunohistochemistry

Embryonic retinas were left in the head and fixed overnight at 4°C in 4% PFA and washed in PBS for 30 minutes. Heads were equilibrated in 15% sucrose overnight and flash frozen in OCT medium. Postnatal retinas were dissected out of the animal and the lens was removed from the eyecup. Intact retinas were fixed at room temperature for 30 minutes in 4% PFA. Retinas were washed in PBS for 30 minutes and equilibrated in a sequential gradient of 10%, sucrose, 20% sucrose and 30% sucrose overnight. Tissue was sectioned on a cryostat at 16-25μm. Tissue sections were blocked in a PBS solution containing 2% Normal Donkey Serum and 0.2% Triton for 30 minutes, and incubated in primary antibody overnight at 4°C. Sections were washed for 30 minutes and incubated in secondary antibody in a PBS solution containing 2% Normal Donkey Serum for 2-4 hours. Sections were incubated in DAPI to stain nuclei for 10 minutes, washed for 30 minutes, and mounted using Fluoromount medium. The source and concentration of all antibodies utilized in this study are listed in Table 1.

Wholemount retinal staining

Postnatal retinas were dissected out of the animal and the lens was removed from the eyecup. Intact retinas were fixed at room temperature for 30 minutes in 4% PFA. Retinas were incubated in primary antibody diluted in PBS solution containing 2% Normal Donkey Serum and 0.2% Triton for two days at 4°C. Retinas were washed in PBS for one day and incubated in secondary antibody diluted in PBS solution containing 2% Normal Donkey Serum for two days at 4°C, washed for one day in PBS and mounted using Fluoromount medium.

Microscopy

Imaging was performed on a Zeiss Axio Imager M2 upright microscope equipped with an ApoTome.2. Imaging of synapses was performed on a Zeiss Elyra PS.1 with LSM 710 laser-scanning confocal Super-Resolution Microscope with AiryScan. Imaging of retinal waves was performed on a Nikon TiE inverted microscope with full environmental chamber equipped with a Yokogawa CSU-W1 spinning disk confocal unit.

Quantification of cell number and mosaic spacing

For each experiment, 3-4 locations per retina at the midpoint of each lobe were sampled. Cell counts of horizontal cells (Calbindin), apoptotic cells (Cleaved Caspase-3, P0), and starburst amacrine cells (ChAT) were obtained from 500 x 500 μm images and quantified in FIJI. Cell counts of apoptotic cells (Cleaved Caspase-3, e16) and ganglion cells (RPBMS) were obtained from 250 x 250 μm images and quantified in FIJI. Analysis of retinal mosaics (Calbindin, ChAT) were conducted on 500 x 500 μm images by measuring the X-Y coordinates for each cell and Voronoi domains were calculated in FIJI and nearest neighbor measurements calculated with WinDRP. Cell counts of proliferating cells (PH3 positive, e13, e16) were done by counting the number of positive cells in mid-retinal 20μm sections.

Live cell imaging and analysis

Retinas from P1 $DG^{F/+}$; $Six3^{Cre}$; R26-LSL-GCaMP6f and $DG^{F/-}$; $Six3^{Cre}$; R26-LSL-GCaMP6f were dissected into chilled Ames' Medium (Sigma) buffered with sodium bicarbonate and bubbled with carbogen gas (95% O_2, 5% CO_2). The

36

retinas were dissected out of the eyecup, mounted RGC side up on cellulose membrane filters (Millipore) and placed in a glass-bottom petri dish containing Ames' Medium. A platinum harp was used to stabilize the filter paper during imaging. Imaging was performed at 30°C using a 10x0.45 Plan Apo Air objective with a field of 1664 by 1404 μm with a 3Hz imaging timeframe. The field was illuminated with a 488 nm laser. 3-4 retinal fields were imaged per retina, and each field of retina was imaged for a two-minute time series using a 300ms exposure and each field was sampled 3-5 times per imaging session.

Thirty representative control and thirty representative mutant time series were randomly selected for analysis. Only waves that initiated and terminated within the imaging field were used for analysis. To measure wave area, movies were manually viewed using FIJI frame by frame to determine the start and end frame of a wave. A Z-Projection for maximum intensity was used to create an image with the entire wave, and the boundary of the wave was manually traced to determine the area. Wave area per time was calculated by dividing the area of the wave by the duration in seconds of the wave. Any wave lasting less than 2 seconds was not used in analysis, consistent with previous studies (Blankenship et al., 2009).

Results

Dystroglycan is required for inner limiting membrane integrity

Dystroglycan plays a critical role in the developing cortex, where it anchors radial neuroepithelial endfeet to the basement membrane along the pial surface. In the absence of functional dystroglycan, disruptions in the cortical basement

membrane and detachment of neuroepithelial endfeet lead to profound neuronal migration phenotypes (Moore et al., 2002; Myshrall et al., 2012). In the adult retina, dystroglycan is present in blood vessels, in RGCs, at ribbon synapses in the OPL, and at the ILM, which serves as a basement membrane that separates the neural retina from the vitreous space (Montanaro et al., 1995; Omori et al., 2012). However, the role of dystroglycan in regulating neuronal migration, axon guidance or dendritic stratification of specific cell types during retinal development has not been examined in a comprehensive manner. To address this open question, we first examined the expression pattern of dystroglycan in the developing retina. Using immunohistochemistry, we observed dystroglycan expression along radial processes that span the width of the retina, and its selective enrichment at the ILM from embryonic ages (e13) through birth (P0) (Figure 1A). These processes are likely a combination of neuroepithelial cells and the basal process of migrating RGCs. Loss of staining in retinas from an epiblast-specific *dystroglycan* conditional knockout ($DG^{F/-}$; $Sox2^{Cre}$) confirmed the specificity of this expression pattern (Figure 1B).

The first step in the assembly of basement membranes is the recruitment of laminin polymers to the cell surface by sulfated glycolipids, followed by the stabilization of laminin polymers by transmembrane receptors (Yurchenco, 2011). To determine whether dystroglycan is required for the initial formation of the ILM during retinal development, we utilized two complementary genetic models. $ISPD^{L79*/L79*}$ mutants, previously identified in a forward genetic screen, lack the mature glycan chains required for dystroglycan to bind ligands such as laminin

and are a model for severe dystroglycanopathy (Wright et al., 2012). $DG^{F/-}$; $Sox2^{Cre}$ conditional mutants lack dystroglycan in epiblast-derived tissues, including all retinal tissue, and were utilized to confirm that phenotypes observed in $ISPD^{L79*/L79*}$ mice are dystroglycan dependent. The enrichment of laminin at the ILM appeared normal in early retinal development at e13 in both $ISPD^{L79*/L79*}$ and $DG^{F/-}$; $Sox2^{Cre}$ mutants (Figure 1C-E), indicating that dystroglycan is not required for the initial formation of the ILM. However, at e16, we observed a loss of laminin staining and degeneration of the ILM across the entire surface of the retina in $ISPD^{L79*/L79*}$ and $DG^{F/-}$; $Sox2^{Cre}$ mutants (Figure 1D-F). The loss of ILM integrity in $ISPD^{L79*/L79*}$ and $DG^{F/-}$; $Sox2^{Cre}$ mutants was accompanied by the inappropriate migration of retinal neurons, resulting in the formation of an ectopic layer of neurons protruding into the vitreous space.

Following the initial polymerization of laminin on cell surfaces, additional ECM proteins bind and crosslink the nascent basement membrane to increase its stability and complexity. Examination of $ISPD^{L79*/L79*}$ and $DG^{F/-}$; $Sox2^{Cre}$ mutant retinas at P0 revealed a loss of the ECM proteins Collagen IV (red), and Perlecan (green), coinciding with the disruptions in Laminin (purple) (Figure 2A, B, C). These data suggest that while dystroglycan is not required for the initial formation of the ILM, it is essential for its maturation and maintenance. Furthermore, dystroglycan is critical for the ILM to function as a structural barrier to prevent the ectopic migration of neurons into the vitreous space.

Dystroglycan is required for vascular and optic fiber layer development

The hyaloid vasculature in the embryonic retina normally regresses as astrocytes and the retinal vascular plexus emerge through the optic nerve head beginning around birth (Fruttiger, 2007). Previous studies have found that defects in ILM integrity disrupt the emergence and migration of astrocytes and the retinal vasculature (Edwards et al., 2010; Lee et al., 2005; Takahashi et al., 2011; Tao and Zhang, 2016). In agreement with these findings, we observe that at embryonic ages in *ISPD$^{L79*/L79*}$* mutant retinas, the hyaloid vasculature becomes embedded within the ectopic retinal neuron layer at e16 (Figure 3A), and fails to regress at P0 (Figure 3B). In addition, the emergence of the retinal vasculature and astrocytes is stunted in *ISPD$^{L79*/L79*}$* mutants (Figure 3B).

We have shown previously that the organization of the basement membrane by dystroglycan provides a permissive growth substrate for axons in the developing spinal cord (Wright et al., 2012). In addition, contact with laminin in the ILM stabilizes the leading process of newly generated RGCs to direct the formation of the nascent axon (Randlett et al., 2011). These axons remain in close proximity to the ILM as they extend centrally towards the optic nerve head, forming the optic fiber layer (OFL). Therefore, we examined whether the disruptions in the ILM affected the guidance of RGC axons in *ISPD$^{L79*/L79*}$* and *DG$^{F/-}$; Sox2^{Cre}* mutants. At e13, axons in both control and mutant retinas formed a dense and continuous network in the basal retina, directly abutting the ILM (Figure 4A). In contrast, at e16 (Figure 4B) and P0 (Figure 4C), RGC axons in

ISPD^{L79*/L79*} and *DG^{F/-}; Sox2^{Cre}* mutants were disorganized, exhibiting both defasciculation (asterisks) and hyperfasciculation (arrowheads).

To gain further insight into the specific defects that occur in RGC axons, we used a flat mount retina preparation. Regardless of their location in the retina, all RGCs orient and extend their axons towards the center of the retina, where they exit the retina through the optic nerve head (Bao, 2008). In control retinas at e16 (Figure 4D, left panel) and P0 (Figure 4E, left panel) axons traveled towards the optic nerve head in fasciculated, non-overlapping bundles. In contrast, we frequently observed defasciculated RGC axons that grew in random directions without respect to their orientation to the optic nerve head in both *ISPD^{L79*/L79*}* and *DG^{F/-}; Sox2^{Cre}* mutants. To further characterize the mutant phenotype, we utilized a previously described Hb9-GFP transgenic reporter to sparsely label a subset of RGCs on the *ISPD* background (Duan et al., 2014). In controls (Supplemental Figure 1A), RGCs extend a single axon towards the optic nerve head. In *ISPD^{L79*/L79*}* mutants, while some RGCs appear to have developed normally, we do observe several defects in axon growth and guidance. A subset of cells extend a single axon away from the optic nerve head; this axon eventually turns around and grows back towards the optic nerve head (Supplemental Figure 1B). Other axons that are initially misoriented will regain a trajectory towards the optic nerve head upon contact with another axon that is correctly oriented (Supplemental Figure 1C, D). An additional subset of cells appears to grow multiple axons, with the secondary axon either growing towards (Supplemental Figure 1E) or away from (Supplemental Figure 1F, G) the optic

nerve head. Together, these data show that proper growth and guidance of RGC axons to the optic nerve head requires dystroglycan to maintain an intact ILM as a growth substrate.

Dystroglycan is required for axonal targeting, dendritic lamination, and cell spacing in the postnatal retina

Our results in $ISPD^{L79*/L79*}$ and $DG^{F/-}$; $Sox2^{Cre}$ mutants demonstrate that dystroglycan is required for ILM integrity and to prevent the ectopic migration of neurons into the vitreous (Figure 1). However, the specific neuronal subtypes affected in models of dystroglycanopathy are unknown, and the role of dystroglycan in regulating postnatal aspects of retinal development has not been examined. The synaptic layers of the retina develop postnatally, with tripartite synapses between the photoreceptors, bipolar cells and horizontal cells forming in the OPL, and synapses between bipolar cells, amacrine cells and retinal ganglion cells forming in the IPL. The development of these synaptic layers requires the precise stratification of both axons and dendrites that occurs between P0 and P14. Since $ISPD^{L79*/L79*}$ and $DG^{F/-}$; $Sox2^{Cre}$ mutant mice exhibit perinatal lethality, we deleted $dystroglycan$ selectively from the early neural retina using a $Six3^{Cre}$ driver (Furuta et al., 2000) (Figure 5A).

Analysis of $DG^{F/-}$; $Six3^{Cre}$ retinas confirmed that dystroglycan protein was lost along the neuroepithelial processes and at the ILM (Figure 5B). We next confirmed that $DG^{F/-}$; $Six3^{Cre}$ mice recapitulated the retinal phenotypes identified in $ISPD^{L79*/L79*}$ and $DG^{F/-}$; $Sox2^{Cre}$ mice. We observed a degeneration of the ILM (laminin, purple) accompanied by ectopic migration of neurons into the vitreous

(Figure 5C), abnormal fasciculation and guidance of RGC axons (Figure 5D), and defective emergence and migration of astrocytes and the vascular plexus (Figure 5E). While fully penetrant, the ILM degeneration and neuronal migration defects in $DG^{F/-}$; $Six3^{Cre}$ mice were milder than in $DG^{F/-}$; $Sox2^{Cre}$ mice, exhibiting a patchiness that was distributed across the retina (Figure 5F). The defects in $DG^{F/-}$; $Six3^{Cre}$ mice contrast the finding that conditional deletion of *dystroglycan* with *Nestin*^{Cre} does not affect the overall structure of the retina (Satz et al., 2009). We find that this difference is likely due to the onset and pattern of *Cre* expression, as recombination of a *Cre*-dependent reporter (*Rosa26-lox-stop-lox-TdTomato; Ai9*) occurred earlier and more broadly in $Six3^{Cre}$ mice than in *Nestin*^{Cre} mice (Figure 5A, data not shown).

$DG^{F/-}$; $Six3^{Cre}$ mice are healthy and survive into adulthood, allowing us to examine the role of dystroglycan in postnatal retinal development. We analyzed DG; $Six3^{Cre}$ retinas at P14 when migration is complete and the laminar specificity of axons and dendrites has been established (Morgan and Wong, 1995). The overall architecture of the ONL appeared unaffected by the loss of dystroglycan in $DG^{F/-}$; $Six3^{Cre}$ mice, and cell body positioning of photoreceptors appeared similar to controls (Figure 6A). Within the INL, the laminar positioning of rod bipolar cell bodies (PKC, Figure 6B), cone bipolar cell bodies (SCGN, Figure 6C), horizontal cells (arrows, Calbindin, Figure 6E), and Müller glia cell bodies (Figure 6H) and the targeting of their processes to the OPL appeared normal in $DG^{F/-}$; $Six3^{Cre}$ mutants. However, bipolar cell axons that are normally confined to the synaptic layers in the IPL, and Müller glia processes that are normally

43

concentrated at the ILM both extended aberrant projections into the ectopic clusters (Figure 6B-C, H).

In contrast to the normal laminar architecture of the outer retina, the inner retina was disorganized in $DG^{F/-}; Six3^{Cre}$ mutants. Subsets of amacrine and ganglion cells labeled by ChAT (starburst amacrine cells, Figure 6D), calbindin (Figure 6E), and calretinin (Figure 6F) that are normally confined to the INL and GCL were present in the ectopic clusters that protrude into the vitreous space. Glycinergic amacrine cells (GlyT1, Figure 6G), whose cell bodies are normally found in a single layer within the INL, were also present within ectopic clusters. Compared to the OPL, which appeared grossly normal, dendritic stratification within the IPL in $DG^{F/-}; Six3^{Cre}$ mutant retinas was disrupted. The laminated dendritic strata appeared expanded (Figure 6D), fragmented (Figure 6D-F) and occasionally lacked an entire lamina (Figure 6E). These defects were restricted to regions of the retina where ectopic neuronal clusters were present, whereas regions of the $DG^{F/-}; Six3^{Cre}$ mutant retina with normal cellular migration and lamination also had normal dendritic stratification (Figure 5F). These results demonstrate that the ectopic clusters consisted of multiple subtypes of amacrine cells and ganglion cells that normally reside in the INL and GCL, and that the disorganization of the dendritic strata are likely secondary to the cell migration defects.

Over the course of retinal development, multiple cell types, including horizontal cells and amacrine cells, develop mosaic spacing patterns that ensure cells maintain complete and non-random coverage over the surface of the retina

(Wassle and Riemann, 1978). This final mosaic pattern is established by both the removal of excess cells through apoptosis and the lateral dispersion of "like-subtype" cells via homotypic avoidance mechanisms (Kay et al., 2012; Li et al., 2015). To determine whether the defects in establishing proper laminar positioning of retinal subtypes in $DG^{F/-}$; $Six3^{Cre}$ mutants extends to mosaic spacing, we performed nearest neighbor analysis. For horizontal cells, which exhibit normal lamination in $DG^{F/-}$; $Six3^{Cre}$ mutant retinas, we observed a small, but significant reduction in the number of cells (Figure 7A-B, Two-Way ANOVA, $p<0.0001$, Tukey HSD post-hoc test ***$p<0.0001$). Despite the reduction in horizontal cell number, nearest neighbor curves between controls and mutants are the same shape, indicating that horizontal cell mosaics are maintained in dystroglycan mutants (Figure 7A-B).

ChAT positive starburst amacrine cells are present in two distinct lamina that form mosaic spacing patterns independent from one another. Consistent with this, ChAT labeled cells in the INL showed normal mosaic cell spacing (Figure 7C, top, Figure 7D, top, Two-Way ANOVA, Tukey HSD post-hoc test *$p=0.0494$). In contrast, the GCL contained prominent ChAT positive clusters that corresponded to the ectopic protrusions that extend into the vitreous, resulting in a decrease in cell spacing as determined by nearest neighbor analysis (Figure 7C, bottom, Figure 7D, bottom, Two-Way ANOVA, $p<0.0001$, Tukey HSD post-hoc test ***$p<0.0001$). These results demonstrate that laminar migration defects in $DG^{F/-}$; $Six3^{Cre}$ mutants degrade the mosaic spacing of cells in the GCL, and

45

that contact with an intact ILM is likely required for the proper lateral dispersion of these cells.

Deletion of dystroglycan leads to a loss of photoreceptors, horizontal cells and ganglion cells

During development, normal physiological apoptotic cell death during the first two postnatal weeks plays an important role in retinal maturation (Young, 1984). This process is critical for establishing the proper numbers and spacing of some subtypes of cells across the mature retina, as well as removing cells that fail to connect to appropriate synaptic targets (Braunger et al., 2014). Degeneration of the ILM during development can lead to a reduction in the number of ganglion cells, and previous analysis of dystroglycanopathy mutants has noted thinning of the retina (Chan et al., 2010; Halfter et al., 2005b; Lee et al., 2005; Satz et al., 2008; Takahashi et al., 2011). In agreement with these results, we observed that the retinas of $DG^{F/-}; Six3^{Cre}$ mutants are thinner (Figure 6, 8). However, the specific cell types affected by the loss of dystroglycan in the retina are unknown.

To investigate the mechanism by which loss of dystroglycan contributes to retinal thinning, we began by measuring the distance between the edges of the inner and outer retina in control and $DG^{F/-}; Six3^{Cre}$ mutants by DAPI staining and found that there was a significant reduction in overall retinal thickness by approximately 20% in mutants (Figure 8A, blue, Figure 8B, t test, p=0.0039). We next investigated which specific cell types contribute to retinal thinning. In the outer retina, the thickness of the photoreceptor layer (recoverin, Figure 8A, green, Figure 8C, t-test, p=0.0163) was reduced by approximately 20% and the

density of horizontal cells had a small, yet significant reduction in $DG^{F/-}$; $Six3^{Cre}$ mutants (calbindin, Figure 8G, t-test, p=0.0112). In contrast, the thickness of the bipolar cell layer (Chx10, Figure 8A, purple, Figure 8D, t-test, p>0.05) was normal. In the inner retina, there was a 50% reduction in the density of ganglion cells (Figure 8H, I, t-test, p<0.0001), while the density of ChAT-positive starburst amacrine cells in both the INL and GCL was normal in $DG^{F/-}$; $Six3^{Cre}$ mutants (Figure 8E, F, t-test, p>0.05). Thus, a reduction in the number of photoreceptors, horizontal cells and RGCs contribute to the overall thinning of $DG^{F/-}$; $Six3^{Cre}$ retinas.

To determine whether the reduction in photoreceptors, horizontal cells and RGCs in the absence of dystroglycan was due to defects in proliferation of retinal progenitors, we examined phospho-Histone H3 (PH3) staining at embryonic ages. PH3 positive mitotic progenitors were localized along the apical surface of the retina, and were present at the normal number in $ISPD^{L79*/L79*}$ mutants at e13 and e16 and (Figure 9 A, B, t-test, p>0.05). To determine whether the reduced number of neurons in mutant retinas was due to increased apoptosis, we quantified the number of caspase-3 positive cells. At e13, we observed no difference between in the number of caspase-3 positive cells in $ISPD^{L79*/L79*}$ mutants and controls (data not shown). In contrast, there was a significant increase in caspase-3 positive cells in $ISPD^{L79*/L79*}$ mutants at e16 (Figure 9D, t-test, p<0.0001) and P0 (Figure 9C, D, t-test, p<0.0001) that was restricted to the ganglion cell layer. Similarly, we observed an increased number of cleaved caspase-3 positive cells in the ganglion cell layer in $DG^{F/-}$; $Six3^{Cre}$ mutants at P0

(Figure 9C, D, t-test, p=0.0279). These results led us to conclude that the loss of RGCs in $DG^{F/-}$; $Six3^{Cre}$ mutants is due to increased apoptotic cell death.

Dystroglycan functions non-cell autonomously as an extracellular scaffold in the developing retina

We next sought to provide mechanistic insight into how dystroglycan regulates retinal development *in vivo*. In the cerebral cortex, the loss of dystroglycan results in breaches of the pial basement membrane and detachment of neuroepithelial endfeet from the pial surface, depriving neurons of a migratory scaffold. In addition, the cortical basement membrane defects cause the mis-positioning of Cajal-Retzius cells, which are the source of Reelin that regulates somal translocation of neurons as they detach from the neuroepithelial scaffold (Nakagawa et al., 2015). Deletion of *dystroglycan* specifically from postmitotic cortical neurons does not result in a migration phenotype (Satz et al., 2010b), supporting a model in which the cortical migration phenotypes arise due to disrupted interactions between the basement membrane and neuroepithelial scaffold. In contrast to the cerebral cortex, the basal migration of RGCs does not involve contact with the neuroepithelial scaffold. Instead, newly born RGCs migrate via somal translocation using an ILM-attached basal process that eventually becomes the nascent axon (Icha et al., 2016; Randlett et al., 2011). Dystroglycan's expression in ILM-attached basal processes (Figure 1A) and RGCs (Montanaro et al., 1995) and the restriction of neuronal migration and axon guidance defects to the GCL raise the possibility that dystroglycan could be functioning cell-autonomously in the basal processes of newly born RGCs. To

48

test this possibility, we generated $DG^{F/-}; Isl1^{Cre}$ conditional knockouts. *Islet1* is expressed in the majority of ganglion cells as they differentiate from the retinal progenitor pool (Pan et al., 2008b). Analysis of $Isl1^{Cre}$ mice at e13 confirmed recombination occurs in the majority of newly born ganglion cells, but not in neuroepithelial progenitors (Figure 10A). Interestingly, dystroglycan protein expression in $DG^{F/-}; Isl1^{Cre}$ mutants was not altered compared to controls, suggesting that RGCs do not provide a significant source of dystroglycan at the ILM (Figure 10B). Examination of $DG^{F/-}; Isl1^{Cre}$ mutants indicated that deletion of *dystroglycan* selectively from RGCs did not affect ILM integrity (Figure 10C). Neuronal migration (Figure 10C, E and F), axon guidance (Figure 10C and D) and the stratification of dendrites in the IPL (Figures 10 E and F) all appeared normal in $DG^{F/-}; Isl1^{Cre}$ mutants. These results demonstrate that dystroglycan is not required within RGCs themselves during retinal development.

Dystroglycan consists of two subunits that can play distinct roles in the overall function of the protein. The extracellular α-subunit is heavily glycosylated and functions as an extracellular scaffold by binding to extracellular matrix components such as laminin. The β-subunit contains a transmembrane and intracellular domain, and can bind directly to the intracellular scaffolding protein dystrophin and other modifiers of the actin cytoskeleton, as well as initiate intracellular signaling cascades (Moore and Winder, 2010). The intracellular domain of dystroglycan is required for the localization of dystrophin to the ILM, and mice lacking the intracellular domain of dystroglycan ($DG^{-/\beta cyt}$) (Satz et al., 2009) or the predominant retinal isoform of dystrophin (Mdx^{3Cv}) (Blank et al.,

1999) have abnormal scotopic electroretinograms, suggesting a defect in retinal function. While these mice do not have any disruptions in the ILM or gross malformations in the retina, whether dystroglycan signaling through dystrophin is required for neuronal migration, axon guidance or dendritic stratification has not been examined. Consistent with the original report, examination of the ILM and overall architecture of the retina is normal in $DG^{-/\beta cyt}$ mice (Figure 11A). In addition, we find that neuronal migration, axon guidance and stratification of dendritic lamina are unaffected in $DG^{-/\beta cyt}$ mice (Figure 11A-D). Therefore, intracellular signaling, including through dystrophin, is not required for these aspects of retinal development. Taken together with our results in $DG^{F/-}$; $Isl1^{Cre}$ mutants, these findings indicate that dystroglycan primarily functions within neuroepithelial cells as an extracellular scaffold to regulate the structural integrity of the ILM. The progressive degeneration of the ILM then leads to secondary defects including aberrant migration, axon guidance and dendritic stratification that primarily affect the inner retina.

Dystroglycan is dispensable for the generation of spontaneous retinal waves

One of the critical functions for laminar targeting in neural circuit development is to ensure that the axons and dendrites of appropriate cell types are in physical proximity to one another during synaptogenesis. In addition to regulating the laminar positioning of neurons in the cortex and retina, dystroglycan is required for the development of a subset of inhibitory synapses in the brain (Fruh et al., 2016). Therefore, we investigated the possibility that the

loss of dystroglycan disrupts synapse formation in the retina. Previous studies have shown that ribbon synapses in the OPL are dysfunctional in the absence of dystroglycan or its ligand pikachurin (Sato et al., 2008). These synapses are normal at the resolution of light microscopy, but electron microscopy reveals that dystroglycan and pikachurin are required for the insertion of bipolar cell dendrite tips into ribbon synapse invaginations (Omori et al., 2012). Consistent with these results, we found that pre- and post-synaptic markers for ribbon synapses are present in $DG^{F/-}$; $Six3^{Cre}$ mutants (Figure 12A). In the inner retina, markers for excitatory synapses (VGLUT1, Figure 12B) and inhibitory synapses (VGAT, Figure 12C) were present in the IPL, and were also present in the mis-localized ectopic cell clusters that protrude into the vitreous (asterisks). This finding is similar to a recent study in which mice lacking the Cas family of intracellular adaptor proteins express synaptic markers localized to aberrant neuronal ectopia that protrude into the vitreous (Riccomagno et al., 2014). These results suggest that mis-laminated neurons in the retina are still able to recruit synaptic partners, despite their abnormal location.

The presence of synaptic markers in ectopic neuronal clusters in the inner retina does not guarantee normal function of these neurons. Recording synaptic activity in RGCs in response to light stimuli in $DG^{F/-}$; $Six3^{Cre}$ mutants is not feasible due to the requirement for dystroglycan at photoreceptor ribbon synapses. We instead analyzed retinal waves, which are spontaneous bursts of activity that propagate across the retina prior to eye opening and are independent of light stimulation. During early postnatal development, these

waves are initiated by acetylcholine (ACh) release from starburst amacrine cells and propagate along the starburst amacrine cell network prior to transmission to RGCs (Xu et al., 2016). In $DG^{F/-}; Six3^{Cre}$ mutants, ChAT positive starburst amacrine cells are present in normal numbers, and while they are normally localized and mosaically spaced in the INL, they are disorganized in the GCL. Therefore, we expected that these defects might affect the propagation of retinal waves through the starburst amacrine cell and RGC network. As disruptions in the ILM in $DG^{F/-}; Six3^{Cre}$ mutants would lead to unequal bulk loading of cell permeable calcium indicators, we utilized the genetically-encoded calcium indicator GCaMP6f crossed onto the $DG; Six3^{Cre}$ line to visualize retinal waves.

Retinal waves in control $DG^{F/+}; Six3^{Cre}; R26-LSL-GCaMP6f$ retinas at P1-P2 were robust and had similar spatiotemporal features (area, rate of propagation, refractory period) to waves measured using cell-permeable calcium indicators (Arroyo and Feller, 2016). Consistent with previous reports, there is a broad distribution of wave area in control retinas (Figures 13A, C, Movie 1). Neighboring waves do not overlap with one another, but rather tile the retinal surface during the two-minute imaging period. To our surprise, retinal waves were present and appeared grossly normal in $DG^{F/-}; Six3^{Cre}; R26-LSL-GCaMP6f$ mutants (Figure 13B, Movie 2). Waves in control and mutant retinas exhibited a similar distribution in wave area (Figure 13C), and the average wave area showed no statistical difference. The rate of wave propagation showed a similar distribution between controls and mutants (Figure 13D). The average rate of wave propagation showed a small, but statistically significant, decrease

(Wilcoxon Rank Sum test, p=0.0493). Thus, despite the dramatic disorganization of ChAT positive starburst amacrine cells in the GCL of $DG^{F/-}$; $Six3^{Cre}$ mutants, the generation and propagation of retinal waves persisted.

Discussion

While defects in retinal structure and function are observed in both human patients and mouse models of dystroglycanopathy, the mechanism of dystroglycan function in the mammalian retina and the consequence of its loss on specific cell types are poorly understood (Chan et al., 2010; Lee et al., 2005; Satz et al., 2008; Satz et al., 2009; Takahashi et al., 2011; Takeda et al., 2003). Our study establishes a critical role for dystroglycan in maintaining the integrity of the ILM, which is required for intra-retinal axon guidance and establishing laminar architecture and mosaic spacing in the inner retina. Mechanistically, we show that dystroglycan functions non-cell autonomously as an extracellular scaffold, as mice with selective deletion of *dystroglycan* from postmitotic RGCs (DG; $Isl1^{Cre}$) and mice lacking the intracellular domain of dystroglycan ($DG^{-/\beta cyt}$) appear phenotypically normal. Despite the dramatic disruptions in cellular lamination in the GCL and dendritic stratification in the IPL in DG; $Six3^{Cre}$ mutants, dystroglycan appears dispensable for the formation of synapses and the generation of spontaneous, light-independent activity in the retina.

Requirement for dystroglycan at the ILM during retinal development.

Using two genetic models for the complete loss of functional dystroglycan ($ISPD^{L79*}$ and DG; $Sox2^{Cre}$), we demonstrated that after the ILM forms, it rapidly degenerates in the absence of dystroglycan. These results suggest that

dystroglycan is not required for the formation of the nascent ILM, but rather plays a critical role in maintaining ILM structure as it expands to accommodate the growing retina. Recruitment of laminin is a critical early step in the assembly of the ILM, and several laminin mutants have similar disruptions in ILM integrity (Edwards et al., 2010; Gnanaguru et al., 2013; Pinzon-Duarte et al., 2010). In contrast to *Xenopus*, where depletion of *dystroglycan* results in degeneration of both the ILM in the inner retina and Bruch's membrane in the outer retina, Bruch's membrane is unaffected by the loss of *dystroglycan* or isoforms of *Laminin* (Lunardi et al., 2006; Pinzon-Duarte et al., 2010). Mice lacking β-1 *Integrin* in the retina exhibit a similar defect to *dystroglycan* mutants, raising the possibility that these laminin receptors may be functionally redundant (Riccomagno et al., 2014). Surprisingly however, mice in which both *dystroglycan* and β-1 *Integrin* are deleted from the retina (*DG*; *ItgB1*; *Six3^{Cre}*) still formed an ILM at e13 (Supplemental Figure 1A), and the subsequent degeneration of the ILM at P0 was indistinguishable from *DG*; *Six3^{Cre}* mutants (Supplemental Figure 2B). Therefore, sulfated glycolipids alone are likely sufficient for the recruitment of laminin during the initial formation of the ILM.

The ILM is required for neuronal migration and axon outgrowth in the retina

In the developing cortex, the loss of functional dystroglycan leads to degeneration of the radial glia processes and ectopic clustering of reelin-secreting Cajal-Retzius neurons, which are thought to be the principal drivers of structural brain defects in dystroglycanopathies (Booler et al., 2016; Myshrall et al., 2012; Nakagawa et al., 2015). Retinal neurons do not migrate along the

neuroepithelial scaffold, and there is no cue analogous to reelin to signal termination of migration, suggesting that while dystroglycan functions primarily in neuroepithelial cells in the retina, the functional implications are distinct from its role in cortical neuroepithelial cells. In the cortex of *dystroglycan* deficient mice, the organization of neurons across all lamina is affected, whereas within the retina, migration defects are restricted to amacrine cells and RGCs in the inner retina. In contrast, migration defects in dystroglycan-deficient *Xenopus* retinas are more widespread and also affect outer retinal neurons, likely reflecting the requirement for dystroglycan at both the ILM and Bruch's membrane (Lunardi et al., 2006). What is the driving force behind the selective localization of amacrine cells and RGCs to the ectopic clusters that protrude into the vitreous in the mammalian retina? While the elimination of RGCs does not affect the lamination of other neurons, other neurons will organize themselves around mislocalized RGCs, resulting in an overall disorganization of retinal lamination (Icha et al., 2016; Kay et al., 2004; Wang et al., 2001). In *dystroglycan* mutants, RGCs that encounter the degenerating ILM and inappropriately migrate into the vitreous may then actively recruit later born neurons such as amacrine cells to inappropriate locations.

The establishment of retinal mosaics requires tangential migration that is regulated by short range interactions between immature neurites of neighboring cells (Galli-Resta et al., 2002; Galli-Resta et al., 1997; Huckfeldt et al., 2009; Reese et al., 1999). A key feature of this process is that it requires homotypic cells to be localized within the same lamina, and cells in which mosaic spacing is

disrupted are no longer restricted to a two-dimensional plane (Fuerst et al., 2008; Kay et al., 2012). In *dystroglycan* mutants, the laminar organization and mosaic spacing is normal in horizontal cells and INL starburst amacrine cells, but disrupted in starburst amacrine cells in the GCL. This defect is not due to dystroglycan functioning within starburst amacrine cells, as mosaic spacing was normal in *DG*; *Isl1^{Cre}* mutant retinas (data not shown). Rather, the selective defects in mosaic spacing of GCL starburst amacrine cells suggests that this is likely a consequence of disrupting the two-dimensional organization of the GCL. Alternatively, mosaic spacing of cells within the GCL may require cues present in the ILM for their tangential dispersion.

Basement membranes are highly dynamic structures that contain pro-axon growth ECM molecules such as laminins and collagens, and also regulate the distribution of secreted axon guidance cues (Chai and Morris, 1999; Halfter et al., 1987; Wright et al., 2012; Xiao et al., 2011). A number of secreted cues direct intraretinal axon guidance of RGCs. Deletion of Netrin (Deiner et al., 1997) specifically affects exit of RGC axons through the optic nerve head, and deletion of Slits (Thompson et al., 2006b) or Sfrps (Marcos et al., 2015) leads to the invasion of RGC axons into the outer retina. In contrast, the randomized growth and defasciculation of axons we observed in *ISPD^{L79*}* and *DG*; *Six3^{Cre}* mutant retinas is more consistent with defects observed upon deletion of adhesion receptors (Bastmeyer et al., 1995; Brittis et al., 1995; Ott et al., 1998). Our results also suggest that axons may be appropriate growth substrates for each other in the absence of an ILM. In our model, the ILM breaks down after e13, when some

axons have already appropriately exited the retina through the optic nerve head. Using the Hb9-GFP reporter at e15 reveals that some axons, while initially on an aberrant trajectory away from the optic nerve head, do have the ability to reorient if they encounter an axon that is already normally oriented (Supplemental Figure 1 C, D). The initial aberrant trajectory may be caused by a loss of laminin cue that normally directs axons to grow in the right direction. These results suggest that dystroglycan primarily functions to organize the ILM as a substrate for axonal adhesion.

Loss of retinal neurons in the absence of dystroglycan

While previous studies of mouse models of dystroglycanopathy have consistently noted retinal thinning, it was unclear which retinal cell types were affected. Our comprehensive analysis found that lack of dystroglycan led to reductions in photoreceptor layer thickness, horizontal cell number, and RGC number (Figure 8). Analysis of e13, e16 and P0 retinas from *ISPD^{L79*}* and *DG; Six3^{Cre}* mutants indicated that the loss of RGCs was not due to altered proliferation of retinal progenitors, but was primarily due to increased apoptosis of cells in the GCL that preceded and extended into the normal window of developmental apoptotic cell death. This increase in apoptotic cell death did not persist in adult (P56) *DG; Six3^{Cre}* mutants (data not shown), suggesting it was likely restricted to the developing retina. Why are RGCs lost at such a high rate in *DG; Six3^{Cre}* mutants, while displaced amacrine cell number in the GCL remains normal? One possibility is that RGCs are selectively affected since they are the only cell type to project out of the retina. Indeed, we observed profound guidance

defects of RGCs at the optic chiasm in *ISPD^{L79*}* and *DG; Six3^{Cre}* mutants (unpublished observations). This result is similar to *Isl1* and *Brn3b* deficient mice, in which axon growth defects at the optic chiasm precede an increase in RGC apoptosis (Gan et al., 1999; Pan et al., 2008a). The death of RGCs whose axons fail to reach retinorecipient regions of the brain is consistent with the need for target-derived factors to support their survival, although the identity of these factors remains elusive.

While we did not observe increased caspase-3 reactivity in photoreceptors or horizontal cells at P0, it is possible that the loss of cells occurred gradually during the first two postnatal weeks. Dystroglycan is required for the proper formation of ribbon synapses between photoreceptors, horizontal cells and bipolar cells in the OPL (Omori et al., 2012; Sato et al., 2008). Therefore, the loss of appropriate synaptic contact in the absence of dystroglycan may lead to the elimination of a proportion of photoreceptors and horizontal cells.

Persistence of retinal waves in the absence of dystroglycan

The defects in lamination and dendritic stratification of starburst amacrine cells in *DG; Six3^{Cre}* mutants led us to hypothesize that this would affect their ability to generate retinal waves. These waves are initiated by the spontaneous activity of starburst amacrine cells, independent of light stimuli, allowing us to circumvent the requirement for dystroglycan in proper transmission at ribbon synapses. Contrary to our expectations, retinal waves were present and propagated normally in *DG; Six3^{Cre}* mutants (Figure 13). The persistence of retinal waves even in the context of disrupted cellular organization supports the

model that these waves are the product of volume release of ACh from starburst amacrine cells that can trigger extra-synaptic responses in cells that are not physically connected (Ford et al., 2012). Therefore, the relatively normal organization of INL starburst amacrine cells may be sufficient to overcome the disorganization of GCL starburst amacrine cells.

Conclusion

Retinal dysplasia and optic nerve hypoplasia are frequently observed in patients with severe forms of dystroglycanopathy (Manzini et al., 2008). Using multiple mouse models, we demonstrate that dystroglycan is required for multiple aspects of retinal development. We show that dystroglycan functions within neuroepithelial cells in the retina to regulate the structural integrity of a basement membrane (the ILM), which is required for the coordination of neuronal migration, axon guidance and dendritic stratification in the inner retina. In addition, we find that there is a significant loss of photoreceptors, horizontal cells and almost 50% of RGCs due to increased apoptotic cell death. Our data suggest that the disorganization of the inner retina resulting from degeneration of the ILM is a key contributor to visual impairment in dystroglycanopathies.

Figure 1

Figure 1: The inner limiting membrane undergoes progressive degeneration in the absence of functional dystroglycan. (A) Dystroglycan (β-DG) is expressed throughout the developing retina, with an enrichment at the inner limiting membrane (ILM). (B) Dystroglycan expression is lost in *DG^{F/-}; Sox2^{Cre}* mice. (C-E) The initial assembly of the ILM (laminin, green) occurs normally in the absence of functional dystroglycan in (D) *ISPD^{L79*/L79*}* and (E) *DG^{F/-}; Sox2^{Cre}* retinas. The ILM in *ISPD^{L79*/L79*}* and *DG^{F/-}; Sox2^{Cre}* retinas undergoes progressive degeneration at e16 (middle) and P0 (right), and retinal neurons migrate into the vitreous. (F) The ILM in *ISPD^{L79*/L79*}* retinas undergoes degeneration (right panel) that is present across the entire span of the retina at e16. Arrowheads indicate ILM, asterisks indicate non-specific staining of blood vessels. Scale bar, 50μm A-E, 200 μm F.
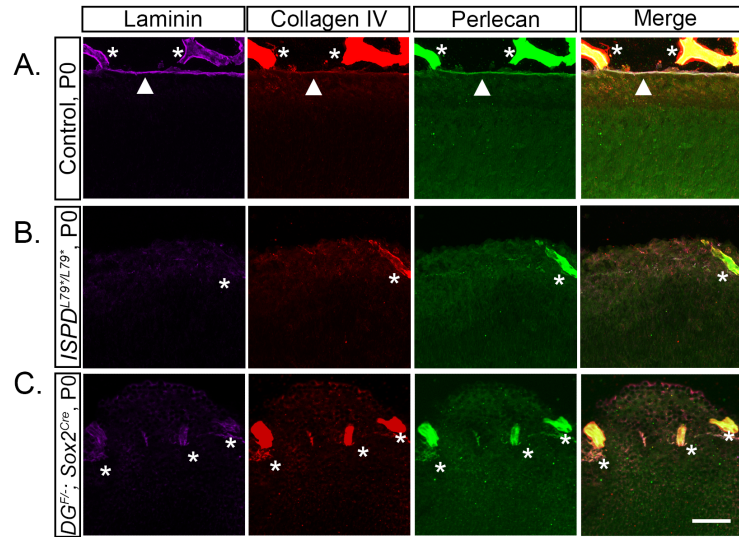
Figure 2

Figure 2: Dystroglycan is required to localize ECM proteins at the ILM. (A) Multiple extracellular matrix proteins, including laminin (purple), collagen IV (red), and perlecan (green), localize to the ILM in controls. (B-**C**) Localization of extracellular matrix proteins is disrupted in the ILM in the absence of functional dystroglycan in *ISPD$^{L79*/L79*}$* (B) and *DG$^{F/-}$; Sox2^{Cre}* (C) retinas at P0. Arrowheads indicate ILM, asterisks indicate blood vessels. Scale bar, 50μm.

Figure 3
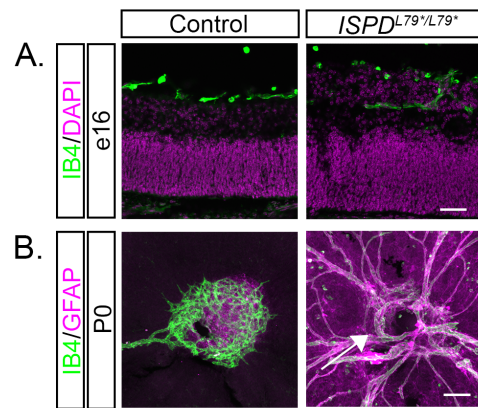
Figure 3: Dystroglycan regulates normal retinal vasculature development.

(A) IB4 labeled hyaloid vasculature is present in the vitreous adjacent to the GCL in control retinas (left) but is embedded within ectopic cell clusters $ISPD^{L79*/L79*}$ (right) retinas at e16. (B) Flat mount retinas at P0 show the emergence of the primary vascular plexus (IB4, green) and astrocytes (GFAP, purple) in controls (left). In $ISPD^{L79*/L79*}$ retinas (right), the emergence of astrocytes and the primary vascular plexus into the retina is delayed (arrow) and there is a persistence of hyaloid vasculature. Scale bar 50 μm A, 100 μm B.
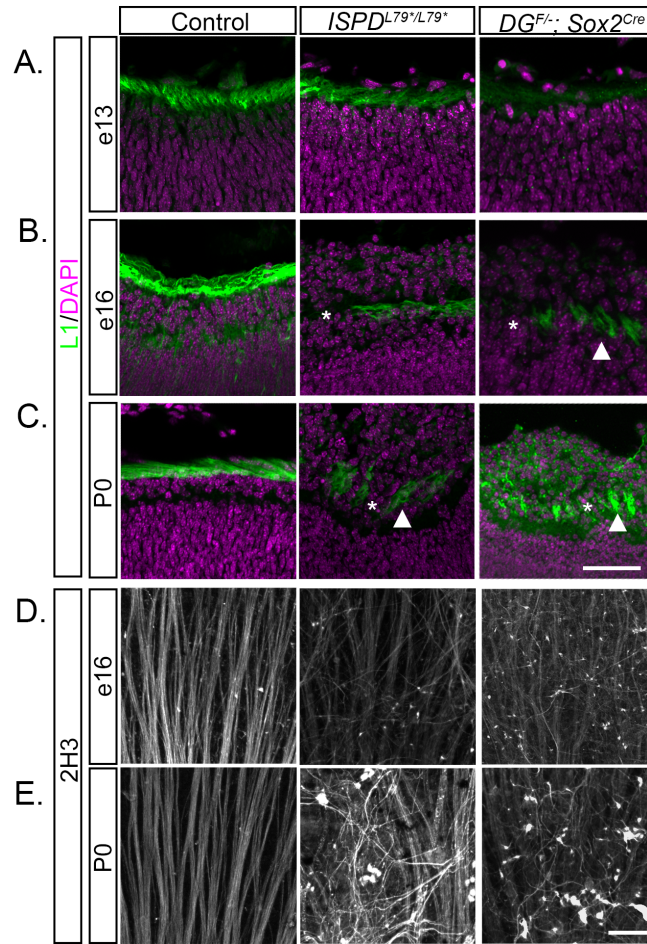
Figure 4

Figure 4: Dystroglycan is required for intraretinal axon guidance, (A) L1 positive axons in the optic fiber layer (OFL) initially appear normal in *ISPD$^{L79*/L79*}$* (middle), and *DG$^{F/-}$; Sox2^{Cre}* retinas (right) at e13. (B, C) As the ILM degenerates in *ISPD$^{L79*/L79*}$* and *DG$^{F/-}$; Sox2^{Cre}* retinas at e16 (B) and P0 (C), axons hyperfasciculate (arrowhead) and exhibit defasciculation (asterisk) within the OFL. (D, E). Flat mount preparations from *ISPD$^{L79*/L79*}$* and *DG$^{F/-}$; Sox2^{Cre}* retinas at e16 (D) and P0 (E) show progressive disruption of axon tracts (Neurofilament, 2H3). Scale bar, 50 μm.

Figure 5

A. *Ai9; Six3^{Cre}*, Tomato, DAPI, e13

	Control	*DG^{F/-}; Six3^{Cre}*
B. β-Dystroglycan		
C. Laminin/2H3/DAPI (P0)		
D. 2H3		
E. IB4/GFAP (P14)		

F. *DG^{F/-}; Six3^{Cre}*, Calbindin, DAPI, P7
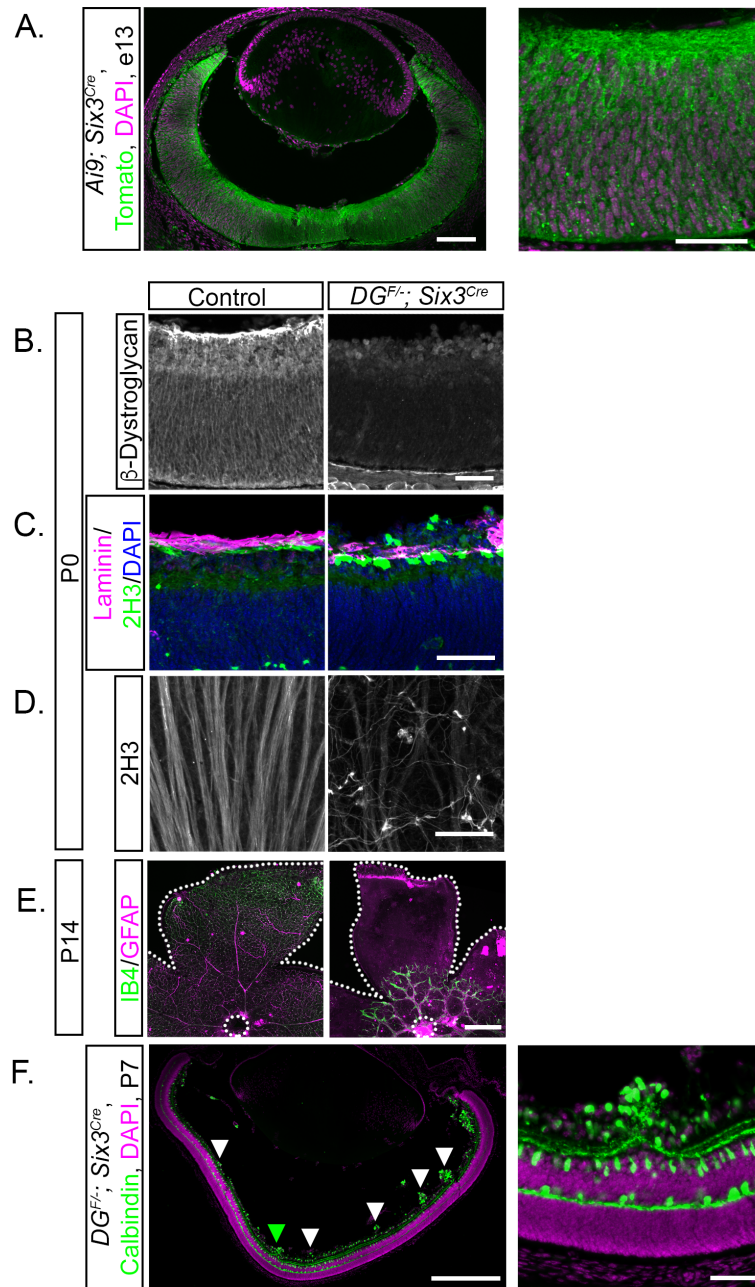
Figure 5: Conditional deletion of *dystroglycan* in the developing retina results in migration and axon guidance defects. (A) Recombination pattern of *Rosa26-lox-stop-lox-TdTomato; Ai9* reporter (green) by *Six3^{Cre}* shows expression throughout the retina and in axons at e13. (B) Dystroglycan protein expression is lost in *DG$^{F/-}$; Six3^{Cre}* mice. (C, D) *DG$^{F/-}$; Six3^{Cre}* (right) mice exhibit inner limiting membrane degeneration (top, purple, laminin) and abnormal axonal fasciculation and guidance (top, green, bottom, 2H3). (E) Primary vascular plexus (IB4, green) and astrocytes (GFAP, purple) migrate from the optic nerve head (dashed circle) to the edge of the retina (dashed line) in control retinas at P14 (right). Vascular and astrocyte migration is stunted in *DG$^{F/-}$; Six3^{Cre}* retinas. (F) Focal migration defects (arrowheads) in P7 *DG$^{F/-}$; Six3^{Cre}* retinas are present across the entire span of the retina. Green arrowhead indicates high magnification image in F (right). Scale bars: A, left panel 100 μm, right panel 50μm; B-D, 50μm; E 500μm; F left panel 500μm, right panel 50μm.
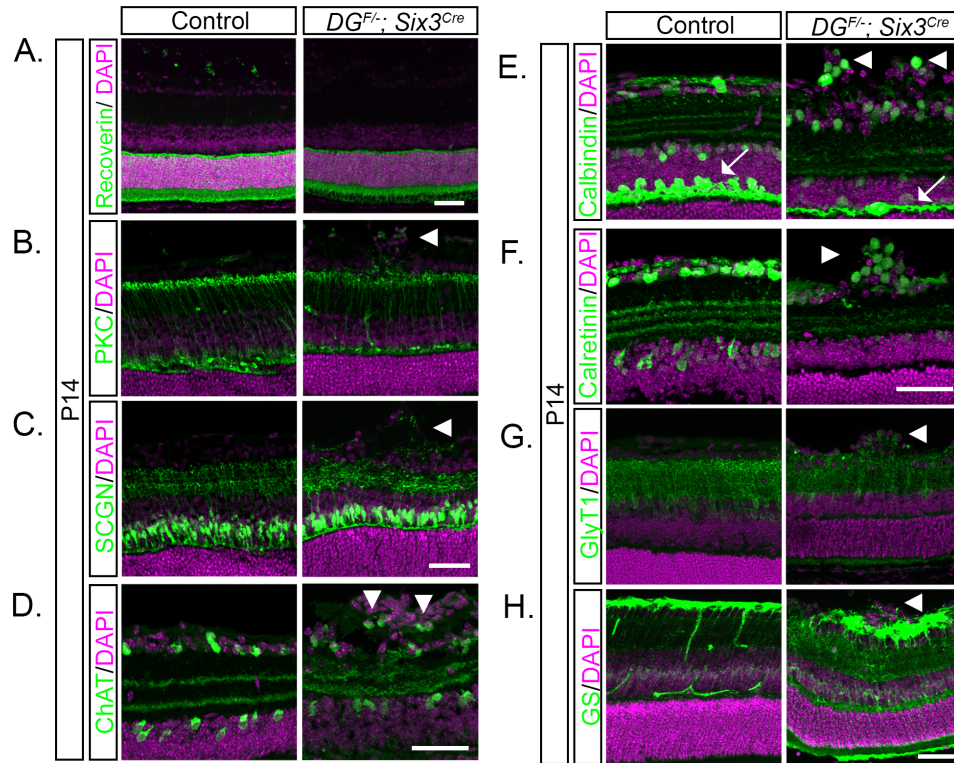
Figure 6

Figure 6: Disrupted postnatal circuit formation in the inner retina of *dystroglycan* mutants. (A) Photoreceptors (recoverin) have normal lamination in P14 $DG^{F/-}$; $Six3^{Cre}$ retinas (right). (B-C) The cell bodies of bipolar cells (PKC, B, SCGN, C) exhibit normal lamination patters, while their axons extend into ectopic cellular clusters in the ganglion cell layer. (D-G) Abnormal cellular lamination and disruptions in dendritic stratification of multiple amacrine and retinal ganglion cell types is observed in $DG^{F/-}$; $Six3^{Cre}$ retinas. (D) ChAT labels starburst amacrine cells, (E) calbindin and (F) calretinin label amacrine and ganglion cells, and (G) GlyT1 labels glycinergic amacrine cells. (H) Müller glia (glutamine synthetase) cell bodies are normally positioned while their inner retinal processes extend into ectopic cellular clusters. Arrowheads indicate axons or cell bodies in ectopic clusters, arrows indicate horizontal cell layer. Scale bar, 50 μm.
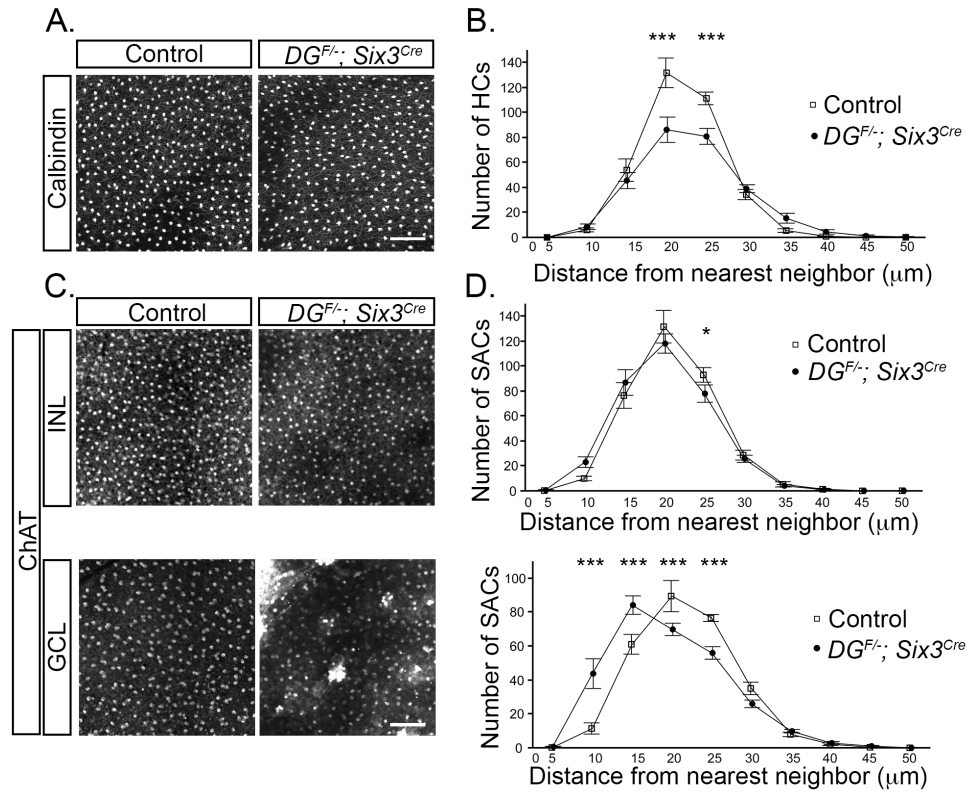
Figure 7

Figure 7: Dystroglycan is required for mosaic cell spacing in the ganglion cell layer. (A, B). Horizontal cells (calbindin) in flat mount P14 adult retinas have reduced cellular density, but normal mosaic cell spacing curves (Nearest neighbor analysis, $p < 0.0001$, Two-Way ANOVA, Tukey HSD post-hoc test ***$p < 0.0001$, n=20 samples from 5 control retinas, 18 samples from 5 mutant retinas). (C, D) Mosaic cell spacing of starburst amacrine cells (ChAT) in the inner nuclear layer is normal (Nearest neighbor analysis, Two-Way ANOVA, Tukey HSD post-hoc test *$p = 0.0494$, n=10 samples from 3 control retinas, 10 samples from 3 mutant retinas), while the ectopic clustering of starburst amacrine cells in the ganglion cell layer results in a significant disruption of mosaic spacing (Nearest neighbor analysis, $p < 0.0001$, Two-Way ANOVA, Tukey HSD post-hoc test ***$p < 0.0001$, n=10 samples from 3 control retinas, 10 samples from 3 mutant retinas). Scale bar 100μm.
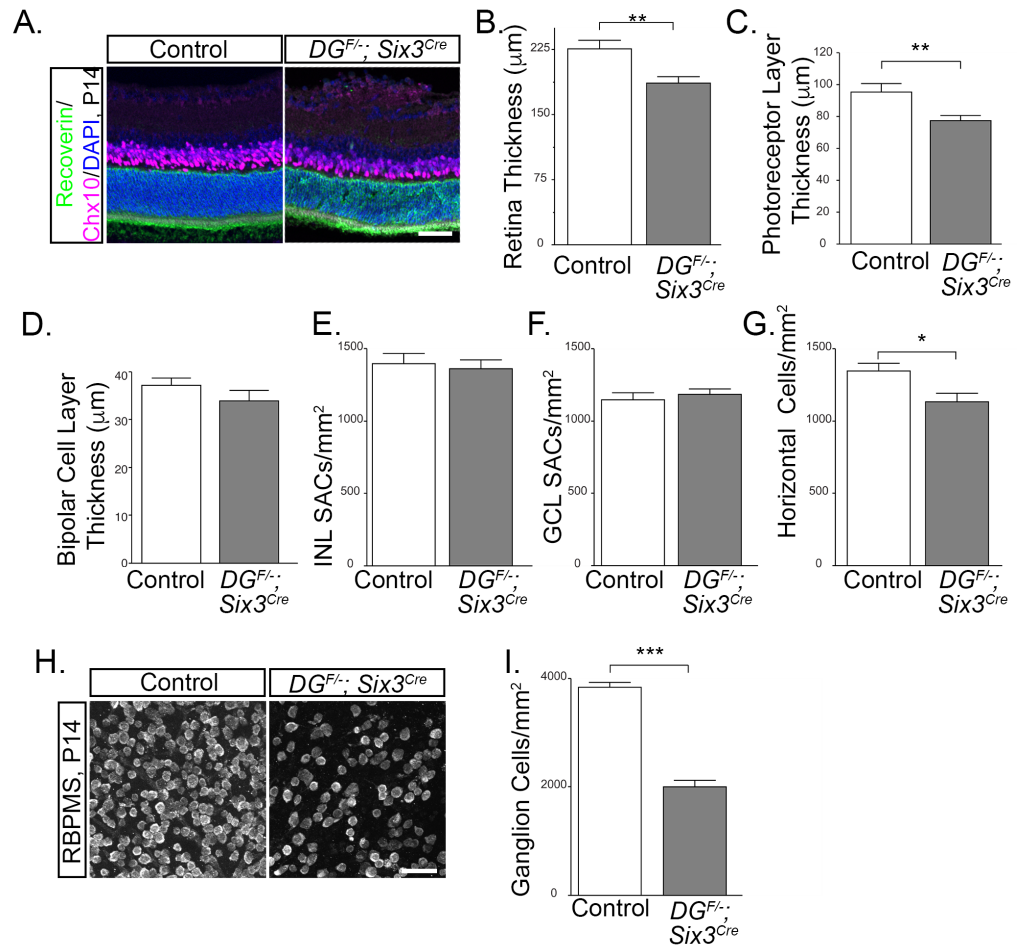
Figure 8

Figure 8: Retinal thinning in *dystroglycan* mutants. (A-D) P14 $DG^{F/-}$; $Six3^{Cre}$

retinas show decreased retinal thickness (DAPI, p=0.0039, t test, n=7 control, 7

mutant), a decreased thickness of the photoreceptor layer (C, Recoverin, green,

p=0.0163, t-test, n=7 control, 7 mutant) and no change in thickness of the bipolar

cell layer (D, Chx10, purple, p>0.05, t-test, n=7 control, 7 mutant). Starburst

amacrine cell density is normal in both the INL (E, p>0.05, t-test, n=10 samples

from 3 control retinas, 10 samples from 3 mutant retinas) and GCL (F, p>0.05, t-

test, n=10 samples from 3 control retinas, 10 samples from 3 mutant retinas),

while horizontal cells show a slight reduction in cell density (G) in P14 $DG^{F/-}$;

$Six3^{Cre}$ retinas (p=0.0112, t test, n=20 samples from 5 control retinas, 18 samples

from 5 mutant retinas). (H, I) Ganglion cell density (RNA binding protein with

multiple splicing, RBPMS) is reduced by approximately 50% in P14 $DG^{F/-}$; $Six3^{Cre}$

retinas (p<0.0001, t-test, n=12 samples from 3 control retinas, 12 samples from 3

mutant retinas). Scale bar 50 μm.

Figure 9

A.
	Control	ISPD$^{L79*/L79*}$
PH3/DAPI	e13	
	e16	

B.
e13   e16

PH3 positive cells

Control ISPD$^{L79*/L79*}$ Control ISPD$^{L79*/L79*}$

C.
Cleaved Caspase-3, P0

| Control | ISPD$^{L79*/L79*}$ | DG$^{F/-}$; Six3^{Cre} |

D.
e16

Caspase positive cells/mm^2

***   ***   P0   **   P0

Control ISPD$^{L79*/L79*}$ Control ISPD$^{L79*/L79*}$ Control DG$^{F/-}$; Six3^{Cre}
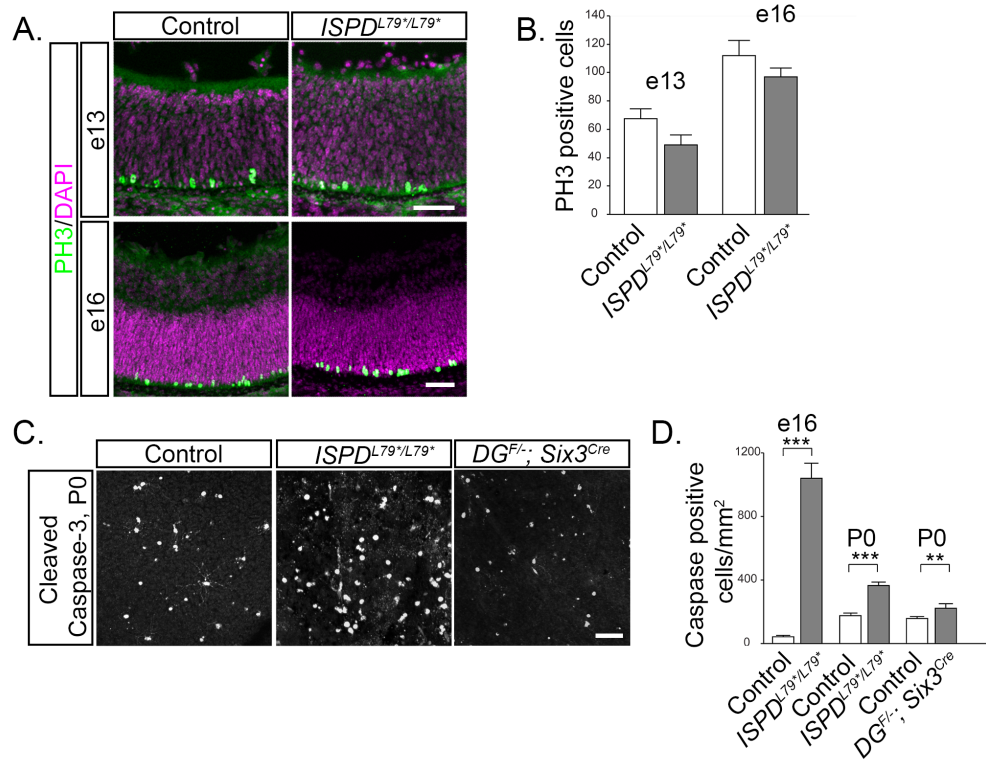
Figure 9: Loss of dystroglycan results in increased developmental cell death. (A) Immunohistochemistry for mitotic cells (PH3) at e13 (top) and e16 (bottom) shows normally positioned mitotic retinal progenitor cells adjacent to the RPE. (B) Quantification of mitotic cells shows no difference between control and ISPD$^{L79*/L79*}$ mutants (p>0.05, t test, n=4 control and 4 mutant retinas at e13, p>0.05, t test, n=4 control and 4 mutant retinas at e16). (C-D) Immunohistochemistry for cleaved caspase-3 in a flat mount preparation of P0 *DG$^{F/-}$; Six3^{Cre}* retinas shows an increase in apoptotic cells. (p=0.0279, t test, n=18 samples from 6 control retinas, 17 samples from 6 mutant retinas). (D) Quantification of cleaved caspase-3 positive cells shows an increase in apoptotic cells at e16 (p<0.0001, t test, n=18 samples from 6 control retinas, 18 samples from 8 mutant retinas) and P0 (C, D p<0.0001, t test, n=18 samples from 6 control retinas, 15 samples from 5 mutant retinas) between control (left) and *ISPD$^{L79*/L79*}$* (middle) retinas. Scale bar 50 μm.
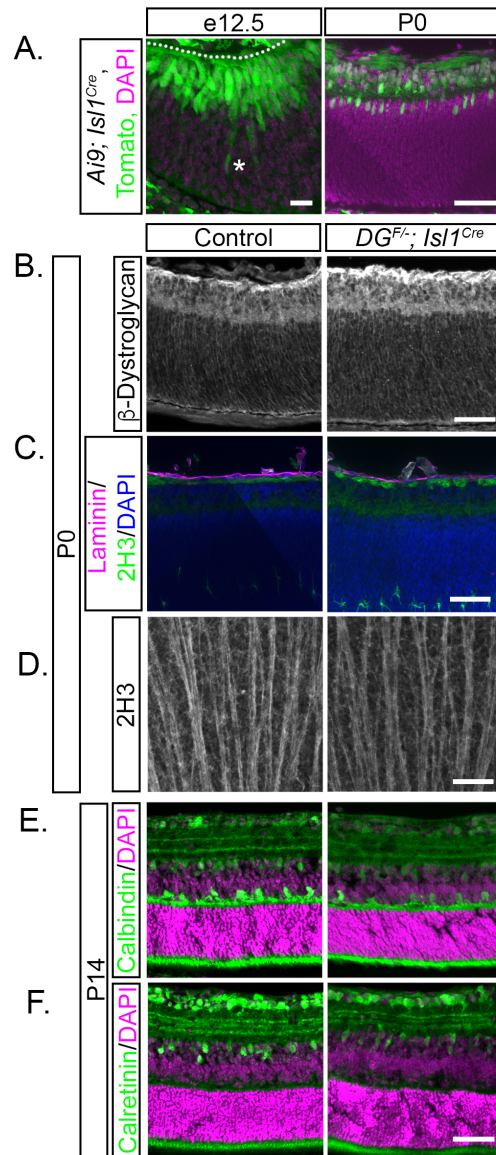
Figure 10

Figure 10: Dystroglycan is not required within RGCs for their migration and axon outgrowth. (A) Recombination pattern of *Rosa26-lox-stop-lox-TdTomato; Ai9* reporter (green) by *Isl1^Cre* by shows expression the majority of differentiated ganglion cells at e12.5 (left) and P0 (right). (B) Dystroglycan expression at the ILM is unchanged between control and *DG^F/-; Isl1^Cre* retinas. (C) The ILM (laminin, purple) and axons in the OFL (2H3, green) in *DG^F/-; Isl1^Cre* retinas appear similar to control. (D) Flat mount preparations show normal axon fasciculation (2H3) in *DG^F/-; Isl1^Cre* retinas. (E-F) *DG^F/-; Isl1^Cre* (right panel) retinas (P14) have normal cellular lamination and dendritic stratification. Dashed line indicates ILM. Asterisk notes a differentiated ganglion cell body that is still migrating toward the ILM. Scale bar 20 μm A left panel, scale bar 50 μm A right panel, B-F.

Figure 11
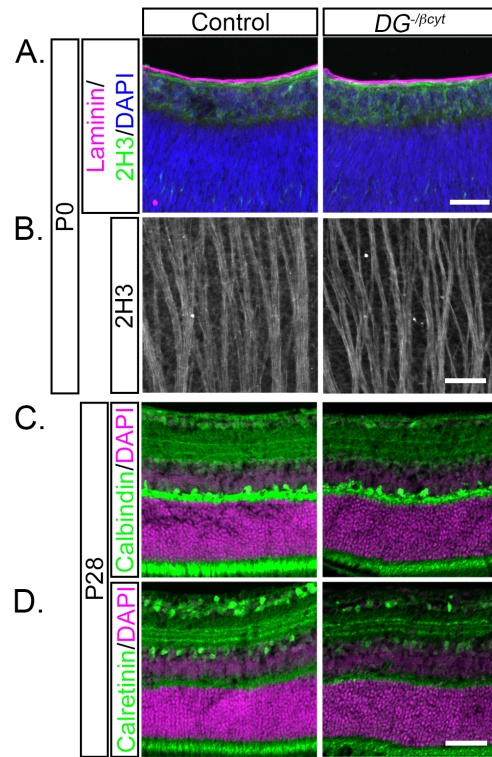
Figure 11: The intracellular signaling domain of dystroglycan is not required for proper retinal development. (A) ILM integrity (laminin, purple), neuronal migration (DAPI, blue) and axon outgrowth (2H3, green) all appear normal in mice lacking the intracellular domain of dystroglycan ($DG^{-/\beta cyt}$) at P0. (B) Flat mount preparations show normal axon fasciculation (2H3) in $DG^{-/\beta cyt}$ retinas. (C-D) $DG^{-/\beta cyt}$ retinas (P28) have normal cellular lamination and dendritic stratification. Scale bar, 50 μm.
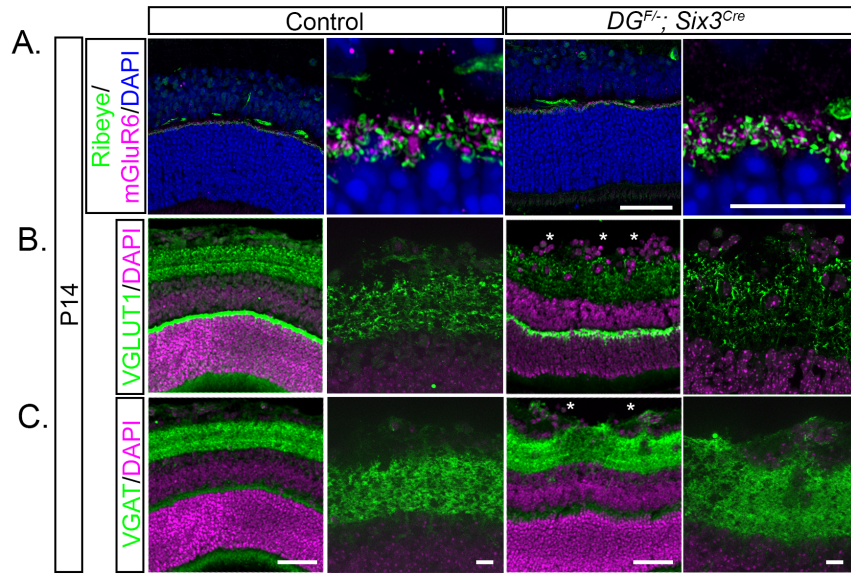
Figure 12

Figure 12: Synaptic markers are present in the retina of *dystroglycan* mutants. (A) Markers for outer retinal ribbon synapses (Ribeye, presynaptic and mGluR6, postsynaptic) appear structurally normal in the absence of dystroglycan. The density of (B) excitatory (VGLUT1) and (C) inhibitory (VGAT) presynaptic markers appear similar to control in the inner retinas of $DG^{F/-}; Six3^{Cre}$ mutants.   Synapses are also present within ectopic clusters (asterisks). Scale bar, 50 μm wide view, scale bar,10 μm enlarged view.

Figure 13

A.

DG^{F/+}; Six3^{Cre}, P1

0   900   1800   2700

3600   4500   5400   6300

B.

DG^{F/-}; Six3^{Cre}, P1

0   900   1800   2700

3600   4500   5400   6300

C.

D.

85
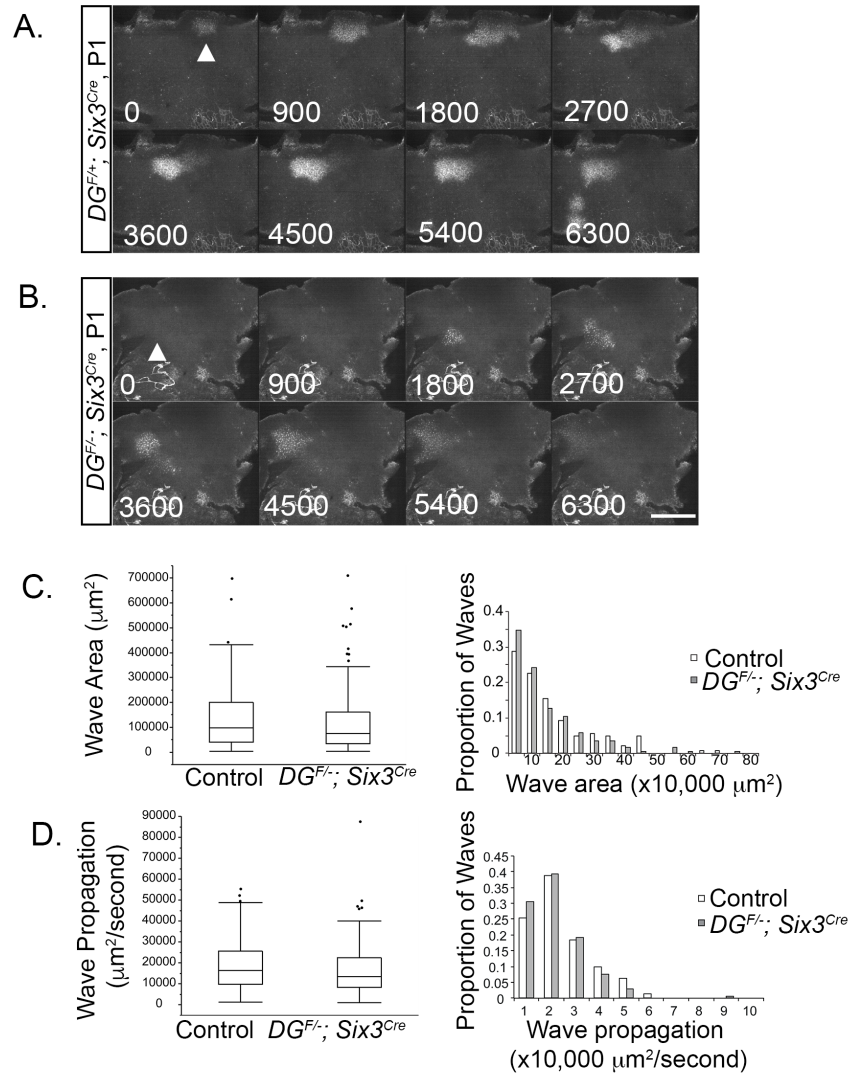
Figure 13: Dystroglycan is dispensable for the generation and propagation of retinal waves. (A-B) At P1, waves propagate normally across the retina in $DG^{F/+}$; $Six3^{Cre}$; $R26$-LSL-$GCaMP6f$ (A) and DG^{F-}; $Six3^{Cre}$; $R26$-LSL-$GCaMP6f$ mice (B). (C) Distributions of wave areas show no difference between controls and mutants (Wilcoxon rank sum test, p>0.05). (D) Wave propagation rate is slightly slower in mutant retinas (Wilcoxon rank sum test, p=0.0493). Wave parameters were calculated from 142 control waves obtained from 6 retinas from 3 control mice and 173 mutant waves obtained from 8 retinas from 5 mutant mice. Arrowheads indicate the initiation site of a retinal wave. Scale bar 500 μm. Time displayed in milliseconds.

Movie 1
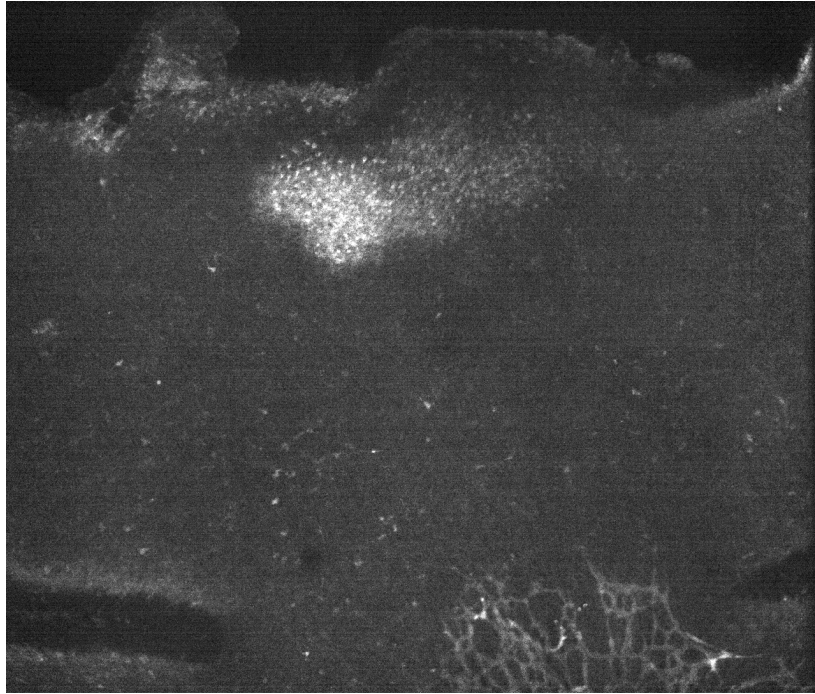
Movie 1: Retinal waves in *DG^{F/+}; Six3^{Cre}; R26-LSL-GCaMP6f* mice. 15frames/sec, total of 21 frames

Movie 2
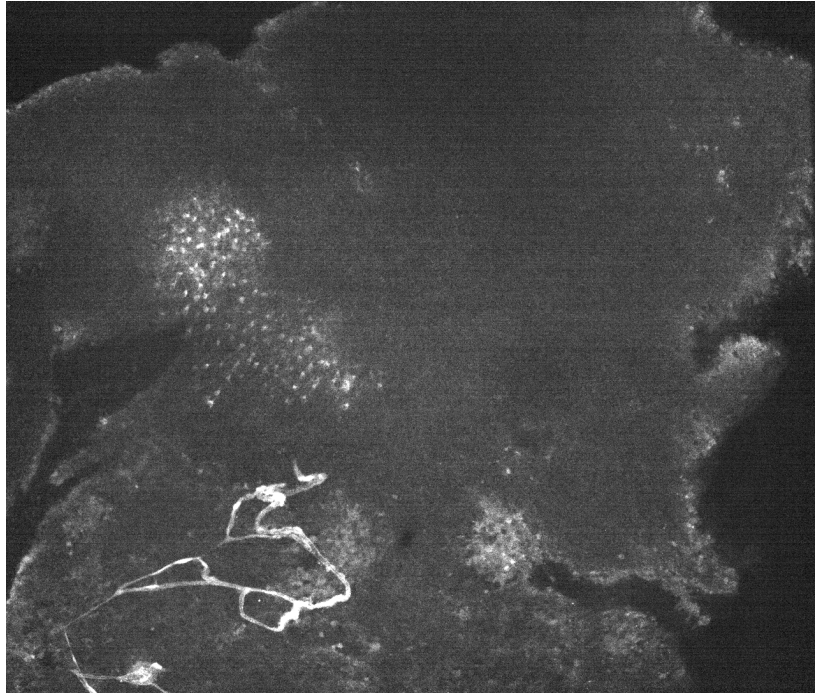
Movie 2: Retinal waves in *DG^{F/-}; Six3^{Cre}; R26-LSL-GCaMP6f* mice. 15frames/sec, total of 21 frames

Supplemental Figure 1
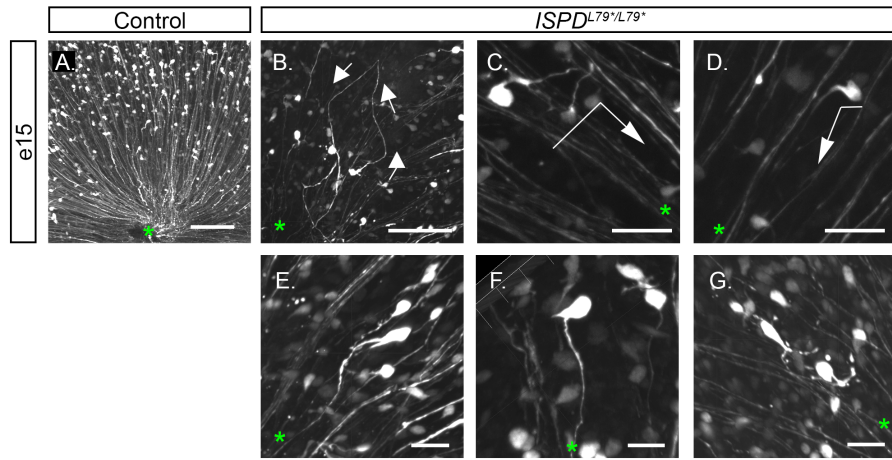
Supplemental Figure 1: Axon growth defects in *ISPD*$^{L79*/L79*}$ retinas are revealed by single cell labeling. (A) RGCs sparsely labeled with the Hb9-GFP reporter in controls show cell bodies with a single axon oriented and growing towards the optic nerve head. (B-D) In *ISPD*$^{L79*/L79*}$ mutants, RGCs exhibit axon orientation and extension defects. Some RGCs extend an axon away from and then back towards the optic nerve head (B). Other axons are initially mispolarized but regain an appropriate growth trajectory when they encounter a cluster of appropriately-oriented axons. Direction of axon growth indicated by arrows. (E-G) RGCs in mutant retinas show formation and stabilization of multiple axons or primary neurites. These neurites may all point towards the optic nerve head (E), or some combination of towards and away from the optic nerve head (F, G). Asterisk in each image marks direction of optic nerve head. Scale bars: A, B, 100μm; C-G, 30 μm.

Supplemental Figure 2
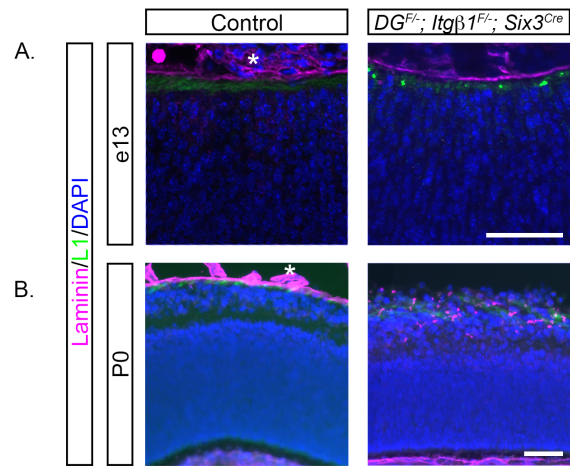
Supplemental Figure 2: The inner limiting membrane forms and degenerates in *dystroglycan, β1 Integrin* mice. (A) At e13, the ILM forms normally in *DG^F/-^; ItgB1^F/-^; Six3^Cre^* retinas. (B). At P0, the ILM has degenerated and retinal neurons have migrated into the vitreous. Asterisks indicate blood vessel staining. Scale bar, 50μm.

Table 1: Antibodies

Target	Host species	Dilution	Company/ origin	Catalog #	RRID
2H3	mouse	1:1000	DSHB	2h3	AB_531793
β-Dystroglycan	mouse	1:500	DSHB	MANDAG2 (7D11)	AB_2618140
β-Dystroglycan	rabbit	1:100	Santa Cruz Biotech	sc-28535	AB_782259
Calbindin	rabbit	1:10,000	Swant	CB 38	AB_10000340
Calretinin	rabbit	1:10,000	Swant	CG 1	AB_2619710
ChAT	goat	1:500	Millipore	AB144P-200UL	AB_11214092
Chx10	goat	1:500	Santa Cruz Biotech	sc-21690	AB_2216006
Cleaved Caspase-3	rabbit	1:500	Cell Signaling	9661S	AB_2341188
Collagen IV	goat	1:250	Southern Biotech	1340-01	AB_2082646
Glutamine Synthetase	mouse	1:1000	BD Biosciences	610517	AB_397879
GlyT1	rabbit	1:800	gift from Dr. David Pow		
IB4		1:250	Life Technologies	I21411	AB_2314662
L1	rat	1:500	Millipore	MAB5272	AB_2133200
Laminin	rabbit	1:1000	Sigma	L9393	AB_477163
MGluR6	sheep	1:100	gift from Dr. Catherine Morgans		
Perlecan	rat	1:500	Millipore	MAB1948P	AB_10615958
PH3	Rat	1:250	Abcam	Ab10543	AB_2295065
PKC	mouse	1:500	Sigma	P5704	AB_477375
RBPMS	guinea pig	1:500	Phospho Solutions	1832-RBPMS	AB_2492226
Recoverin	rabbit	1:200	Millipore	AB5585	AB_2253622
Ribeye/Ctbp2	mouse	1:1000	BD Biosciences	612044	AB_399431
Secretagogin	rabbit	1:4000	Biovendor	rd181120100	AB_2034060
VGAT	rabbit	1:500	Synaptic Systems	131-003	AB_887869
VGLUT1	guinea pig	1:500	Millipore	AB5905	AB_2301751

Table 1: List of Antibodies. Antibodies utilized throughout the study, including target, host species, dilution, manufacturer, catalog number and RRID.

Chapter 2

Dystroglycan at the Optic Chiasm Determines Retinal Ganglion Cell Axon Targeting to the Brain

Reena Clements[1] and Kevin M. Wright[1,2]

1) Neuroscience Graduate Program, 2) Vollum Institute, Oregon Health & Science University, Portland, OR 97239, USA

This chapter is in preparation to be published as a short format journal article.

Extended figures will not be submitted for peer review.

Abstract

During neural development, neurons extend axons to synapse with downstream targets. Several molecules have been implicated in guiding axons in the developing visual system, but the role of extracellular matrix molecules in this process remains poorly understood. Additionally, postnatal axon guidance to visual targets when there are guidance defects at the optic chiasm has not been well studied. Dystroglycan is a laminin-binding, cell-surface protein important for formation and maintenance of the extracellular matrix and basement membranes and which has previously been implicated in axon guidance. To study how the loss of the structure and components of the extracellular matrix affects axon guidance in the visual system, we use two genetic models of functional dystroglycan loss, $ISPD^{L79*/L79*}$, and $DG^{F/-}; Six3^{Cre}$. We found that dystroglycan maintenance of laminin at the optic chiasm is necessary for correct contralateral and ipsilateral axon sorting. However, missorted axons still correctly target the retinorecipient brain regions, and these inappropriate projections persisted in adult mice even after axon pruning was complete. Our results highlight the importance of the extracellular matrix for axon sorting at an intermediate choice point in the developing visual circuit.

Introduction

The development of neural circuits is dependent on neurons establishing precise connectivity during development. One aspect of circuit formation is axon guidance, in which neurons extend axons long distances to synapse with appropriate downstream targets. In the mammalian visual system, the axons of

95

retinal ganglion cells (RGCs) leave the retina and cross the optic chiasm in the ventral forebrain *en route* to multiple retinorecipient areas of the brain. RGC axons terminate and synapse in two visual-forming brain regions, the lateral geniculate nucleus (LGN) and the superior colliculus (SC), as well as in non-image forming brain regions, including the suprachiasmatic nucleus (SCN), olivary pretectal nucleus (OPN), nucleus of the optic tract (NOT) and medial terminal nucleus (MTN) (Zhang et al., 2017).

Axon guidance to target regions is dependent on numerous short- and long-range secreted cues. Slits are responsible for keeping axons confined within fasciculated tracts at the optic chiasm (Plump et al., 2002), while axon crossing is regulated by local EphrinB2/EphB1 signaling (Williams et al., 2003) and remote Shh signaling (Peng et al., 2018). In the brain, projections of functionally distinct RGCs are guided by molecular cues to specific but different regions of the visual system. For example, the molecular cues Cadherin-6, EphrinA2, and EphrinA5 have been shown to play a role in RGC guidance to the LGN (Feldheim et al., 1998; Osterhout et al., 2011). In the SC, the axons of off-αRGCs are restricted to lower lamina (Huberman et al., 2008b), while the axons of the on-off direction selective ganglion cells project to the superficial lamina (Sun et al., 2015). Numerous factors such as EphBs, EphrinAs, EphrinBs, Sema3D, and Wnt3 contribute to retinotopic mapping in the SC (Erskine and Herrera, 2007), while specific molecular cues responsible for normal axonal targeting to the SC are less understood. Interestingly, Reelin, an extracellular matrix (ECM) molecule, has been shown to direct guidance into the LGN (Su et al., 2011), raising the

possibility that proteins other than traditional axon guidance cues may play a role in axonal targeting.

Basement membranes, which consist of ECM proteins such as laminin, are crucial for providing scaffolds in the developing nervous system. In the cortex, disruption of the basement membrane leads to detachment of radial glial endfeet and failure of neurons to migrate into normal cortical layers, causing lissencephaly. Dystroglycan is responsible for stabilizing laminin in basement membranes, and loss of functional dystroglycan causes profound neuronal migration defects in the developing brain and retina (Clements et al., 2017; Wright et al., 2012). Recently, dystroglycan was also shown to regulate axon guidance in the spinal cord by localizing the axon guidance cue Slit in the basement membrane (Wright et al., 2012). However, little is known about how the ECM contributes to axon guidance during development. Here, we describe how the loss of dystroglycan from the optic chiasm disrupts ipsilateral and contralateral axon sorting and results in inappropriate innervation of visual target regions in the brain.

Materials and Methods

Animals

Animal procedures were approved by the OHSU Institutional Animal Care and Use Committee and conformed to the National Institutes of Health *Guide for the care and use of laboratory animals*. Embryonic day 0 (e0) was the day of vaginal plug observation and postnatal day 0 (P0) was the day of birth. Animals were euthanized with CO_2. Controls were *ISPD*$^{+/L79*}$, and *DG*$^{F/+}$; *Six3*^{Cre} or *DG*$^{F/+}$

age matched littermates. *ISPD^(L79*/L79*)* (Wright et al., 2012) and *DG^(F/F)* (Moore et al., 2002) mice and genotyping have been described previously. Generic cre primers were used for *Six3^(Cre)* (Furuta et al., 2000) and *Isl1^(Cre)* (Yang et al., 2006) genotyping.

Statistical Analysis

All analysis was performed on n≥3 mice from at least two litters. Statistics were conducted using JMP Pro 13.0 software (SAS Institute). A Student's t-test was used to compare means of two groups, and an ANOVA with Tukey post-hoc test was used to compare means of two or more groups. A significance threshold of 0.05 was used for all statistical tests. * indicates $p<0.05$; ** indicates $p<0.01$; *** indicates $p<0.001$.

Labeling and Analysis of the Optic Chiasm

DiI injections were performed at e13 and P0. Animals were decapitated and heads were fixed in 4% PFA at 4°C overnight. The left eye was enucleated and a crystal of DiI approximately the size of the optic disc was placed inside the optic disc. Low melting point 2.5% agarose was placed into the eyecup to hold the crystal in place. Heads were incubated at 37°C for three days at e13, one week at P0. Projections were visualized by removing the lower jaw, tongue, and palate. Images were acquired on a Zeiss AxioZoom.V16.

Analysis of DiI projections at P0 (Figure 1) was conducted by tracing the area of the projections in FIJI and dividing by the total area of all projections for each mouse.

Labeling and Analysis of Retinorecipient Brain Regions

Cholera Toxin Subunit B (CTB) injections to label anterograde axonal projections were performed at P0 or P1 for P2 analysis, at P0-P4 for P10 analysis, and at P26 for P28 analysis. Mice between P0-P4 were anesthetized on ice, and mice aged P26 were anesthetized with isofluorane. Glass capillary needles were backfilled with CTB conjugated to Alexa-488 or Alexa-555. The right eye was injected with CTB-488 and the left eye was injected with CTB-555. Injections were performed using a picospritzer injecting for 15 milliseconds at 30 PSI. At P2 or P10, brains were removed and drop fixed in 4% PFA at 4°C overnight. At P28, animals were perfused, and brains were post-fixed in 4% PFA at 4°C overnight. Whole mount images of the superior colliculus were obtained prior to fixation on a Zeiss AxioZoom.V16. After fixation, brains were washed in PBS for 30 minutes, embedded in 2.5% low melting point agarose, and sectioned on a vibratome at 150 μm. Sections were incubated in DAPI overnight and mounted using Fluoromount medium. Brain sections were imaged on a Zeiss Axio Imager M2 upright microscope equipped with an ApoTome.2. Analysis of superior colliculus misprojections (Figure 4) was conducted on whole mount colliculus images by tracing the regions with inappropriate ipsilateral projections, adding to determine total area, and dividing by the area of the superior colliculus.

A threshold-dependent analysis method was used to determine the proportion of contralateral and ipsilateral projections to the dLGN based on previously described methods (Jaubert-Miazza et al., 2005). Briefly, the region corresponding to the LGN was thresholded in FIJI to determine the pixels that

corresponded to contralateral signal and ipsilateral signal. Threshold values were the same between corresponding contralateral and ipsilateral images. The total area of pixels in each image, and the overlap between the two areas, was measured.

A threshold-independent method was utilized to confirm results and analyze segregation between contralateral and ipsilateral projections (Torborg and Feller, 2004). We applied a rolling ball filter of 200 pixels to the LGN to subtract background. The logarithm of the intensity ratio (R) was calculated for each pixel to compare the intensity of ipsilateral (F_I) and contralateral (F_C) fluorescence, where $R = \log_{10}(F_I/F_C)$. This generates a distribution of R-values for each LGN image. We then computed the variance for each R-distribution. Smaller variances reflect greater overlap, and less segregated axonal input, whereas larger variances reflect decreased overlap and more segregated axonal input.

Brains containing fluorescent markers to detect cre expression in retinorecipient brain regions were processed the same way as brains injected with CTB.

Retrograde CTB Injection

To trace projections from the superior colliculus to the retina, retrograde CTB injections were performed. CTB was prepared as described for retina injections. Mice at P0 were anesthetized on ice and CTB 555 was injected into the left superior colliculus through the skull. Injections were performed using a picospritzer injecting for 60 milliseconds at 2 PSI. Three injections were made

into the rostromedial, caudomedial, and caudolateral regions of the superior colliculus. At P2, brains were dissected and the superior colliculus imaged to ensure full CTB fill and no leakage into the right superior colliculus. Retinas were flat mounted and imaged for retrograde projections.

Immunohistochemistry

Embryos to be used for immunohistochemistry were decapitated and fixed in 4% PFA at 4°C overnight. Tissue was washed in PBS for 30 minutes and equilibrated in 15% sucrose at 4°C overnight. Tissue was flash frozen in embedding media and sectioned at 20 μm on a cryostat. Sections were blocked with PBS containing 2% Normal Donkey Serum and 0.2% Triton for 30 minutes, and incubated in antibody diluted in this solution at 4°C overnight. Tissue was washed for 30 minutes and incubated in secondary antibody diluted in a PBS solution containing 2% Normal Donkey Serum for 2-4 hours. Tissue was incubated in PBS containing DAPI for 10 minutes, washed in PBS for 20 minutes, and mounted using Fluoromount medium. Sections were imaged on a Zeiss Axio Imager M2 upright microscope equipped with an ApoTome.2. Preparation of P0 retinas (Supplemental Figure 2) was performed as previously described (Clements et al., 2017). Antibody information is contained in Table 1.

<u>**Results and Discussion**</u>

Dystroglycan is required for axon sorting at the optic chiasm

In the mouse, after they exit the retina, approximately 95% of RGC axons cross at the optic chiasm (Petros et al., 2008). At e13, axons only make a contralateral projection (Figure 1A, green), with the ipsilateral projection (Figure

1A, blue) forming from e14-e17 (Petros et al., 2008). Previous work using the *ISPD^{79*/79*}* model, in which dystroglycan cannot bind to laminin or other ECM proteins due to loss of glycosylation, has shown intraretinal axon guidance defects due to loss of the retinal ILM and crossing defects of sensory axons in the spinal cord (Clements et al., 2017; Wright et al., 2012). We used this model to test whether similar axon guidance defects occur at the optic chiasm. DiI injections at e13 showed a normal, contralateral projection in controls (Figure 1B). In mutants at e13, we observed stalling of axons at the chiasm, a failure of all axons to project into the contralateral optic tract, and an early projection into the ipsilateral optic tract (Figure 1B). In control animals at P0, approximately 80% of axons project contralaterally, and 20% of axons project ipsilaterally. In mutants, while axons do eventually exit the chiasm, approximately 50% of axons make a contralateral projection, and the remainder of the axons are evenly split between projecting ipsilaterally and projecting to the contralateral eye (Figure 1C, D, ANOVA, Tukey HSD *post hoc* test, p<0.01).

We hypothesize that there is some developmental abnormality at e13 that makes initial axon trajectory through the chiasm stall. In chiasm cross sections stained for laminin (Figure 1 E, G) and axons (L1, Figure 1 F, G), controls show continuous laminin in the basement membrane with fasciculated bundles of axons growing along it. In *ISPD^{79*/79*}* mutants at e13, laminin in the basement membrane has become discontinuous, and axon bundles defasciculate and some fibers appear to grow inappropriately into the ventral forebrain. Additional basement membrane component proteins such as Perlecan (Supplemental

Figure 1B, D) and Collagen IV (Supplemental Figure 1C, D) colocalize with laminin (Supplemental Figure 1A, D) and also exhibit disruptions and discontinuity at the chiasm in mutants at e13. Radial glia at the midline are intact in mutants at e13 (Figure 1H), revealing that there is no structural defect at the chiasm that might cause axonal misrouting. These initial observations suggest that dystroglycan plays a role as an adhesion receptor to concentrate laminin in the basement membrane as an axonal growth substrate.

Additional genetic tools may be utilized to study axon dynamics during an encounter with a broken basement membrane at the chiasm. Previous reports have shown that axons exhibit various growth cone dynamics depending on their trajectory at the chiasm. Growth cones classified as simple are long and streamlined with few filopodial processes. These axons are actively growing and represent the contralateral projection. In contrast, axons that pause or turn exhibit complex growth cone dynamics, which are more circular with many filopodial processes. These growth cones represent axons making an ipsilateral projection (Godement et al., 1994; Marcus et al., 1995). The Hb9-GFP transgenic mouse labels a subset of RGCs (Duan et al., 2014). We can utilize this mouse to label RGCs and their axons as they traverse the optic chiasm. In sections at e13 in controls, we can trace axons from the retina to the optic chiasm (arrowheads, Extended Figure 1A). Within the chiasm, we observe axons with both complex (Extended Figure 1B) and simple (Extended Figure 1C) growth cone dynamics. This tool may be utilized to study growth cone dynamics *in vivo* in *ISPD*$^{79*/79*}$ mutants. Specifically, observing an increased proportion of complex growth

cones at e13 would indicate that more axons were either stalled or projecting ipsilaterally. Our data using DiI injections also cannot tell us what proportion of axons that stall at the chiasm at e13 remain stuck, and what proportion eventually exit. Using a sparse RGC label such as the Hb9-GFP will allow us to conduct further experiments to address this question. Specifically, we have previously shown that there is extensive apoptosis of $ISPD^{79*/79*}$ RGCs in the retina that begins earlier than the normal window of cell death (Clements et al., 2017). This previous data leads us to hypothesize that RGCs die in the retina because their axons remain stuck at the chiasm and never make it to appropriate targets.

Dystroglycan functions at the optic chiasm to stabilize the basement membrane as an axonal growth substrate

To test whether the crossing phenotype we observed is due to loss of dystroglycan, and not ISPD off target effects, we generated $DG^{F/-}; Six3^{Cre}$ mice to delete dystroglycan in the retina and ventral forebrain. To verify the cre expression pattern, we bred a *R26-LSL-H2B:mCherry* reporter to the $Six3^{Cre}$ driver. Cre is expressed in all retinal progenitor cells in the retina (Figure 2A), consistent with previous reports (Furuta et al., 2000), as well as in cells surrounding the optic chiasm in the ventral forebrain (asterisk, Figure 2B). $DG^{F/-};$ $Six3^{Cre}$ mice recapitulate the phenotypes observed in $ISPD^{79*/79*}$ mice. At the optic chiasm at P0, we observe apparent axon stalling but eventual exit from the chiasm (Figure 2C). In control chiasm sections at e15, there is a continuous basement membrane of laminin on which axons grow (Figure 2D, F). In mutant

mice, the laminin-rich basement membrane is lost (Figure 2D, F), and axons begin to inappropriately invade the ventral forebrain (Figure 2E, F).

Our initial phenotypic observations show axon sorting defects and basement membrane breakdown at the optic chiasm. The phenotype could be due solely to dystroglycan's role in binding to and stabilizing laminin at basement membranes. Alternatively, the phenotype may be the result of dystroglycan function in the retina, as previous work has shown severe defects in retinal development due to loss of dystroglycan (Clements et al., 2017). In order to these possibilities, we utilized several approaches.

In addition to dystroglycan, β1-Integrin is also a laminin receptor. A previous study characterizing a β1-Integrin mutant showed defects in retinal development but no crossing defects at the optic chiasm (Riccomagno et al., 2014). One possibility is that deleting β1-Integrin and dystroglycan together enhances the phenotype we observe in single *dystroglycan* null mice. We generated a *DG$^{F/-}$; Itgβ1 $^{F/-}$; Six3^{Cre}* mouse to test this question. In controls at P0, we observe a normal large contralateral projection and small ipsilateral projection (Extended Figure 2A). Heterozygous mice that lack *dystroglycan* and do not conditionally knock out β1-Integrin (Extended Figure 2B) present with an indistinguishable phenotype from double conditional knockouts (Extended Figure 2C), which includes a bigger ipsilateral projection and projections to the contralateral eye. Therefore, dystroglycan function by itself is sufficient to cause axonal sorting defects at the optic chiasm.

To test the role of dystroglycan function in the retina, we first generated a $DG^{F/-}$; $Isl1^{Cre}$ conditional knockout mouse, in which dystroglycan is deleted in RGCs, but only some cells in the ventral forebrain (Pan et al., 2008b). Cre recombination shows expression in cell bodies (Supplemental Figure 2A, left panel) of RGCs and in their axons at the chiasm (asterisk, Supplemental Figure 2A). A whole mount view of the chiasm labeled with DiI at P0 did not reveal any differences in axon crossing between controls and mutants at P0 (Supplemental Figure 2B). Based on our previous work showing that the retinal inner limiting membrane is normal in $DG^{F/-}$; $Isl1^{Cre}$ conditional knockout animals (Clements et al., 2017), we predict that the chiasm basement membrane is also normal.

Because of the presence of an early ipsilateral projection in mutants, we next focused on whether the molecular cues that specify this projection are intact. At the chiasm, radial glia express EphrinB2, a repulsive axon guidance cue. Axons that project ipsilaterally at the chiasm express EphB1, the receptor for EphrinB2. When they reach the chiasm, they are repulsed, causing them to enter the ipsilateral optic tract instead of crossing at the chiasm (Petros et al., 2008). Cells in the ventrotemporal retina form the ipsilateral projection and are specified by the transcription factor Zic2 (Herrera et al., 2003). In the mutant retina, immunostaining for Zic2 at e13, the timepoint when we observe an early ipsilateral projection, did not reveal a population of specified cells anywhere in the retina, including the ventrotemporal region (Supplemental Figure 3A, B). At e16, when the ipsilateral projection should be specified, a population of cells is labeled in the ventrotemporal retina for Zic2 (Supplemental Figure 3C, D). We

predict that EphrinB2 is normally localized to radial glia due to the sound structure of the chiasm that we observe (Figure 1H). We also predict that SSEA-1 cells, which pioneer the formation of the chiasm (Marcus and Mason, 1995), would also be localized normally. Dystroglycan loss in RCGs ($DG^{F/-}$; $Isl1^{Cre}$) does not impact their ability to navigate at the chiasm, and dystroglycan loss does not alter the molecular specification of the ipsilateral projection. Therefore, dystroglycan maintains the structural integrity of the basement membrane at the chiasm as a growth substrate for axons.

Axon mistargeting occurs within visual target regions due to loss of dystroglycan at the optic chiasm

Previous models of chiasm crossing defects in *Slit* or *Robo* mutants report phenotypes including failure of axons to remain fasciculated at the chiasm, and aberrant projections to the ventral forebrain (Plachez et al., 2008; Plump et al., 2002). One previous model studying a growth cone protein knockout presents with a stalling phenotype similar to what we observe in *dystroglycan* mice (Strittmatter et al., 1995a). Another model describes a mutant in which there are forebrain abnormalities and an early ipsilateral projection at the optic chiasm (Rachel et al., 2000). After axons traverse the optic chiasm, they travel to and synapse with both image-forming and non-image forming visual target regions in the brain. In *Slit* mutants at e16.5, after axons have left the chiasm, they aberrantly project out of the optic tract and into the telencephalon (Thompson et al., 2006a). *Circletail* mutant axons fail to stop growing at the thalamus and grow

across the midline at e15 (Rachel et al., 2000). However, no previous studies have characterized the impact that missorting at the chiasm has on RGC axon guidance to and pruning within appropriate visual targets after birth. The trajectory of axons to the brain over the course of visual map refinement, specifically after birth, remains largely unknown. $ISPD^{79*/79*}$ mice die perinatally possibly due to a respiratory defect. We are able to utilize the $DG^{F/-}$; $Six3^{Cre}$ model to circumvent the early lethality of $ISPD^{79*/79*}$ and other models with chiasm axon guidance defects to understand the impacts of chiasm missorting on axon targeting in the brain. This provides a novel opportunity to determine what effect neuronal misrouting at an intermediate choice point has on final targeting in the brain. We explored the possibilities that in the absence of normal routing at the chiasm, RGC axons either 1) randomly project into the brain or 2) correctly navigate to retinorecipient regions.

To ensure that phenotypes in the brain are due to initial axon missorting at the chiasm, and not failure of target regions to pattern normally, we utilized a $R26$-LSL-$H2B$:$mCherry$ marker to label nuclei and identify regions of $Six3^{Cre}$ recombination in the brain. The LGN, located below the hippocampus (hippocampus designated by asterisk, Supplemental Figure 4A) does not express $Six3^{Cre}$, and the SC also does not express $Six3^{Cre}$ (Supplemental Figure 4B). Therefore, any axon guidance defects we observe are the result of missorting at the chiasm, and not the result of dystroglycan loss causing mispatterning of target regions.

To visualize axon tracts from each eye, we performed dual-color Cholera Toxin Subunit B (CTB) injections. CTB coupled to a fluorophore acts as both an anterograde and retrograde axon tracer. We use this as a tool to label axon projections from the retina to target regions in the brain. At the optic chiasm in P2 controls, we observed axons segregating according to their eye of origin (Figure 3A). Because the ipsilateral projection in mouse is very small, we cannot observe it in the chiasm by CTB-labeling. However, in $DG^{F/-}$; $Six3^{Cre}$ mutants, we observe overlapping projections, with axons from each eye projecting to both sides of the brain (Figure 3A). The axonal projections into the ventral forebrain that we observe at embryonic ages (Figure 1F, G, Figure 2 E, F) are no longer present at P2. In the LGN (Figure 3B), contralaterally projecting axons (purple) innervate an outer shell region, and ipsilateral axons (green) are beginning to grow into the inner core. In stark contrast, *dystroglycan* mutant axons correctly target the LGN but show overlapping contralateral and ipsilateral innervation (Figure 3B). Threshold-independent analysis of the dLGN projections yields a statistically significant decreased variance of R in mutants, meaning that the projections have less segregation and more overlap (Figure 3F, t-test, p=0.038). In the SC (Figure 3D, E), we observe normal contralaterally segregated innervation in controls. Normally, a small proportion of axons do project to the ipsilateral SC, but we do not observe it at the resolution of our images. In mutants, axons correctly target the SC, but exhibit overlapping contralateral and ipsilateral projections that span the entirety of the SC (Figure 3D, E). The relative faintness of projections to the colliculus (Figure 3E) is likely due to early and widespread

RGC death (Clements et al., 2017), leading to fewer overall axons innervating the SC. Normal axonal targeting also occurs to the MTN, a component of the non-image forming visual system (Figure 3C). Thus, all retinorecipient regions receive retinal innervation with no RGC axons ectopically growing into non-visual brain regions. However, the innervation we observe is abnormally binocular, with many axons targeting the appropriate retinorecipient region on the inappropriate side of the brain.

Previous work has shown that different genetically distinct subtypes of RGCs project to different retinorecipient regions of the brain (Herrera et al., 2003; Kim et al., 2010b; Osterhout et al., 2014). In order to determine if a specific population of RGCs is specifically misrouted, we performed unilateral retrograde CTB labeling. This is a tool to label the retinal origins of SC axons. In P2 control retinas, we observe that the entire contralateral retina is labeled, and only the ventrotemporal portion of the ipsilateral retina is labeled (Extended Figure 3A). This indicates that the contralateral retina and a small portion of the ipsilateral retina project to the contralateral SC. In contrast, injections into $DG^{F/-}; Six3^{Cre}$ mutants reveal labeling across the retina in both contralateral and ipsilateral retinas (Extended Figure 3B). Specifically, the labeling in the ipsilateral mutant retina appears to be random. Therefore, in mutants, no specific subtype of RGCs appears to be selectively misrouted, instead, any axon that should normally project ipsilaterally may be misrouted to the contralateral SC.

In the LGN and SC, axon projections refine after birth to form a specific lamination pattern (Godement et al., 1984; Jaubert-Miazza et al., 2005).

Refinement in both nuclei is mediated by spontaneous bursts of activity from the retina, known as retinal waves (Butts et al., 2007; McLaughlin et al., 2003). We have previously shown that the spontaneous retinal waves necessary for map refinement in the LGN and SC are preserved in *dystroglycan* null mice (Clements et al., 2017). We performed CTB injections at postnatal timepoints including prior to eye opening at P10, when eye segregation is almost complete, and after eye opening at P28, when eye segregation is complete (Furman and Crair, 2012). We wanted to determine whether, despite initial binocular innervation, axon pruning within the LGN and SC still occurred normally. Surprisingly, while pruning does occur after P2, ipsilateral axons that have inappropriately invaded contralateral nuclei persist. At the optic chiasm at P10 (Figure 4A) and P28 (Figure 4E), we observe axons traveling to both sides of the brain. In the LGN, (Figure 4B, F), both the dorsal and ventral LGN are innervated and there are no ectopic projections into the brain. However, axons fail to prune in a way that correctly innervates the contralateral shell and ipsilateral core, they are instead present in patchy, random distributions. We next tested if the appropriate proportions of axons are still present, despite inappropriate innervation. To achieve this, we measured the area occupied by contralateral, ipsilateral, and overlapping axons. In P10 dLGN, we observe a significantly greater proportion of ipsilateral innervation than in controls (Figure 4I, p<0.05, t-test). The contralateral and overlapping projections do not show any difference in total area occupied within the dLGN at P10 or P28 (Figure 4I, p>0.05, t-test). To corroborate these results, we utilized a threshold-independent method to measure segregation

111

between contralateral and ipsilateral projections. We calculated the variance of the intensity ratio (R) to determine the amount of segregation. Higher variances indicate increased segregation and organization. Axons in the dLGN of mutants appear to be more segregated, although the comparison is not statistically significant (Figure 4J, p>0.05, t-test). Because retinal waves are intact, it is likely that axonal segregation in the LGN occurs at a normal level, despite the inappropriate lamination of the axons.

In the SC (Figure 4C, D, G, H), clusters of ipsilaterally originating axons invade the contralateral colliculus, evident in both sections and whole mounts. Analysis of the whole mount colliculus reveals that at P10, before eye opening when pruning is almost complete, approximately 20% of axons innervate the wrong side of the brain, which persists throughout eye opening and into adulthood (ANOVA, Tukey HSD *post hoc* test, p<0.0001, Figure 4K). In the SC, specific subsets of RGCs target either the upper or lower lamina (Kim et al., 2010a). Our data show that inappropriate ipsilateral projections span the entirety of the SC, leading us to conclude that no specific type of RGC is selectively misrouted at the chiasm. We can draw three conclusions from our data in the LGN and SC. First, we show that pruning mechanisms are generally intact, but do not show a preference for inappropriate ipsilateral axons. Second, as a result of failure of ipsilateral axons to prune, axons do not innervate the LGN and SC with appropriate spatial positioning. Finally, we initially observe at P2 that there is axonal overlap in both the LGN and SC that prunes into patchy clusters of axons.

We speculate that these represent regions of the retina where correlated activity from retinal waves remains.

We also observed defects in non-image forming components of the visual pathway. The SCN, dorsal to the optic chiasm, responsible for circadian rhythms, normally receives binocular input. Binocularity is still present in $DG^{F/-}$; $Six3^{Cre}$ mutants (Supplemental Figure 5A, D), however, it appears that at P28, there is a greater proportion of input from one eye over the other (Supplemental Figure 5D). The optic tract, like the chiasm, contains projections from both eyes, and also appears thinner at P28 (Supplemental Figure 5B, E). This thinning is likely due to early and specific ganglion cell death in this model, leading to fewer RGC axons traveling to the brain, as previously described (Clements et al., 2017). The MTN, which is involved in smooth pursuit, is normally monocularly innervated, but receives binocular innervation in *dystroglycan* mutant mice (Supplemental Figure 5C, F). Deletion of *dystroglycan* has been shown to impair visual transmission in the retina (Sato et al., 2008), meaning that we cannot use visual stimuli and behavioral tests to determine what impact that mislamination in the LGN, SC, and abnormal binocularity in the accessory optic system has on visual perception. We predict that if visual transmission was preserved, we would observe mice that are unable to correctly localize spatial cues or correctly track objects in motion.

The density of axonal innervation to image-forming and non-image forming retinorecipient regions appears to be complete, despite loss of ganglion cells in $DG^{F/-}$; $Six3^{Cre}$ animals. Axons that survive may arborize to a greater

extent in target regions to account for this loss. Further analysis using transgenic lines is necessary to understand the consequences of axonal arborization in mutants. The persistence of inappropriate ipsilateral projections across the visual targets suggests that these neurons are capable of integrating into the mature circuit, potentially because neurotrophins in the target may not selectively act on contralateral or ipsilateral axons. Our findings also raise interesting questions about downstream visual processing. First, are ocular dominance columns in V1 bilaterally innervated or otherwise inappropriately formed? Two recent studies show that retinogeniculate and corticothalamic axons interact and may rely on one another for correct innervation of the LGN (Seabrook et al., 2013; Shanks et al., 2016). If the visual cortex is not innervated correctly in our model because of failure of RGC axons to appropriately laminate the LGN, it may play an additional role in retinogeniculate innervation. More work with additional and specific *cre* mice would be necessary to dissect this question.

Summary and Conclusions

Dystroglycan is required to maintain the basement membrane at the optic chiasm as a substrate for axonal growth. When dystroglycan is lost, axons do not sort correctly resulting in compromised innervation of retinorecipient brain regions. We observe clusters of contralateral and ipsilateral axons that form patches across the LGN and SC that are stable and persist throughout adulthood. Our study is the first to characterize the mature visual brain circuit that arises due to a developmental abnormality at the optic chiasm. Our data show

114

that despite this initial misrouting, neurons are still able to correctly target the brain and prune, but specificity of refinement is lost.
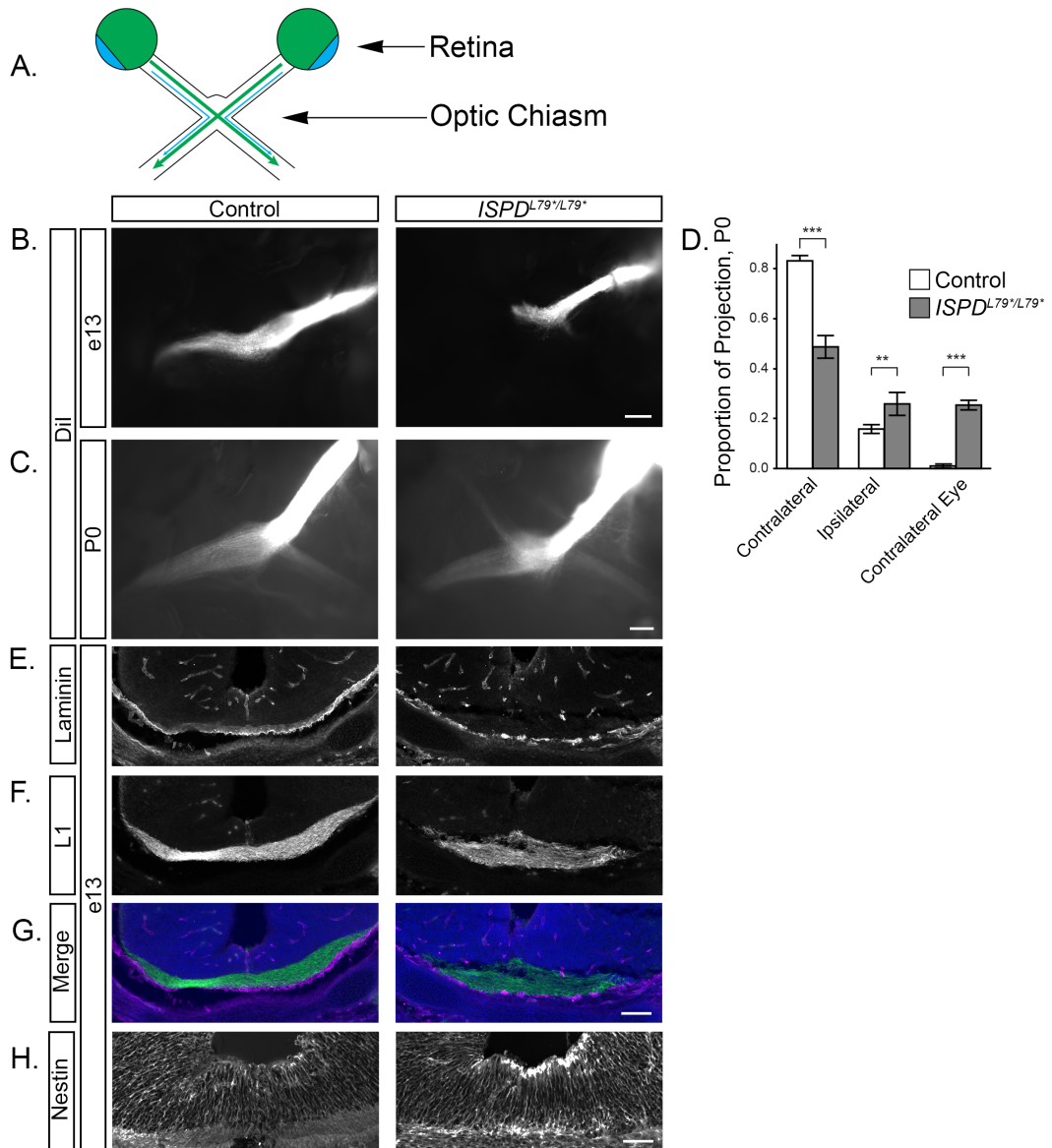
Figure 1

Figure 1: Loss of functional dystroglycan causes axon guidance defects at the optic chiasm. (A) Schematic of axon crossing at the optic chiasm. The contralateral projection is designated in green, and the ipsilateral projection is designated in blue. (B) Axons (DiI) at e13 in controls form a contralateral projection (left). Axons in *ISPD*$^{L79*/L79*}$ chiasms stall and form an early ipsilateral projection (right). (C) At P0, control axons make a contralateral and ipsilateral projection (left). In *ISPD*$^{L79*/L79*}$ mutants, axons project contralaterally, ipsilaterally, and to the contralateral eye (right). (D) At P0, mutant axons have a reduced contralateral projection and increased projection to the ipsilateral optic tract and the contralateral eye (ANOVA, Tukey HSD *post hoc* test, $p<0.01$). (E-G) Sections of the optic chiasm at e13 reveal that the basement membrane (laminin, E, purple, G) becomes discontinuous in mutants, and that mutant axons (L1, F, green, G) become defasciculated and enter the ventral forebrain. Laminin staining above the chiasm (E) is blood vessel labeling. (H) Radial glia at the optic chiasm labeled with nestin are structurally intact in both controls and *ISPD*$^{L79*/L79*}$ mutants. Scale bars: B, C, 200μm; E-G, 100 μm; H, 50 μm.

Figure 2

A. Retina — *R26-LSL-H2B: mCherry; Six3^Cre*, P0

B. OC

C. DiI / P0 — Control | *DG^F/-; Six3^Cre*

D. Laminin

E. 2H3 / e15

F. Merge
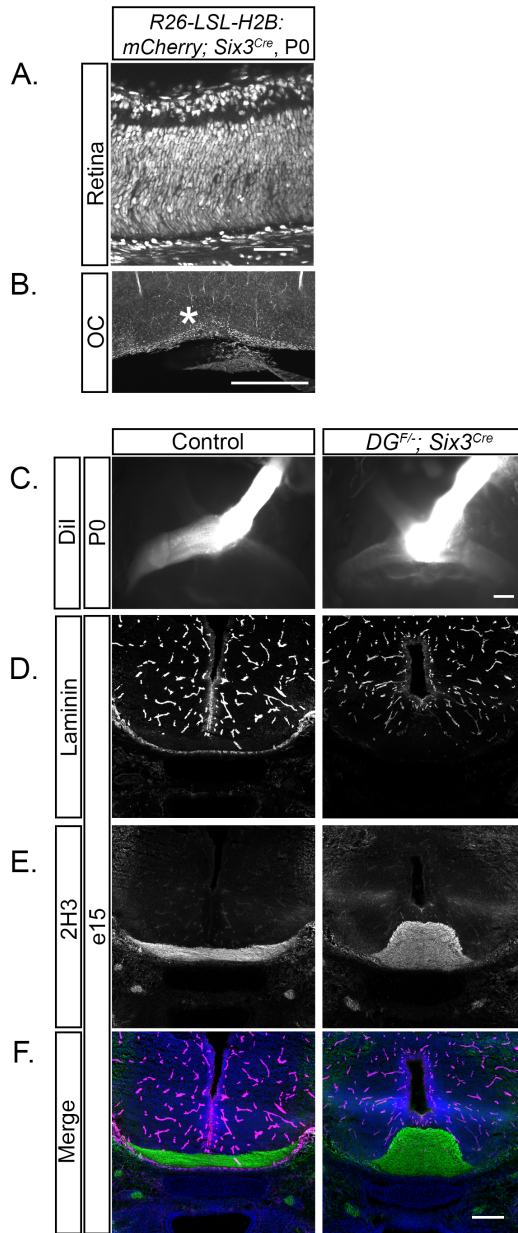
Figure 2: Deletion of *dystroglycan* in the retina and ventral forebrain recapitulate phenotype seen in *ISPD$^{L79*/L79*}$*. (A-B) Expression of *Six3^{Cre}* by *Rosa26-lox-stop-lox-H2B:mCherry* shows expression in all retinal cells (A) and the ventral forebrain (B) at P0. (C) Axons in *DG$^{F/-}$; Six3^{Cre}* chiasms stall and make smaller projections into the contralateral and ipsilateral optic tracts than in controls. (D-F). Sections in e15 *DG$^{F/-}$; Six3^{Cre}* mice reveal a loss of laminin at the basement membrane at the chiasm (D, F purple) and axons (2H3) that inappropriately grow into the ventral forebrain (E, F green). Laminin staining above the chiasm (D) represents blood vessel staining. Scale bars: A, 50 μm; B, 500μm; C-F, 200μm.
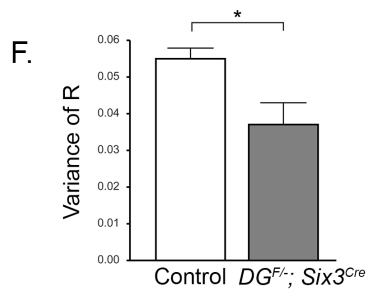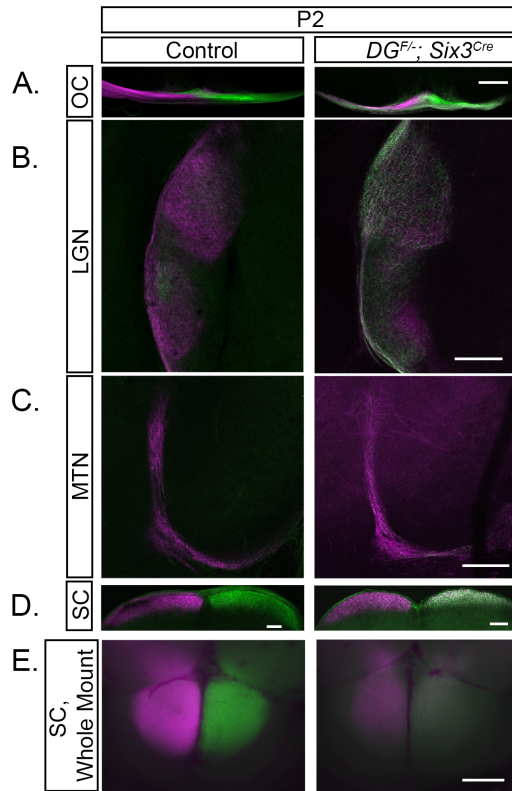
Figure 3

Figure 3: Retinal ganglion cell axons target appropriate visual regions in *dystroglycan* null mice. (A) CTB labeled axons at the optic chiasm show eye-specific segregation in controls at P2 (left panel) and overlapping projections in $DG^{F/-}$; $Six3^{Cre}$ chiasms (right). (B) Contralateral axons (purple) in controls (left) at P2 innervate the dorsal and lateral LGN while ipsilateral axons (green) begin to grow into the dorsal and lateral LGN cores. Mutant (right) axons originating from contralateral and ipsilateral eye overlap across the LGN. (C) In the MTN of the accessory optic system, controls are monocularly innervated from the contralateral eye (left), and in mutants (right), the MTN is correctly innervated with several ipsilaterally originating axons invading the nucleus. (D, E) In sections (D) and whole mounts (E) of the SC, controls (left) show segregation of eye input. In $DG^{F/-}$; $Six3^{Cre}$ mice (left), contralateral and ipsilateral inputs overlap across the span of the colliculus. (F) Threshold-independent analysis of LGN projections (B) shows a significantly greater axonal overlap in mutants than controls (t-test, p=0.038). Scale bar 200μm.
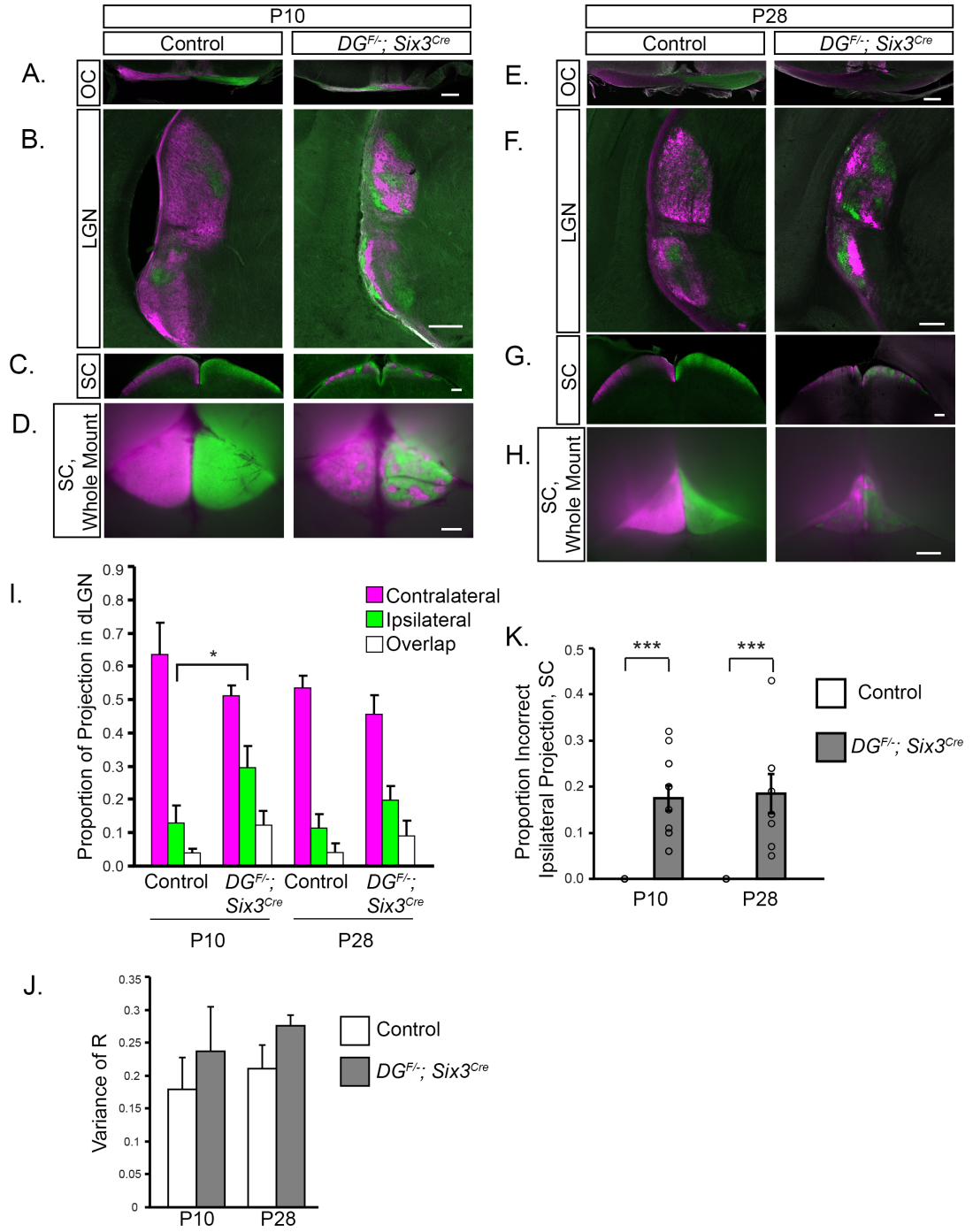
Figure 4

Figure 4: Retinal ganglion cell axons do not laminate appropriately in dystroglycan null mice. (A) CTB injected axons at the optic chiasm in $DG^{F/-}$; $Six3^{Cre}$ at P10 maintain overlap. (B) Pruning occurs in $DG^{F/-}$; $Six3^{Cre}$ P10 dorsal and lateral LGN, but axons do not prune into the appropriate contralateral shell and ipsilateral core. (C, D) SC sections (C) and whole mounts (D) in P10 $DG^{F/-}$; $Six3^{Cre}$ mice reveal pruning has occurred into discrete contralateral and ipsilateral patches. (E-H). Analysis of CTB injected axons in the optic chiasm (E), LGN (F), and SC (G, H) at P28 in $DG^{F/-}$; $Six3^{Cre}$ show that inappropriate ipsilateral projections remain after eye opening. (I) Threshold-dependent measures of the total area of contralateral, ipsilateral, and overlapping projections in the dLGN show that the ipsilateral innervation $DG^{F/-}$; $Six3^{Cre}$ at P10 is significantly greater (p=0.04, t-test). (J) Threshold-independent analysis does not show a difference in segregation between controls and mutants at P10 or P28 (t test, p>0.05). (K) Approximately 20% of axons are inappropriate ipsilateral projections in the SC at P10 and P28 (ANOVA, Tukey HSD *post hoc* test, p<0.0001). Scale bars: A-C, E-G, 200μm; D, H, 500μm.

Supplemental Figure 1
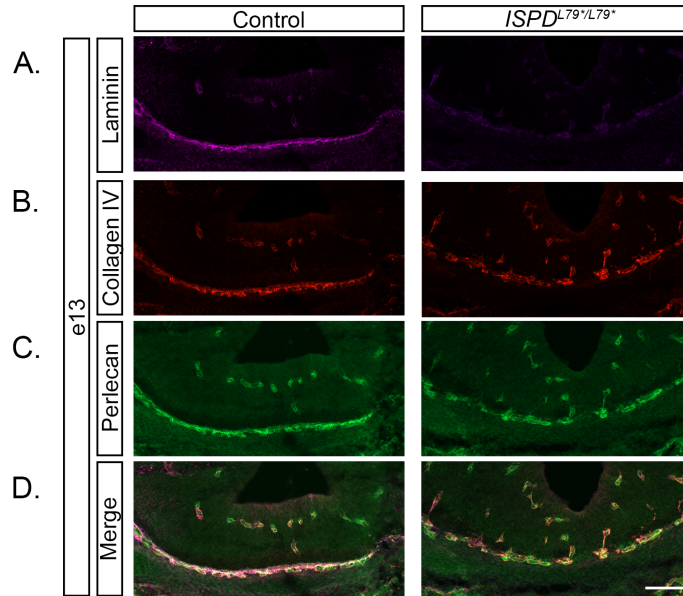
Supplemental Figure 1: Dystroglycan stabilizes multiple ECM proteins at the chiasm. (A-D) In controls (left) at e13, multiple ECM proteins including laminin (A), Collagen IV (B), and perlecan (C) colocalize at the basement membrane of the optic chiasm. In $ISPD^{L79*/L79*}$ chiasms (right), the basement membrane becomes patchy and appropriate localization of ECM proteins is lost. Scale bar: 100μm.

Supplemental Figure 2

A.

Retina	Optic Chiasm

Ai9; Isl1^{Cre}, Tomato, DAPI, P0

B.

Control	*DG^{F/-}; Isl1^{Cre}*

P0
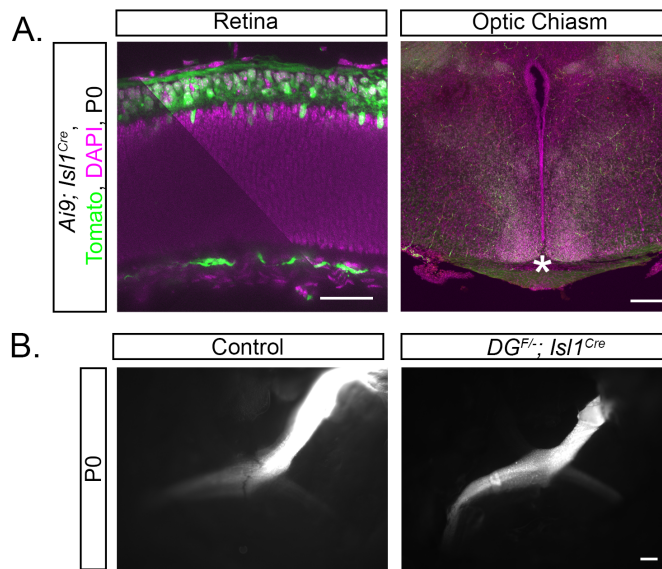
Supplemental Figure 2: Dystroglycan does not function in RGC axons to regulate crossing at the chiasm. (A) Expression of *Isl1^Cre* by *Rosa26-lox-stop-lox-TdTomato; Ai9* reporter (green) shows expression in RGC cell bodies in the retina (left) and RGC axons at the chiasm (asterisk, right). (B) Axon crossing at the chiasm is normal in *DG^{F/-}; Isl1^Cre* chiasms. Scale bars: A left, 50μm; A right, B 200μm.

Supplemental Figure 3
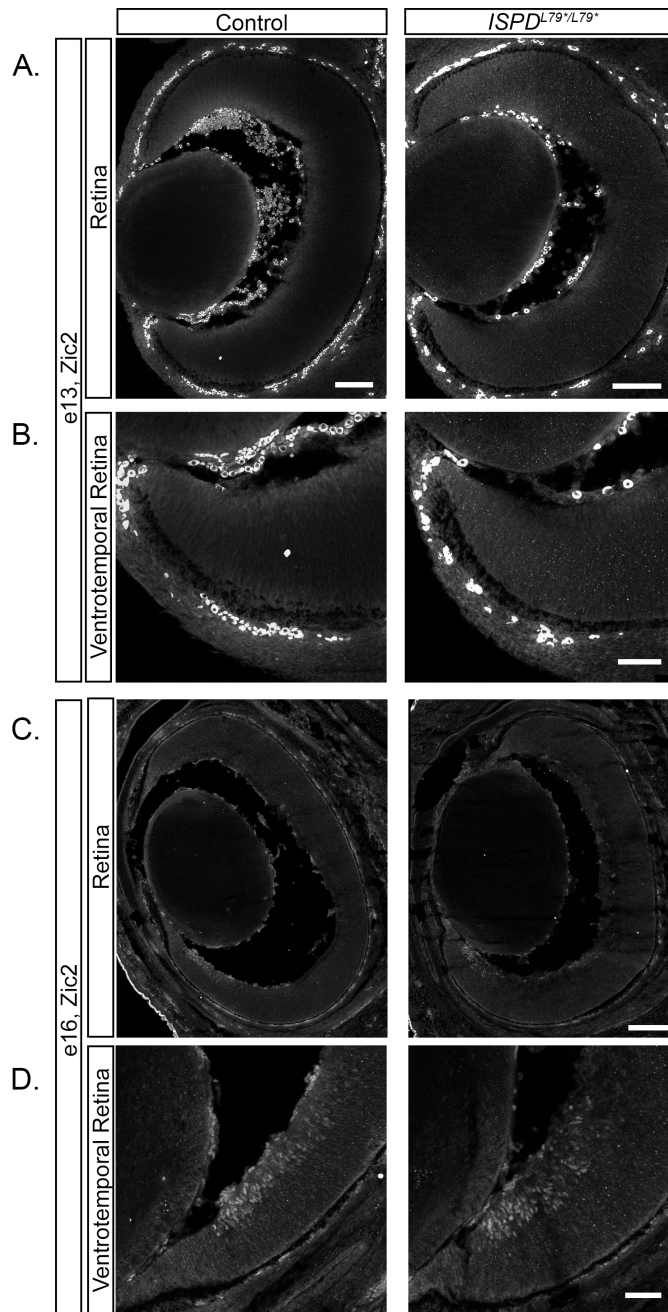
Supplemental Figure 3: Loss of dystroglycan does not cause misspecification of the ipsilateral projection. (A, B) Immunohistochemistry for Zic2 at e13 in *ISPD^(L79*/L79*)* retinas does not reveal a population of ipsilateral cells specified early in either the whole retina (A) or the ventrotemporal retina (B). (C, D) An appropriately specified population of cells positive for Zic2 is present in the ventrotemporal retina (D) in *ISPD^(L79*/L79*)* retinas at e16. Scale bars: A, 100μm; B, 50μm; C, 200μm; D, 50μm.

Supplemental Figure 4

| | *R26-LSL-H2B: mCherry; Six3^Cre*, P0 | *R26-LSL-H2B: mCherry; Six3^Cre*, P28 |

A. dLGN

B. SC
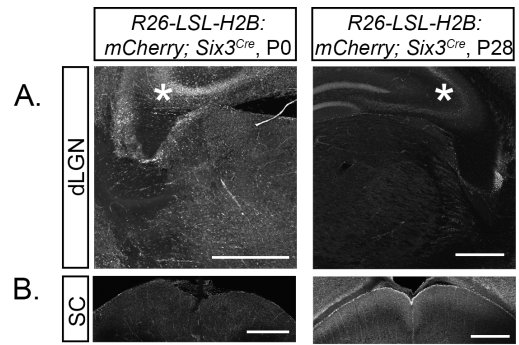
Supplemental Figure 4: *Six3^{Cre}* **is not expressed in retinorecipient brain**

regions. (A, B) Expression of *Six3^{Cre}* by *Rosa26-lox-stop-lox-H2B:mCherry* does

not show expression in the LGN (A) or SC (B) at P0 or P28. Asterisk denotes

hippocampus. Scale bar: 500μm.

Supplemental Figure 5
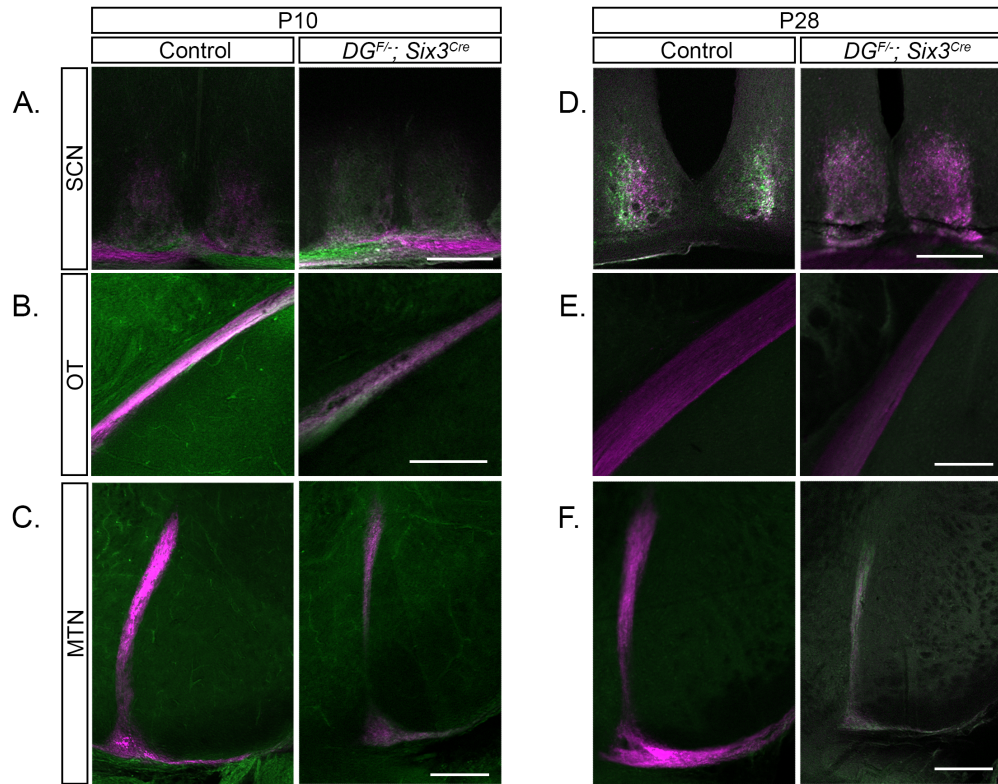
Supplemental Figure 5: Binocular innervation of the accessory optic system. (A) The SCN at P10 begins to receive binocular innervation. (B) The optic tract contains visible contralateral and ipsilateral RGC axons in $DG^{F/-}$; $Six3^{Cre}$ mutants at P10. (C) The MTN receives inappropriate binocular innervation in $DG^{F/-}$; $Six3^{Cre}$ mutants at P10. (D) Binocular innervation is present but perturbed in $DG^{F/-}$; $Six3^{Cre}$ mutants at P28. (E) The optic tract at P28 in $DG^{F/-}$; $Six3^{Cre}$ mutants is thinner and contains contralateral and ipsilateral RGC axons. (F) The MTN at P28 receives inappropriate binocular innervation in mutants. Scale bar: 200μm.

Extended Figure 1
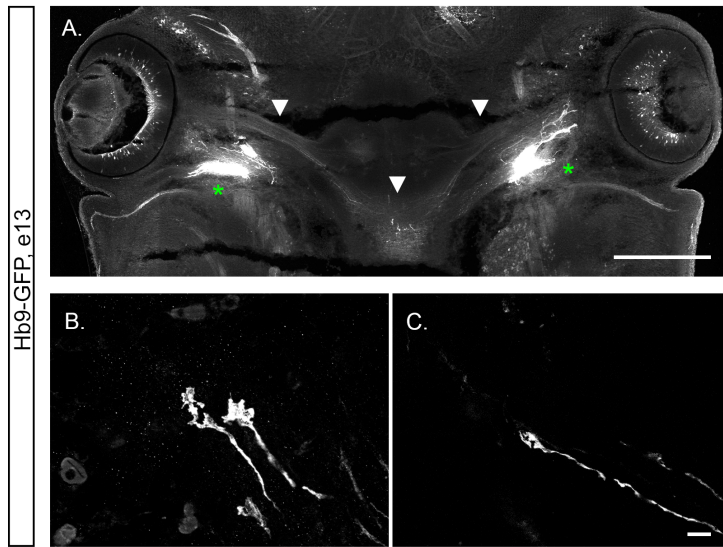
Extended Figure 1: Hb9-GFP allows for growth cone visualization at the optic chiasm. (A) Hb9-GFP labels cell bodies and axons of retinal ganglion cells. Arrowheads indicate axons in optic tract and optic chiasm, asterisks indicate oculomotor nerve. (B, C) Growth cones of retinal ganglion cells are visible in the optic chiasm *in vivo*. Scale bar: A, 500µm, B, C, 10µm.

Extended Figure 2

	Control	*DG^{F/-}; Itgβ1^{F/+}; Six3^{Cre}*	*DG^{F/-}; Itgβ1^{F/-}; Six3^{Cre}*
P0	A.	B.	C.
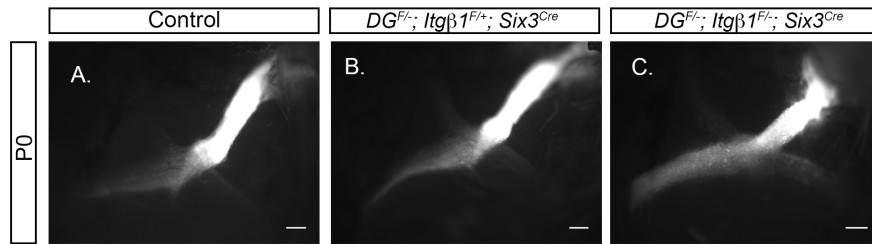
Extended Figure 2: Dystroglycan and β1-Integrin do not have additive functions at the optic chiasm. (A) At P0 in controls, axons predominantly make a contralateral projection at the optic chiasm with a small ipsilateral projection. (B) In *dystroglycan* mutants, the contralateral and ipsilateral projections are more diffuse and there appear to be fewer axons. (C) The *dystroglycan* and *β1-Integrin* phenotype at the optic chiasm is not worse than the single *dystroglycan* mutation. Scale bar: 200μm.

Extended Figure 3
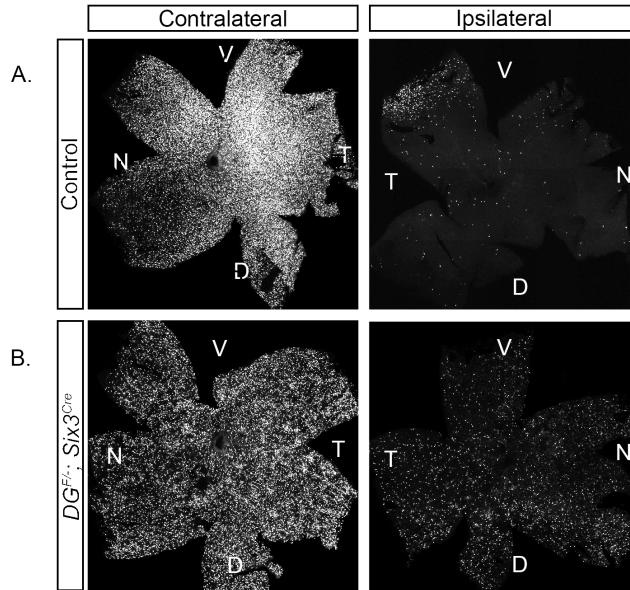
Extended Figure 3: Ipsilateral axons are randomly misrouted in dystroglycan mutants. (A) At P2 in controls, retinal axons labeled retrogradely from CTB injections show that collicular projections originate from the entirety of the contralateral eye (left panel) and the ventrotemporal region of the ipsilateral eye (left panel). (B) In *dystroglycan* mutants, both the contralateral and ipsilateral eyes show widespread projections to the contralateral SC.

Table 1: Antibodies

Target	Host	Dilution	Company/ origin	Catalog #	RRID
2H3	mouse	1:1000	Developmental Studies Hybridoma Bank	2h3	AB_531793
Collagen IV	goat	1:250	Southern Biotech	1340-01	AB_2082646
L1	rat	1:500	Millipore	MAB5272	AB_2133200
Laminin	rabbit	1:1000	Sigma	L9393	AB_477163
Nestin	mouse	1:100	Developmental Studies Hybridoma Bank	Rat-401	AB_2235915
Perlecan	rat	1:500	Millipore	MAB1948P	AB_10615958
Zic2	rabbit	1:500	Millipore	AB15392	AB_1977437

Table 1: List of Antibodies. Antibodies and associated information (host species, dilution, manufacturer, catalog number, and RRID) are presented here.

Conclusions and Future Directions

Current neuroscience research aims to dissect the molecular mechanisms that regulate development. Dystroglycan has been the subject of extensive study throughout recent years for its role in regulating development outside of muscle cells. In the cortex, it plays a scaffolding role to stabilize the cortical basement membrane and anchor radial neuroepithelial endfeet to the pial surface, and thus regulates neuronal migration. Recent work has also implicated dystroglycan in spinal cord axon guidance (Wright et al., 2012). My research in the visual system was motivated by two fundamental open-ended questions. First, does dystroglycan play a similar role in the retina as it does in the cortex and spinal cord to regulate neuronal migration and axon guidance? Second, what function does dystroglycan serve in visual-associated brain regions? Human patients with non-functional dystroglycan present with brain malformations and visual abnormalities. While we understand the molecular role dystroglycan plays in brain malformations, we do not yet understand in detail the role dystroglycan plays in the visual system. Understanding dystroglycan's role in the developing visual system also provides insight into general mechanisms of circuit development.

I show in the retina that dystroglycan functions in a similar manner as in the cortex, in that it stabilizes the retinal inner limiting membrane to regulate cell migration. Due to the loss of the inner limiting membrane, cells migrate into the vitreous and many RGC axons are unable to correctly exit the retina. The inner

retina is selectively impacted, with the outer retina being grossly normal. This is in contrast to the cortex, where all layers are affected, and is likely due to glial-independent cell migration that occurs in the retina. Within the inner retina, RGCs and cells in the ganglion cell layer display abnormal phenotypes, with displaced amacrine cells showing clustered mosaic cell spacing, and RGCs undergoing early and extensive apoptosis. I show that the phenotypes are due to dystroglycan's maintenance of the ILM, and that dystroglycan does not function cell autonomously in RGCs. Retinal waves, spontaneous bursts of activity before eye opening, are normal despite the profound defects in ILM integrity and cellular positioning. Outside the retina, some RGC axons are able to successfully travel to the chiasm. Non-functional dystroglycan causes the basement membrane at the chiasm to be fragmented, and as a result, axons stall and exhibit an early ipsilateral projection. This crossing defect is due to the loss of an intact basement membrane as a growth substrate, and not due to any molecular misspecifications within axons. Past the chiasm, axons do target the appropriate retinorecipient brain regions, but fail to laminate them correctly.

The data presented in this thesis is novel in two ways. First, while dystroglycan has previously been shown to play a role in retinal development and that retinal thinning occurs in mutants, my study is the first to characterize the specific implications of dystroglycan loss on each cell type thoroughly. Second, previous studies have not characterized the impact of developmental axon guidance defects on formation and maturation of the postnatal circuit. My study describes a novel phenotype of axon innervation to target regions in the

142

postnatal animal, which occurs as the result of embryonic missorting at an intermediate choice point.

Cellular growth and maturation dynamics in the retina

The work presented in Chapter 1, pertaining to dystroglycan's role in the retina, gives me the opportunity to perform several new experiments to study cellular development dynamics. Upon close examination, not all axons in $ISPD^{L79*/L79*}$ mutants exhibit defasciculation or aberrant trajectories away from the optic nerve head (Chapter 1, Figure 4 D, E, Supplemental Figure 1). There is a set of axons that appears to fasciculate and exit the retina normally. RGCs are the first cell type born in the retina and their differentiation from retinal progenitor cells continues through birth. My prediction is that the subset of axons that appears normal is from the early-born population of RGCs, at or around e13, before the ILM has broken down, and that the subset that exhibits an aberrant trajectory is born after e14-e15, after the ILM has broken down, and therefore does not have a growth substrate for proper pathfinding to the optic nerve head. To test this, I propose the following set of experiments. First, I need a way to visualize RGC axons and label them by birth date. To accomplish this, I would use the $Cdh4\text{-}^{CreER}$ or $Cdh6\text{-}^{CreER}$, which express cre in RGC axons (Martersteck et al., 2017). I would use either of these mouse lines in conjunction with a *Cre*-dependent reporter such as *Rosa26-lox-stop-lox-TdTomato; Ai9*, so that neurons expressing *cre* would be labeled with Td-Tomato for visualization. Using a Cre^{ER} driver would allow me to have temporal control over *Cre* and TdTomato expression. Both the *Cre* reporter and TdTomato would be crossed to the *ISPD*

line, so that I would label a population of RGCs on the mutant background of interest. I would pulse with tamoxifen to label cells at e12 and e15, analyze retinas at P0, and counterstain with 2H3 to label all axons. Only RGCs born at the time of the tamoxifen pulse would express TdTomato. I anticipate that for the e12 tamoxifen pulsed retina, all labeled TdTomato axons would be normally fasciculated and guided to the optic nerve head, while some of the 2H3 labeled axons would display inappropriate trajectories. In contrast, I expect that in the e15 tamoxifen pulse set of animals, both normal trajectory and abnormal trajectory axons would be labeled with TdTomato. I would conclude from the results of this experiment that only axons born after e12-e13 undergo pathfinding defects.

When cortical neurons divide and differentiate, they undergo a multipolar phase with exploratory processes before stabilizing an axon and dendrites (Tabata and Nakajima, 2003). In contrast, RGCs very rapidly stabilize an axon that is oriented towards the basal side of the retina. Recent work has shown that this is due to neurite contact with laminin at the ILM. In the absence of laminin, RGCs do undergo a multipolar phase, reminiscent of cells in the cortex (Randlett et al., 2011). Our model is a useful tool to study these axon emergence dynamics *in vivo* as not all newborn RGCs will make contact with laminin. Additionally, our model presents with a slightly different phenotype. In static images, we observe neurons that often have one clearly defined axon and multiple other stable neurites (Chapter 1, Supplemental Figure 1). RGCs with this morphology are located in the ganglion cell layer, and thus have presumably stabilized their cell

body at the correct location in the circuit. It is undetermined whether these extra neurites are also axons or some other stabilized process. Static images do not provide sufficient information to determine whether these neurites are transient and will eventually retract, or if the RGCs are in fact stuck in a multipolar phase. Live imaging of retinal whole mounts is possible using previously described techniques (Sharpe and Wong, 2011). I can visualize RGCs in a live prep using the Hb9-GFP transgenic reporter bred to the *ISPD* mouse. Long-term live retinal imaging will allow me to further characterize axon formation dynamics and determine if the multiple neurites that I observe (Chapter 1, Supplemental Figure 1) are transient or truly stable.

The impact of axonal missorting on visual processing

RGC axons synapse in the brain to send information necessary for cortical visual processing. The work presented in Chapter 2 raises several interesting questions regarding how visual processing occurs when a target region is severely mislaminated. Despite loss of visual input in the $DG^{F/-}$; $Six3^{Cre}$ model due to transduction failure between photoreceptors and bipolar cells (Sato et al., 2008), my data suggest that RGCs are still able to integrate into the visual circuit to both receive and send information. In Chapter 1, I show that retinal waves, spontaneous bursts of activity generated by amacrine cells and received by RGCs, are grossly normal. In Chapter 2, I show that pruning of contralateral and ipsilateral input to the LGN, mediated by retinal waves, also occurs relatively normally. In previous models with LGN pruning defects caused by disrupted retinal waves, such as the $\beta2$ and *nob* models, there is a persistence of

contralateral and ipsilateral overlap that is restricted to the area immediately around the ipsilateral core (Demas et al., 2006; Rossi et al., 2001; Torborg and Feller, 2004). I do not see persistence of overlap in the $DG^{F/-}$; $Six3^{Cre}$ model (Chapter 2, Figure 4J), further evidence that retinal waves are functionally intact and that retinogeniculate projections transmit information.

Although retinal waves are normal and the LGN and SC are completely innervated, the level of resolution of CTB injections does not provide information about specific pruning of axonal arbors. Several studies show pruning defects in the SC due to either loss of guidance cues or disruption of retinal waves (Huberman et al., 2008a; McLaughlin et al., 2003). I have shown that ganglion cells undergo extensive cell death due to loss of dystroglycan (Chapter 1, Figure 8 H, I, Figure 9 C, D), leading to fewer axonal projections into the brain. While pruning does occur in mutants between P2 and P10 (Chapter 2, Figure 3B, Figure 4B), it is unclear if the axons take up a larger amount of space to compensate for fewer projections. This kind of pruning defect has not been described before in the visual system. To determine how axons get pruned in the *dystroglycan* model, I will take advantage of genetic approaches to label subsets of axons. First, I can breed the $DG^{F/-}$; $Six3^{Cre}$ mouse with transgenic lines that label ganglion cells with known patterns of central projections (Martersteck et al., 2017). Three results may occur. First, I might observe an axon that has pruned to the appropriate size but is in the wrong location in its target nucleus. This would mean that axons prune correctly and only undergo localization defects. Second, I could see an axon in the correct location in its target nucleus but with a bigger

arbor. This would suggest that axons localize correctly but do not fully prune, likely to compensate for fewer RGC projections into the brain. Third, I might observe an axon with both a larger arbor and in an inappropriate location, suggesting that both pruning and laminar targeting are impaired in the *dystroglycan* model. In addition to transgenic labeling, I could label RGC axons using cre-dependent AAV-GFP or single neuron tracing using rabies virus (Rompani et al., 2017; Yonehara et al., 2013). However, both of these methods label cells at random, meaning that cell types between controls and mutants would be different. Because the phenotype in the mutant is so severe, it is important to have extremely specific controls. Injections of AAV or rabies means the data is likely unable to be interpreted. I will focus on utilizing a robust transgenic line to study pruning and localization defects. Axons that exhibit larger arbors likely contain misrepresentations of their receptive field. The next set of experiments I propose will determine how the inappropriate laminar targeting I observe in the LGN and SC impacts visual processing.

Although dystroglycan is present at some synapses (Früh et al., 2016), it is unlikely that any defects that occur in visual processing in the LGN or V1 are due to the function of dystroglycan at synapses in the brain. Instead, any defects are likely to be a secondary effect of mislamination of target regions that occurs because of axonal missorting at the optic chiasm. One way to check whether information transmission from the retina to LGN is intact is to perform simultaneous recordings. Pioneering work by Hubel and Wiesel show that on/off, center/surround receptive fields are preserved between the retina and LGN

(Hubel and Wiesel, 1961). Additional studies have described methods to record from the retina with a single electrode and the LGN with a multielectrode while the animal views a visual stimulus (Usrey et al., 1999). Because *dystroglycan* animals undergo loss of visual transmission, such experiments would have to be performed by stimulating cells instead of presenting a visual stimulus. These kinds of experiments have been described in mouse (Bickford et al., 2015). Numerous transgenic lines exist that label RGCs with specific response properties, including ON and OFF RGCs (Sanes and Masland, 2015). I would breed any of these transgenic lines to the $DG^{F/-}; Six3^{Cre}$ mouse to have a specific population of cells to study. In my experiment, I would target and stimulate transgenic-labeled RGCs while recording in the LGN. This would confirm if RGCs in the $DG^{F/-}; Six3^{Cre}$ model are truly able to transmit meaningful and appropriate visual information, even if the axon of the particular RGC is localized to the wrong place in the LGN.

What happens to visual cortex lamination as a result of laminar targeting defects in the LGN? Ocular dominance columns in V1 are blob regions which respond to either contralateral or ipsilateral light input (Hubel and Wiesel, 1959). The first experiment I would perform is to confirm that ocular dominance columns form in mutants using cytochrome oxidase staining. As a control experiment, to confirm that defects I see are due to initial axon missorting, and not any defect in retinal waves, which would cause a failure to form ocular dominance columns at all, I will block retinal waves in controls using epibatidine (Ackman et al., 2012; Huberman et al., 2006; Sun et al., 2008) and compare maps between controls,

mutants, and epibatidine-treated animals. Spontaneous retinal waves can cause correlated activity in neurons downstream in the visual pathway (Huberman et al., 2008a). Studies in ferrets have shown that correlated activity bursts are involved in visual map formation (Chiu and Weliky, 2002). This fits with classic plasticity rules: neurons from the periphery sending action potentials will connect with neurons in the brain, thus causing the brain to create a representation of the periphery. If there is no sensory information, such as during monocular deprivation, then the amount of cortical area dedicated to the deprived eye will shrink (Wiesel and Hubel, 1963). I predict that because the LGN is targeted normally, pruning occurs, and that there is no axonal overlap, maps will also form in visual cortex and there will be no abnormal binocular columns. However, cytochrome oxidase staining may not be sufficient to elucidate the spatial misplacement of afferents or misrepresentation of receptive fields that I would expect to see in V1. More advanced techniques, such as simultaneous recordings between the retina and V1 using extracellular recordings and GCaMP, respectively, would be necessary to determine the exact eye-specific input locations in V1. Overall, I predict that because initial overlap in the LGN is pruned away, combined with the finding that there are not a significantly higher number of ipsilateral projections in the LGN at P28 (Chapter 2, Figure 4), ocular dominance columns and visual maps in V1 may resolve somewhat normally. Defects in visual processing therefore would be due to mislocalization of columns or misrepresentation of receptive fields, not failure of columns to form.

Another interesting experiment would be to examine the interactions between the retinogeniculate and corticothalamic afferents. One previous report suggests that retinogeniculate input is necessary to drive corticothalamic projections (Seabrook et al., 2013), while another claims that retinogeniculate innervation is incomplete without prior corticothalamic projections (Shanks et al., 2016). Regardless of which model is correct, these papers demonstrate that there are interactions between the two populations of axons. I propose a basic characterization of corticothalamic axon projections in the *dystroglycan* model. In preliminary experiments, I would utilize a τ-GFP, which labels axons from cortical Layer VI (Jacobs et al., 2007), bred to the $DG^{F/-}$; $Six3^{Cre}$ mouse to label corticothalamic projections in mutants. If the transgenic reporter labels too many axons to elucidate a phenotype, I would perform sparse and specific injections into Layer VI in visual cortex using either CTB, AAV, or DiI.

Summary: Dystroglycan in the developing visual system

Due to the complexity of the nervous system, we still have much to understand regarding the molecular cues that guide the development of functional neural circuits. Deletion of proteins using genetic tools can inform us both about the function of a particular protein on a particular circuit, and the general mechanisms of how a circuit forms. Here, I present a role for dystroglycan in the developing visual system. I characterize dystroglycan function as a stabilizing protein for basement membranes. In turn, basement membranes provide growth substrates for migrating neurons and axons. In addition, my study provides new information about the general wiring of visual systems. Most

notably, I find that retinal waves are robust even in the presence of severe retinal structural defects, and that they can still function to shape refinement in downstream nuclei. Although most of the defects that I observe are secondary effects of basement membrane breakdown, they provide a new model with which one could study the minutia of cellular development (Future Directions related to Chapter 1) and the representation of visual information in cortex (Future Directions related to Chapter 2).

References

Ackman, J.B., Burbridge, T.J., and Crair, M.C. (2012). Retinal waves coordinate patterned activity throughout the developing visual system. Nature *490*, 219-225.

Arroyo, D.A., and Feller, M.B. (2016). Spatiotemporal Features of Retinal Waves Instruct the Wiring of the Visual Circuitry. Front Neural Circuits *10*, 54.

Austin, C.P., Feldman, D.E., Ida, J.A., Jr., and Cepko, C.L. (1995). Vertebrate retinal ganglion cells are selected from competent progenitors by the action of Notch. Development *121*, 3637-3650.

Bao, Z.Z. (2008). Intraretinal projection of retinal ganglion cell axons as a model system for studying axon navigation. Brain Research *1192*, 165-177.

Barresi, R., and Campbell, K.P. (2006). Dystroglycan: from biosynthesis to pathogenesis of human disease. J Cell Sci *119*, 199-207.

Bassett, E.A., and Wallace, V.A. (2012). Cell fate determination in the vertebrate retina. Trends in neurosciences *35*, 565-573.

Bastiani, M.J., Doe, C.Q., Helfand, S.L., and Goodman, C.S. (1985). Neuronal specificity and growth cone guidance in grasshopper and Drosophila embryos. Trends in Neurosciences *8*, 257-266.

Bastmeyer, M., Ott, H., Leppert, C.A., and Stuermer, C.A. (1995). Fish E587 glycoprotein, a member of the L1 family of cell adhesion molecules, participates in axonal fasciculation and the age-related order of ganglion cell axons in the goldfish retina. J Cell Biol *130*, 969-976.

Batchelor, C.L., Higginson, J.R., Chen, Y.J., Vanni, C., Eva, A., and Winder, S.J. (2007). Recruitment of Dbl by ezrin and dystroglycan drives membrane proximal Cdc42 activation and filopodia formation. Cell Cycle *6*, 353-363.

Beltran-Valero de Bernabe, D., Currier, S., Steinbrecher, A., Celli, J., van Beusekom, E., van der Zwaag, B., Kayserili, H., Merlini, L., Chitayat, D., Dobyns, W.B.*, et al.* (2002). Mutations in the O-mannosyltransferase gene POMT1 give rise to the severe neuronal migration disorder Walker-Warburg syndrome. Am J Hum Genet *71*, 1033-1043.

Berry, M., and Rogers, A.W. (1965). The migration of neuroblasts in the developing cerebral cortex. J Anat *99*, 691-709.

Bickford, M.E., Zhou, N., Krahe, T.E., Govindaiah, G., and Guido, W. (2015). Retinal and Tectal "Driver-Like" Inputs Converge in the Shell of the Mouse Dorsal Lateral Geniculate Nucleus. The Journal of Neuroscience *35*, 10523-10534.

Birgbauer, E., Cowan, C.A., Sretavan, D.W., and Henkemeyer, M. (2000). Kinase independent function of EphB receptors in retinal axon pathfinding to the optic disc from dorsal but not ventral retina. Development *127*, 1231-1241.

Blank, M., Koulen, P., Blake, D.J., and Kroger, S. (1999). Dystrophin and beta-dystroglycan in photoreceptor terminals from normal and mdx3Cv mouse retinae. Eur J Neurosci *11*, 2121-2133.

Blankenship, A.G., Ford, K.J., Johnson, J., Seal, R.P., Edwards, R.H., Copenhagen, D.R., and Feller, M.B. (2009). Synaptic and extrasynaptic factors governing glutamatergic retinal waves. Neuron *62*, 230-241.

Booler, H.S., Williams, J.L., Hopkinson, M., and Brown, S.C. (2016). Degree of Cajal-Retzius Cell Mislocalization Correlates with the Severity of Structural Brain Defects in Mouse Models of Dystroglycanopathy. Brain Pathol *26*, 465-478.

Bramblett, D.E., Pennesi, M.E., Wu, S.M., and Tsai, M.J. (2004). The transcription factor Bhlhb4 is required for rod bipolar cell maturation. Neuron *43*, 779-793.

Braunger, B.M., Demmer, C., and Tamm, E.R. (2014). Programmed cell death during retinal development of the mouse eye. Adv Exp Med Biol *801*, 9-13.

Brittis, P.A., Canning, D.R., and Silver, J. (1992). Chondroitin sulfate as a regulator of neuronal patterning in the retina. Science *255*, 733-736.

Brittis, P.A., Lemmon, V., Rutishauser, U., and Silver, J. (1995). Unique changes of ganglion cell growth cone behavior following cell adhesion molecule perturbations: a time-lapse study of the living retina. Mol Cell Neurosci *6*, 433-449.

Brittis, P.A., and Silver, J. (1995). Multiple factors govern intraretinal axon guidance: a time-lapse study. Mol Cell Neurosci *6*, 413-432.

Brockington, M., Blake, D.J., Prandini, P., Brown, S.C., Torelli, S., Benson, M.A., Ponting, C.P., Estournet, B., Romero, N.B., Mercuri, E.*, et al.* (2001). Mutations in the fukutin-related protein gene (FKRP) cause a form of congenital muscular dystrophy with secondary laminin alpha2 deficiency and abnormal glycosylation of alpha-dystroglycan. Am J Hum Genet *69*, 1198-1209.

Butts, D.A., Kanold, P.O., and Shatz, C.J. (2007). A Burst-Based "Hebbian" Learning Rule at Retinogeniculate Synapses Links Retinal Waves to Activity-Dependent Refinement. PLoS Biology *5*, e61.

Bystron, I., Blakemore, C., and Rakic, P. (2008). Development of the human cerebral cortex: Boulder Committee revisited. Nat Rev Neurosci *9*, 110-122.

Caviness, V.S., Jr., and Sidman, R.L. (1973). Time of origin or corresponding cell classes in the cerebral cortex of normal and reeler mutant mice: an autoradiographic analysis. J Comp Neurol *148*, 141-151.

Centanin, L., and Wittbrodt, J. (2014). Retinal neurogenesis. Development *141*, 241-244.

Cepko, C.L., Austin, C.P., Yang, X., Alexiades, M., and Ezzeddine, D. (1996). Cell fate determination in the vertebrate retina. Proc Natl Acad Sci U S A *93*, 589-595.

Chai, L., and Morris, J.E. (1999). Heparan sulfate in the inner limiting membrane of embryonic chicken retina binds basic fibroblast growth factor to promote axonal outgrowth. Exp Neurol *160*, 175-185.

Chan, Y.M., Keramaris-Vrantsis, E., Lidov, H.G., Norton, J.H., Zinchenko, N., Gruber, H.E., Thresher, R., Blake, D.J., Ashar, J., Rosenfeld, J.*, et al.* (2010). Fukutin-related protein is essential for mouse muscle, brain and eye development and mutation recapitulates the wide clinical spectrums of dystroglycanopathies. Hum Mol Genet *19*, 3995-4006.

Chen, Y.J., Spence, H.J., Cameron, J.M., Jess, T., Ilsley, J.L., and Winder, S.J. (2003). Direct interaction of beta-dystroglycan with F-actin. Biochem J *375*, 329-337.

Chiu, C., and Weliky, M. (2002). Relationship of correlated spontaneous activity to functional ocular dominance columns in the developing visual cortex. Neuron *35*, 1123-1134.

Chow, R.L., Volgyi, B., Szilard, R.K., Ng, D., McKerlie, C., Bloomfield, S.A., Birch, D.G., and McInnes, R.R. (2004). Control of late off-center cone bipolar cell differentiation and visual signaling by the homeobox gene Vsx1. Proc Natl Acad Sci U S A *101*, 1754-1759.

Clay, M.R., and Sherwood, D.R. (2015). Basement Membranes in the Worm: A Dynamic Scaffolding that Instructs Cellular Behaviors and Shapes Tissues. Curr Top Membr *76*, 337-371.

Clements, R., Turk, R., Campbell, K.P., and Wright, K.M. (2017). Dystroglycan Maintains Inner Limiting Membrane Integrity to Coordinate Retinal Development. J Neurosci *37*, 8559-8574.

Cowan, W.M., Fawcett, J.W., O'Leary, D.D., and Stanfield, B.B. (1984). Regressive events in neurogenesis. Science *225*, 1258-1265.

Czeschik, J.C., Hehr, U., Hartmann, B., Lüdecke, H.-J., Rosenbaum, T., Schweiger, B., and Wieczorek, D. (2013). 160 kb deletion in ISPD unmasking a recessive mutation in a patient with Walker-Warburg syndrome. European journal of medical genetics *56*, 689-694.

Deiner, M.S., Kennedy, T.E., Fazeli, A., Serafini, T., Tessier-Lavigne, M., and Sretavan, D.W. (1997). Netrin-1 and DCC mediate axon guidance locally at the optic disc: loss of function leads to optic nerve hypoplasia. Neuron *19*, 575-589.

Demas, J., Sagdullaev, B.T., Green, E., Jaubert-Miazza, L., McCall, M.A., Gregg, R.G., Wong, R.O.L., and Guido, W. (2006). Failure to Maintain Eye-Specific Segregation in nob, a Mutant with Abnormally Patterned Retinal Activity. Neuron *50*, 247-259.

Diamond, J.S. (2017). Inhibitory Interneurons in the Retina: Types, Circuitry, and Function. Annu Rev Vis Sci *3*, 1-24.

Dobyns, W.B., Pagon, R.A., Armstrong, D., Curry, C.J., Greenberg, F., Grix, A., Holmes, L.B., Laxova, R., Michels, V.V., Robinow, M.*, et al.* (1989). Diagnostic criteria for Walker-Warburg syndrome. Am J Med Genet *32*, 195-210.

Dong, X., Liu, O.W., Howell, A.S., and Shen, K. (2013). An extracellular adhesion molecule complex patterns dendritic branching and morphogenesis. Cell *155*, 296-307.

Duan, X., Krishnaswamy, A., De la Huerta, I., and Sanes, J.R. (2014). Type II cadherins guide assembly of a direction-selective retinal circuit. Cell *158*, 793-807.

Durbeej, M., Henry, M.D., Ferletta, M., Campbell, K.P., and Ekblom, P. (1998). Distribution of dystroglycan in normal adult mouse tissues. J Histochem Cytochem *46*, 449-457.

Edwards, M.M., Mammadova-Bach, E., Alpy, F., Klein, A., Hicks, W.L., Roux, M., Simon-Assmann, P., Smith, R.S., Orend, G., Wu, J.*, et al.* (2010). Mutations in Lama1 disrupt retinal vascular development and inner limiting membrane formation. J Biol Chem *285*, 7697-7711.

Erskine, L., and Herrera, E. (2007). The retinal ganglion cell axon's journey: Insights into molecular mechanisms of axon guidance. Developmental Biology *308*, 1-14.

Erskine, L., Reijntjes, S., Pratt, T., Denti, L., Schwarz, Q., Vieira, J.M., Alakakone, B., Shewan, D., and Ruhrberg, C. (2011). VEGF signaling through neuropilin 1 guides commissural axon crossing at the optic chiasm. Neuron *70*, 951-965.

Ervasti, J.M., Ohlendieck, K., Kahl, S.D., Gaver, M.G., and Campbell, K.P. (1990). Deficiency of a glycoprotein component of the dystrophin complex in dystrophic muscle. Nature *345*, 315-319.

Famiglietti, E.V., Jr., and Kolb, H. (1976). Structural basis for ON-and OFF-center responses in retinal ganglion cells. Science *194*, 193-195.

Feldheim, D.A., Kim, Y.I., Bergemann, A.D., Frisen, J., Barbacid, M., and Flanagan, J.G. (2000). Genetic analysis of ephrin-A2 and ephrin-A5 shows their requirement in multiple aspects of retinocollicular mapping. Neuron *25*, 563-574.

Feldheim, D.A., Vanderhaeghen, P., Hansen, M.J., Frisén, J., Lu, Q., Barbacid, M., and Flanagan, J.G. (1998). Topographic Guidance Labels in a Sensory Projection to the Forebrain. Neuron *21*, 1303-1313.

Feng, L., Hatten, M.E., and Heintz, N. (1994). Brain lipid-binding protein (BLBP): a novel signaling system in the developing mammalian CNS. Neuron *12*, 895-908.

Ferletta, M., Kikkawa, Y., Yu, H., Talts, J.F., Durbeej, M., Sonnenberg, A., Timpl, R., Campbell, K.P., Ekblom, P., and Genersch, E. (2003). Opposing roles of integrin alpha6Abeta1 and dystroglycan in laminin-mediated extracellular signal-regulated kinase activation. Mol Biol Cell *14*, 2088-2103.

Field, G.D., and Chichilnisky, E.J. (2007). Information processing in the primate retina: circuitry and coding. Annu Rev Neurosci *30*, 1-30.

Ford, K.J., Felix, A.L., and Feller, M.B. (2012). Cellular mechanisms underlying spatiotemporal features of cholinergic retinal waves. J Neurosci *32*, 850-863.

Freedman, M.S., Lucas, R.J., Soni, B., von Schantz, M., Munoz, M., David-Gray, Z., and Foster, R. (1999). Regulation of mammalian circadian behavior by non-rod, non-cone, ocular photoreceptors. Science *284*, 502-504.

Frisen, J., Yates, P.A., McLaughlin, T., Friedman, G.C., O'Leary, D.D., and Barbacid, M. (1998). Ephrin-A5 (AL-1/RAGS) is essential for proper retinal axon guidance and topographic mapping in the mammalian visual system. Neuron *20*, 235-243.

Früh, S., Romanos, J., Panzanelli, P., Bürgisser, D., Tyagarajan, S.K., Campbell, K.P., Santello, M., and Fritschy, J.-M. (2016). Neuronal Dystroglycan Is Necessary for Formation and Maintenance of Functional CCK-Positive

Basket Cell Terminals on Pyramidal Cells. The Journal of Neuroscience *36*, 10296-10313.

Fruh, S., Romanos, J., Panzanelli, P., Burgisser, D., Tyagarajan, S.K., Campbell, K.P., Santello, M., and Fritschy, J.M. (2016). Neuronal Dystroglycan Is Necessary for Formation and Maintenance of Functional CCK-Positive Basket Cell Terminals on Pyramidal Cells. The Journal of neuroscience : the official journal of the Society for Neuroscience *36*, 10296-10313.

Fruttiger, M. (2007). Development of the retinal vasculature. Angiogenesis *10*, 77-88.

Fuerst, P.G., Bruce, F., Tian, M., Wei, W., Elstrott, J., Feller, M.B., Erskine, L., Singer, J.H., and Burgess, R.W. (2009). DSCAM and DSCAML1 function in self-avoidance in multiple cell types in the developing mouse retina. Neuron *64*, 484-497.

Fuerst, P.G., Koizumi, A., Masland, R.H., and Burgess, R.W. (2008). Neurite arborization and mosaic spacing in the mouse retina require DSCAM. Nature *451*, 470-474.

Fuhrmann, S. (2008). Wnt signaling in eye organogenesis. Organogenesis *4*, 60-67.

Fuhrmann, S. (2010). Eye morphogenesis and patterning of the optic vesicle. Curr Top Dev Biol *93*, 61-84.

Furman, M., and Crair, M.C. (2012). Synapse maturation is enhanced in the binocular region of the retinocollicular map prior to eye opening. J Neurophysiol *107*, 3200-3216.

Furukawa, T., Morrow, E.M., and Cepko, C.L. (1997). Crx, a novel otx-like homeobox gene, shows photoreceptor-specific expression and regulates photoreceptor differentiation. Cell *91*, 531-541.

Furuta, Y., Lagutin, O., Hogan, B.L., and Oliver, G.C. (2000). Retina- and ventral forebrain-specific Cre recombinase activity in transgenic mice. Genesis *26*, 130-132.

Galli-Resta, L., Novelli, E., and Viegi, A. (2002). Dynamic microtubule-dependent interactions position homotypic neurones in regular monolayered arrays during retinal development. Development *129*, 3803-3814.

Galli-Resta, L., Resta, G., Tan, S.S., and Reese, B.E. (1997). Mosaics of islet-1-expressing amacrine cells assembled by short-range cellular interactions. J Neurosci *17*, 7831-7838.

Gan, L., Wang, S.W., Huang, Z., and Klein, W.H. (1999). POU domain factor Brn-3b is essential for retinal ganglion cell differentiation and survival but not for initial cell fate specification. Developmental biology *210*, 469-480.

Gan, L., Xiang, M., Zhou, L., Wagner, D.S., Klein, W.H., and Nathans, J. (1996). POU domain factor Brn-3b is required for the development of a large set of retinal ganglion cells. Proc Natl Acad Sci U S A *93*, 3920-3925.

Ghosh, K.K., Bujan, S., Haverkamp, S., Feigenspan, A., and Wassle, H. (2004). Types of bipolar cells in the mouse retina. J Comp Neurol *469*, 70-82.

Gleeson, J.G., Allen, K.M., Fox, J.W., Lamperti, E.D., Berkovic, S., Scheffer, I., Cooper, E.C., Dobyns, W.B., Minnerath, S.R., Ross, M.E*., et al.* (1998). Doublecortin, a brain-specific gene mutated in human X-linked

lissencephaly and double cortex syndrome, encodes a putative signaling protein. Cell *92*, 63-72.

Gnanaguru, G., Bachay, G., Biswas, S., Pinzon-Duarte, G., Hunter, D.D., and Brunken, W.J. (2013). Laminins containing the beta2 and gamma3 chains regulate astrocyte migration and angiogenesis in the retina. Development *140*, 2050-2060.

Godement, P., Salaun, J., and Imbert, M. (1984). Prenatal and postnatal development of retinogeniculate and retinocollicular projections in the mouse. J Comp Neurol *230*, 552-575.

Godement, P., Wang, L.C., and Mason, C.A. (1994). Retinal axon divergence in the optic chiasm: dynamics of growth cone behavior at the midline. The Journal of neuroscience : the official journal of the Society for Neuroscience *14*, 7024-7039.

Godfrey, C., Foley, a.R., Clement, E., and Muntoni, F. (2011). Dystroglycanopathies: coming into focus. Current opinion in genetics & development *21*, 278-285.

Gollisch, T., and Meister, M. (2010). Eye smarter than scientists believed: neural computations in circuits of the retina. Neuron *65*, 150-164.

Guillery, R.W., Mason, C.A., and Taylor, J.S. (1995). Developmental determinants at the mammalian optic chiasm. J Neurosci *15*, 4727-4737.

Halfter, W., Dong, S., Schurer, B., Ring, C., Cole, G.J., and Eller, A. (2005a). Embryonic synthesis of the inner limiting membrane and vitreous body. Invest Ophthalmol Vis Sci *46*, 2202-2209.

Halfter, W., Reckhaus, W., and Kroger, S. (1987). Nondirected axonal growth on basal lamina from avian embryonic neural retina. J Neurosci *7*, 3712-3722.

Halfter, W., Willem, M., and Mayer, U. (2005b). Basement membrane-dependent survival of retinal ganglion cells. Invest Ophthalmol Vis Sci *46*, 1000-1009.

Hara, Y., Balci-Hayta, B., Yoshida-Moriguchi, T., Kanagawa, M., Beltran-Valero de Bernabe, D., Gundesli, H., Willer, T., Satz, J.S., Crawford, R.W., Burden, S.J.*, et al.* (2011). A dystroglycan mutation associated with limb-girdle muscular dystrophy. N Engl J Med *364*, 939-946.

Harris, W.A. (1997). Cellular diversification in the vertebrate retina. Curr Opin Genet Dev *7*, 651-658.

Hatakeyama, J., Tomita, K., Inoue, T., and Kageyama, R. (2001). Roles of homeobox and bHLH genes in specification of a retinal cell type. Development *128*, 1313-1322.

Hatten, M.E. (1999). Central nervous system neuronal migration. Annu Rev Neurosci *22*, 511-539.

Hayashi, S., Lewis, P., Pevny, L., and McMahon, A.P. (2002). Efficient gene modulation in mouse epiblast using a Sox2Cre transgenic mouse strain. Mechanisms of development *119 Suppl 1*, S97-s101.

Henry, M.D., and Campbell, K.P. (1998). A role for dystroglycan in basement membrane assembly. Cell *95*, 859-870.

Henry, M.D., and Campbell, K.P. (1999). Dystroglycan inside and out. Curr Opin Cell Biol *11*, 602-607.

Herrera, E., Brown, L., Aruga, J., Rachel, R.A., Dolen, G., Mikoshiba, K., Brown, S., and Mason, C.A. (2003). Zic2 patterns binocular vision by specifying the uncrossed retinal projection. Cell *114*, 545-557.

Hindges, R., McLaughlin, T., Genoud, N., Henkemeyer, M., and O'Leary, D. (2002). EphB forward signaling controls directional branch extension and arborization required for dorsal-ventral retinotopic mapping. Neuron *35*, 475-487.

Hojo, M., Ohtsuka, T., Hashimoto, N., Gradwohl, G., Guillemot, F., and Kageyama, R. (2000). Glial cell fate specification modulated by the bHLH gene Hes5 in mouse retina. Development *127*, 2515-2522.

Hu, H., Candiello, J., Zhang, P., Ball, S.L., Cameron, D.A., and Halfter, W. (2010). Retinal ectopias and mechanically weakened basement membrane in a mouse model of muscle-eye-brain (MEB) disease congenital muscular dystrophy. Mol Vis *16*, 1415-1428.

Hubel, D.H., and Wiesel, T.N. (1959). Receptive fields of single neurones in the cat's striate cortex. The Journal of physiology *148*, 574-591.

Hubel, D.H., and Wiesel, T.N. (1961). Integrative action in the cat's lateral geniculate body. The Journal of physiology *155*, 385-398.381.

Huberman, A.D., Feller, M.B., and Chapman, B. (2008a). Mechanisms Underlying Development of Visual Maps and Receptive Fields. Annual review of neuroscience *31*, 479-509.

Huberman, A.D., Manu, M., Koch, S.M., Susman, M.W., Lutz, A.B., Ullian, E.M., Baccus, S.a., and Barres, B.a. (2008b). Architecture and activity-mediated refinement of axonal projections from a mosaic of genetically identified retinal ganglion cells. Neuron *59*, 425-438.

Huberman, A.D., Speer, C.M., and Chapman, B. (2006). Spontaneous Retinal Activity Mediates Development of Ocular Dominance Columns and Binocular Receptive Fields in V1. Neuron *52*, 247-254.

Huckfeldt, R.M., Schubert, T., Morgan, J.L., Godinho, L., Di Cristo, G., Huang, Z.J., and Wong, R.O.L. (2009). Transient neurites of retinal horizontal cells exhibit columnar tiling via homotypic interactions. Nature neuroscience *12*, 35-43.

Ibraghimov-Beskrovnaya, O., Ervasti, J.M., Leveille, C.J., Slaughter, C.A., Sernett, S.W., and Campbell, K.P. (1992). Primary structure of dystrophin-associated glycoproteins linking dystrophin to the extracellular matrix. Nature *355*, 696-702.

Icha, J., Kunath, C., Rocha-Martins, M., and Norden, C. (2016). Independent modes of ganglion cell translocation ensure correct lamination of the zebrafish retina. J Cell Biol *215*, 259-275.

Ilsley, J.L., Sudol, M., and Winder, S.J. (2001). The interaction of dystrophin with beta-dystroglycan is regulated by tyrosine phosphorylation. Cell Signal *13*, 625-632.

Inoue, T., Hojo, M., Bessho, Y., Tano, Y., Lee, J.E., and Kageyama, R. (2002). Math3 and NeuroD regulate amacrine cell fate specification in the retina. Development *129*, 831-842.

Jacobs, E.C., Campagnoni, C., Kampf, K., Reyes, S.D., Kalra, V., Handley, V., Xie, Y.-Y., Hong-Hu, Y., Spreur, V., Fisher, R.S.*, et al.* (2007). Visualization of corticofugal projections during early cortical development in a τ-GFP-transgenic mouse. European Journal of Neuroscience *25*, 17-30.

James, M., Nuttall, A., Ilsley, J.L., Ottersbach, K., Tinsley, J.M., Sudol, M., and Winder, S.J. (2000). Adhesion-dependent tyrosine phosphorylation of (beta)-dystroglycan regulates its interaction with utrophin. J Cell Sci *113 (Pt 10)*, 1717-1726.

Jaubert-Miazza, L., Green, E., Lo, F.S., Bui, K., Mills, J., and Guido, W. (2005). Structural and functional composition of the developing retinogeniculate pathway in the mouse. Vis Neurosci *22*, 661-676.

Jessell, T.M., and Sanes, J.R. (2000). Development. The decade of the developing brain. Curr Opin Neurobiol *10*, 599-611.

Kanagawa, M., and Toda, T. (2017). Muscular Dystrophy with Ribitol-Phosphate Deficiency: A Novel Post-Translational Mechanism in Dystroglycanopathy. Journal of neuromuscular diseases *4*, 259-267.

Kandel, E.R. (2013). Principles of neural science, 5th edn (New York: McGraw-Hill).

Kay, J.N., Chu, M.W., and Sanes, J.R. (2012). MEGF10 and MEGF11 mediate homotypic interactions required for mosaic spacing of retinal neurons. Nature *483*, 465-469.

Kay, J.N., Roeser, T., Mumm, J.S., Godinho, L., Mrejeru, A., Wong, R.O.L., and Baier, H. (2004). Transient requirement for ganglion cells during assembly of retinal synaptic layers. Development (Cambridge, England) *131*, 1331-1342.

Kay, J.N., Voinescu, P.E., Chu, M.W., and Sanes, J.R. (2011). Neurod6 expression defines new retinal amacrine cell subtypes and regulates their fate. Nat Neurosci *14*, 965-972.

Keleman, K., Ribeiro, C., and Dickson, B.J. (2005). Comm function in commissural axon guidance: cell-autonomous sorting of Robo in vivo. Nat Neurosci *8*, 156-163.

Kidd, T., Bland, K.S., and Goodman, C.S. (1999). Slit is the midline repellent for the robo receptor in Drosophila. Cell *96*, 785-794.

Kim, I.-J., Zhang, Y., Meister, M., and Sanes, J.R. (2010a). Laminar Restriction of Retinal Ganglion Cell Dendrites and Axons: Subtype-Specific Developmental Patterns Revealed With Transgenic Markers. The Journal of neuroscience : the official journal of the Society for Neuroscience *30*, 1452.

Kim, I.-J., Zhang, Y., Meister, M., and Sanes, J.R. (2010b). Laminar restriction of retinal ganglion cell dendrites and axons: subtype-specific developmental patterns revealed with transgenic markers. The Journal of neuroscience : the official journal of the Society for Neuroscience *30*, 1452-1462.

Kim, I.J., Zhang, Y., Meister, M., and Sanes, J.R. (2010c). Laminar restriction of retinal ganglion cell dendrites and axons: subtype-specific developmental patterns revealed with transgenic markers. J Neurosci *30*, 1452-1462.

Kim, S., and Wadsworth, W.G. (2000). Positioning of longitudinal nerves in C. elegans by nidogen. Science *288*, 150-154.

Kobayashi, K., Nakahori, Y., Miyake, M., Matsumura, K., Kondo-Iida, E., Nomura, Y., Segawa, M., Yoshioka, M., Saito, K., Osawa, M*., et al.* (1998). An ancient retrotransposal insertion causes Fukuyama-type congenital muscular dystrophy. Nature *394*, 388-392.

Kornack, D.R., and Rakic, P. (1995). Radial and horizontal deployment of clonally related cells in the primate neocortex: relationship to distinct mitotic lineages. Neuron *15*, 311-321.

Kriegstein, A.R., and Noctor, S.C. (2004). Patterns of neuronal migration in the embryonic cortex. Trends Neurosci *27*, 392-399.

Langenbach, K.J., and Rando, T.A. (2002). Inhibition of dystroglycan binding to laminin disrupts the PI3K/AKT pathway and survival signaling in muscle cells. Muscle Nerve *26*, 644-653.

Lee, Y., Kameya, S., Cox, G.A., Hsu, J., Hicks, W., Maddatu, T.P., Smith, R.S., Naggert, J.K., Peachey, N.S., and Nishina, P.M. (2005). Ocular abnormalities in Large(myd) and Large(vls) mice, spontaneous models for muscle, eye, and brain diseases. Mol Cell Neurosci *30*, 160-172.

Lefebvre, J.L., Kostadinov, D., Chen, W.V., Maniatis, T., and Sanes, J.R. (2012). Protocadherins mediate dendritic self-avoidance in the mammalian nervous system. Nature *488*, 517-521.

Lévi, S., Grady, R.M., Henry, M.D., Campbell, K.P., Sanes, J.R., and Craig, A.M. (2002). Dystroglycan Is Selectively Associated with Inhibitory GABAergic

Synapses But Is Dispensable for Their Differentiation. The Journal of Neuroscience *22*, 4274-4285.

Li, S., Sukeena, J.M., Simmons, A.B., Hansen, E.J., Nuhn, R.E., Samuels, I.S., and Fuerst, P.G. (2015). DSCAM Promotes Refinement in the Mouse Retina through Cell Death and Restriction of Exploring Dendrites. Journal of Neuroscience *35*, 5640-5654.

Libby, R.T., Lavallee, C.R., Balkema, G.W., Brunken, W.J., and Hunter, D.D. (1999). Disruption of laminin beta2 chain production causes alterations in morphology and function in the CNS. J Neurosci *19*, 9399-9411.

Lim, L.E., and Campbell, K.P. (1998). The sarcoglycan complex in limb-girdle muscular dystrophy. Curr Opin Neurol *11*, 443-452.

Liu, J., Ball, S.L., Yang, Y., Mei, P., Zhang, L., Shi, H., Kaminski, H.J., Lemmon, V.P., and Hu, H. (2006). A genetic model for muscle-eye-brain disease in mice lacking protein O-mannose 1,2-N-acetylglucosaminyltransferase (POMGnT1). Mech Dev *123*, 228-240.

Liu, J., Wilson, S., and Reh, T. (2003). BMP receptor 1b is required for axon guidance and cell survival in the developing retina. Developmental Biology *256*, 34-48.

Liu, Y., Berndt, J., Su, F., Tawarayama, H., Shoji, W., Kuwada, J.Y., and Halloran, M.C. (2004). Semaphorin3D guides retinal axons along the dorsoventral axis of the tectum. J Neurosci *24*, 310-318.

Livesey, F.J., and Cepko, C.L. (2001). Vertebrate neural cell-fate determination: lessons from the retina. Nature reviews Neuroscience *2*, 109-118.

Lunardi, A., Cremisi, F., and Dente, L. (2006). Dystroglycan is required for proper retinal layering. Developmental biology *290*, 411-420.

MacNeil, M.A., Heussy, J.K., Dacheux, R.F., Raviola, E., and Masland, R.H. (1999). The shapes and numbers of amacrine cells: matching of photofilled with Golgi-stained cells in the rabbit retina and comparison with other mammalian species. J Comp Neurol *413*, 305-326.

MacNeil, M.A., and Masland, R.H. (1998). Extreme diversity among amacrine cells: implications for function. Neuron *20*, 971-982.

Mann, F., Ray, S., Harris, W., and Holt, C. (2002). Topographic mapping in dorsoventral axis of the Xenopus retinotectal system depends on signaling through ephrin-B ligands. Neuron *35*, 461-473.

Manzini, M.C., Gleason, D., Chang, B.S., Hill, R.S., Barry, B.J., Partlow, J.N., Poduri, A., Currier, S., Galvin-Parton, P., Shapiro, L.R*., et al.* (2008). Ethnically diverse causes of Walker-Warburg syndrome (WWS): FCMD mutations are a more common cause of WWS outside of the Middle East. Human mutation *29*, E231-241.

Marcos, S., Nieto-Lopez, F., Sandonis, A., Cardozo, M.J., Di Marco, F., Esteve, P., and Bovolenta, P. (2015). Secreted frizzled related proteins modulate pathfinding and fasciculation of mouse retina ganglion cell axons by direct and indirect mechanisms. J Neurosci *35*, 4729-4740.

Marcus, R., and Mason, C. (1995). The first retinal axon growth in the mouse optic chiasm: axon patterning and the cellular environment. The Journal of Neuroscience *15*, 6389-6402.

Marcus, R.C., Blazeski, R., Godement, P., and Mason, C.A. (1995). Retinal axon divergence in the optic chiasm: uncrossed axons diverge from crossed axons within a midline glial specialization. The Journal of neuroscience : the official journal of the Society for Neuroscience *15*, 3716-3729.

Martersteck, E., Hirokawa, K.E., Evarts, M., Bernard, A., Duan, X., Li, Y., Ng, L., Oh, S.W., Ouellette, B., Royall, J.J.*, et al.* (2017). Diverse Central Projection Patterns of Retinal Ganglion Cells. Cell reports *18*, 2058-2072.

Masland, R.H. (2012). The neuronal organization of the retina. Neuron *76*, 266-280.

Matsumura, K., Chiba, A., Yamada, H., Fukuta-Ohi, H., Fujita, S., Endo, T., Kobata, A., Anderson, L.V., Kanazawa, I., Campbell, K.P.*, et al.* (1997). A role of dystroglycan in schwannoma cell adhesion to laminin. J Biol Chem *272*, 13904-13910.

Matsuoka, R.L., Chivatakarn, O., Badea, T.C., Samuels, I.S., Cahill, H., Katayama, K., Kumar, S.R., Suto, F., Chedotal, A., Peachey, N.S.*, et al.* (2011). Class 5 transmembrane semaphorins control selective Mammalian retinal lamination and function. Neuron *71*, 460-473.

McLaughlin, T., Torborg, C.L., Feller, M.B., and O'Leary, D.D. (2003). Retinotopic map refinement requires spontaneous retinal waves during a brief critical period of development. Neuron *40*, 1147-1160.

Mears, A.J., Kondo, M., Swain, P.K., Takada, Y., Bush, R.A., Saunders, T.L., Sieving, P.A., and Swaroop, A. (2001). Nrl is required for rod photoreceptor development. Nat Genet *29*, 447-452.

Michele, D.E., Barresi, R., Kanagawa, M., Saito, F., Cohn, R.D., Satz, J.S., Dollar, J., Nishino, I., Kelley, R.I., Somer, H*., et al.* (2002). Post-translational disruption of dystroglycan-ligand interactions in congenital muscular dystrophies. Nature *418*, 417-422.

Montanaro, F., Carbonetto, S., Campbell, K.P., and Lindenbaum, M. (1995). Dystroglycan expression in the wild type and mdx mouse neural retina: synaptic colocalization with dystrophin, dystrophin-related protein but not laminin. Journal of neuroscience research *42*, 528-538.

Montanaro, F., Gee, S.H., Jacobson, C., Lindenbaum, M.H., Froehner, S.C., and Carbonetto, S. (1998). Laminin and alpha-dystroglycan mediate acetylcholine receptor aggregation via a MuSK-independent pathway. J Neurosci *18*, 1250-1260.

Moore, C.J., and Winder, S.J. (2010). Dystroglycan versatility in cell adhesion: a tale of multiple motifs. Cell communication and signaling : CCS *8*, 3.

Moore, S.A., Saito, F., Chen, J., Michele, D.E., Henry, M.D., Messing, A., Cohn, R.D., Ross-Barta, S.E., Westra, S., Williamson, R.A*., et al.* (2002). Deletion of brain dystroglycan recapitulates aspects of congenital muscular dystrophy. Nature *418*, 422-425.

Morgan, J., and Wong, R. (1995). Development of Cell Types and Synaptic Connections in the Retina. In Webvision: The Organization of the Retina and Visual System, H. Kolb, E. Fernandez, and R. Nelson, eds. (Salt Lake City (UT)).

Myshrall, T.D., Moore, S.A., Ostendorf, A.P., Satz, J.S., Kowalczyk, T., Nguyen, H., Daza, R.A., Lau, C., Campbell, K.P., and Hevner, R.F. (2012).

Dystroglycan on radial glia end feet is required for pial basement membrane integrity and columnar organization of the developing cerebral cortex. J Neuropathol Exp Neurol *71*, 1047-1063.

Nadarajah, B., Brunstrom, J.E., Grutzendler, J., Wong, R.O., and Pearlman, A.L. (2001). Two modes of radial migration in early development of the cerebral cortex. Nat Neurosci *4*, 143-150.

Nakagawa, N., Yagi, H., Kato, K., Takematsu, H., and Oka, S. (2015). Ectopic clustering of Cajal-Retzius and subplate cells is an initial pathological feature in Pomgnt2-knockout mice, a model of dystroglycanopathy. Scientific reports *5*, 11163.

Nguyen-Ba-Charvet, K.T., and Chedotal, A. (2014). Development of retinal layers. C R Biol *337*, 153-159.

Nishida, A., Furukawa, A., Koike, C., Tano, Y., Aizawa, S., Matsuo, I., and Furukawa, T. (2003). Otx2 homeobox gene controls retinal photoreceptor cell fate and pineal gland development. Nat Neurosci *6*, 1255-1263.

Ohsawa, R., and Kageyama, R. (2008). Regulation of retinal cell fate specification by multiple transcription factors. Brain Res *1192*, 90-98.

Olson, E.C., and Walsh, C.A. (2002). Smooth, rough and upside-down neocortical development. Curr Opin Genet Dev *12*, 320-327.

Omori, Y., Araki, F., Chaya, T., Kajimura, N., Irie, S., Terada, K., Muranishi, Y., Tsujii, T., Ueno, S., Koyasu, T.*, et al.* (2012). Presynaptic dystroglycan-pikachurin complex regulates the proper synaptic connection between

retinal photoreceptor and bipolar cells. The Journal of neuroscience : the official journal of the Society for Neuroscience *32*, 6126-6137.

Osterhout, J.a., El-Danaf, R.N., Nguyen, P.L., and Huberman, A.D. (2014). Birthdate and outgrowth timing predict cellular mechanisms of axon target matching in the developing visual pathway. Cell reports *8*, 1006-1017.

Osterhout, J.A., Josten, N., Yamada, J., Pan, F., Wu, S.W., Nguyen, P.L., Panagiotakos, G., Inoue, Y.U., Egusa, S.F., Volgyi, B.*, et al.* (2011). Cadherin-6 mediates axon-target matching in a non-image-forming visual circuit. Neuron *71*, 632-639.

Osterhout, Jessica A., Stafford, Benjamin K., Nguyen, Phong L., Yoshihara, Y., and Huberman, Andrew D. (2015). Contactin-4 Mediates Axon-Target Specificity and Functional Development of the Accessory Optic System. Neuron *86*, 985-999.

Ott, H., Bastmeyer, M., and Stuermer, C.A. (1998). Neurolin, the goldfish homolog of DM-GRASP, is involved in retinal axon pathfinding to the optic disk. J Neurosci *18*, 3363-3372.

Pan, L., Deng, M., Xie, X., and Gan, L. (2008a). ISL1 and BRN3B co-regulate the differentiation of murine retinal ganglion cells. Development (Cambridge, England) *135*, 1981-1990.

Pan, L., Deng, M., Xie, X., and Gan, L. (2008b). ISL1 and BRN3B co-regulate the differentiation of murine retinal ganglion cells. Development (Cambridge, England) *135*, 1981-1990.

Peng, J., Fabre, P.J., Dolique, T., Swikert, S.M., Kermasson, L., Shimogori, T., and Charron, F. (2018). Sonic Hedgehog Is a Remotely Produced Cue that Controls Axon Guidance Trans-axonally at a Midline Choice Point. Neuron *97*, 326-340.e324.

Peng, Y.R., Tran, N.M., Krishnaswamy, A., Kostadinov, D., Martersteck, E.M., and Sanes, J.R. (2017). Satb1 Regulates Contactin 5 to Pattern Dendrites of a Mammalian Retinal Ganglion Cell. Neuron *95*, 869-883 e866.

Petros, T.J., Rebsam, A., and Mason, C.A. (2008). Retinal axon growth at the optic chiasm: to cross or not to cross. Annual review of neuroscience *31*, 295-315.

Pinzon-Duarte, G., Daly, G., Li, Y.N., Koch, M., and Brunken, W.J. (2010). Defective formation of the inner limiting membrane in laminin beta2- and gamma3-null mice produces retinal dysplasia. Investigative ophthalmology & visual science *51*, 1773-1782.

Plachez, C., Andrews, W., Liapi, A., Knoell, B., Drescher, U., Mankoo, B., Zhe, L., Mambetisaeva, E., Annan, A., Bannister, L.*, et al.* (2008). Robos are required for the correct targeting of retinal ganglion cell axons in the visual pathway of the brain. Mol Cell Neurosci *37*, 719-730.

Plump, A.S., Erskine, L., Sabatier, C., Brose, K., Epstein, C.J., Goodman, C.S., Mason, C.A., and Tessier-Lavigne, M. (2002). Slit1 and Slit2 cooperate to prevent premature midline crossing of retinal axons in the mouse visual system. Neuron *33*, 219-232.

Poche, R.A., and Reese, B.E. (2009). Retinal horizontal cells: challenging paradigms of neural development and cancer biology. Development *136*, 2141-2151.

Pribiag, H., Peng, H., Shah, W.A., Stellwagen, D., and Carbonetto, S. (2014). Dystroglycan mediates homeostatic synaptic plasticity at GABAergic synapses. Proc Natl Acad Sci U S A *111*, 6810-6815.

Qu, Q., and Smith, F.I. (2005). Neuronal migration defects in cerebellum of theLarge myd mouse are associated with disruptions in Bergmann glia organization and delayed migration of granule neurons. The Cerebellum *4*, 261-270.

Rachel, R.A., Murdoch, J.N., Beermann, F., Copp, A.J., and Mason, C.A. (2000). Retinal axon misrouting at the optic chiasm in mice with neural tube closure defects. Genesis *27*, 32-47.

Rakic, P. (1972). Mode of cell migration to the superficial layers of fetal monkey neocortex. J Comp Neurol *145*, 61-83.

Randlett, O., Poggi, L., Zolessi, F.R., and Harris, W.a. (2011). The oriented emergence of axons from retinal ganglion cells is directed by laminin contact in vivo. Neuron *70*, 266-280.

Reese, B.E. (2011). Development of the retina and optic pathway. Vision research *51*, 613-632.

Reese, B.E., Necessary, B.D., Tam, P.P., Faulkner-Jones, B., and Tan, S.S. (1999). Clonal expansion and cell dispersion in the developing mouse retina. Eur J Neurosci *11*, 2965-2978.

Riccomagno, M.M., Sun, L.O., Brady, C.M., Alexandropoulos, K., Seo, S., Kurokawa, M., and Kolodkin, A.L. (2014). Cas adaptor proteins organize the retinal ganglion cell layer downstream of integrin signaling. Neuron *81*, 779-786.

Rompani, S.B., Mullner, F.E., Wanner, A., Zhang, C., Roth, C.N., Yonehara, K., and Roska, B. (2017). Different Modes of Visual Integration in the Lateral Geniculate Nucleus Revealed by Single-Cell-Initiated Transsynaptic Tracing. Neuron *93*, 767-776 e766.

Roscioli, T., Kamsteeg, E.J., Buysse, K., Maystadt, I., van Reeuwijk, J., van den Elzen, C., van Beusekom, E., Riemersma, M., Pfundt, R., Vissers, L.E.*, et al.* (2012). Mutations in ISPD cause Walker-Warburg syndrome and defective glycosylation of alpha-dystroglycan. Nat Genet *44*, 581-585.

Ross, M.E., Allen, K.M., Srivastava, A.K., Featherstone, T., Gleeson, J.G., Hirsch, B., Harding, B.N., Andermann, E., Abdullah, R., Berg, M.*, et al.* (1997). Linkage and physical mapping of X-linked lissencephaly/SBH (XLIS): a gene causing neuronal migration defects in human brain. Hum Mol Genet *6*, 555-562.

Rossi, F.M., Pizzorusso, T., Porciatti, V., Marubio, L.M., Maffei, L., and Changeux, J.-P. (2001). Requirement of the nicotinic acetylcholine receptor β2 subunit for the anatomical and functional development of the visual system. Proceedings of the National Academy of Sciences *98*, 6453-6458.

Russo, K., Di Stasio, E., Macchia, G., Rosa, G., Brancaccio, A., and Petrucci, T.C. (2000). Characterization of the beta-dystroglycan-growth factor receptor 2 (Grb2) interaction. Biochem Biophys Res Commun *274*, 93-98.

Sakagami, K., Chen, B., Nusinowitz, S., Wu, H., and Yang, X.J. (2012). PTEN regulates retinal interneuron morphogenesis and synaptic layer formation. Mol Cell Neurosci *49*, 171-183.

Sakai, J.A., and Halloran, M.C. (2006). Semaphorin 3d guides laterality of retinal ganglion cell projections in zebrafish. Development *133*, 1035-1044.

Sanes, J.R., and Masland, R.H. (2015). The types of retinal ganglion cells: current status and implications for neuronal classification. Annu Rev Neurosci *38*, 221-246.

Sato, S., Omori, Y., Katoh, K., Kondo, M., Kanagawa, M., Miyata, K., Funabiki, K., Koyasu, T., Kajimura, N., Miyoshi, T.*, et al.* (2008). Pikachurin, a dystroglycan ligand, is essential for photoreceptor ribbon synapse formation. Nature neuroscience *11*, 923-931.

Satz, J.S., Barresi, R., Durbeej, M., Willer, T., Turner, A., Moore, S.a., and Campbell, K.P. (2008). Brain and eye malformations resembling Walker-Warburg syndrome are recapitulated in mice by dystroglycan deletion in the epiblast. The Journal of neuroscience : the official journal of the Society for Neuroscience *28*, 10567-10575.

Satz, J.S., Ostendorf, A.P., Hou, S., Turner, A., Kusano, H., Lee, J.C., Turk, R., Nguyen, H., Ross-Barta, S.E., Westra, S.*, et al.* (2010a). Distinct Functions of Glial and Neuronal Dystroglycan in the Developing and Adult Mouse Brain. The Journal of neuroscience : the official journal of the Society for Neuroscience *30*, 14560-14572.

Satz, J.S., Ostendorf, A.P., Hou, S., Turner, A., Kusano, H., Lee, J.C., Turk, R., Nguyen, H., Ross-Barta, S.E., Westra, S.*, et al.* (2010b). Distinct functions

of glial and neuronal dystroglycan in the developing and adult mouse brain. The Journal of neuroscience : the official journal of the Society for Neuroscience *30*, 14560-14572.

Satz, J.S., Philp, A.R., Nguyen, H., Kusano, H., Lee, J., Turk, R., Riker, M.J., Hernández, J., Weiss, R.M., Anderson, M.G.*, et al.* (2009). Visual impairment in the absence of dystroglycan. The Journal of neuroscience : the official journal of the Society for Neuroscience *29*, 13136-13146.

Schmitt, A.M., Shi, J., Wolf, A.M., Lu, C.C., King, L.A., and Zou, Y. (2006). Wnt-Ryk signalling mediates medial-lateral retinotectal topographic mapping. Nature *439*, 31-37.

Schwarzbauer, J. (1999). Basement membranes: Putting up the barriers. Curr Biol *9*, R242-244.

Seabrook, T.A., El-Danaf, R.N., Krahe, T.E., Fox, M.A., and Guido, W. (2013). Retinal Input Regulates the Timing of Corticogeniculate Innervation. The Journal of Neuroscience *33*, 10085-10097.

Seeger, M., Tear, G., Ferres-Marco, D., and Goodman, C.S. (1993). Mutations affecting growth cone guidance in Drosophila: genes necessary for guidance toward or away from the midline. Neuron *10*, 409-426.

Shanks, J.A., Ito, S., Schaevitz, L., Yamada, J., Chen, B., Litke, A., and Feldheim, D.A. (2016). Corticothalamic Axons Are Essential for Retinal Ganglion Cell Axon Targeting to the Mouse Dorsal Lateral Geniculate Nucleus. The Journal of Neuroscience *36*, 5252-5263.

Sharpe, J., and Wong, R.O. (2011). Imaging in developmental biology : a laboratory manual (Cold Spring Harbor, N.Y.: Cold Spring Harbor Laboratory Press).

Sotgia, F., Lee, H., Bedford, M.T., Petrucci, T., Sudol, M., and Lisanti, M.P. (2001). Tyrosine phosphorylation of beta-dystroglycan at its WW domain binding motif, PPxY, recruits SH2 domain containing proteins. Biochemistry *40*, 14585-14592.

Spence, H.J., Chen, Y.J., Batchelor, C.L., Higginson, J.R., Suila, H., Carpen, O., and Winder, S.J. (2004a). Ezrin-dependent regulation of the actin cytoskeleton by beta-dystroglycan. Hum Mol Genet *13*, 1657-1668.

Spence, H.J., Dhillon, A.S., James, M., and Winder, S.J. (2004b). Dystroglycan, a scaffold for the ERK-MAP kinase cascade. EMBO Rep *5*, 484-489.

Sperry, R.W. (1943). Effect of 180 degree rotation of the retinal field on visuomotor coordination. Journal of Experimental Zoology *92*, 263-279.

Sretavan, D.W., and Reichardt, L.F. (1993). Time-lapse video analysis of retinal ganglion cell axon pathfinding at the mammalian optic chiasm: growth cone guidance using intrinsic chiasm cues. Neuron *10*, 761-777.

Sterling, P., and Matthews, G. (2005). Structure and function of ribbon synapses. Trends Neurosci *28*, 20-29.

Stevens, B., Allen, N.J., Vazquez, L.E., Howell, G.R., Christopherson, K.S., Nouri, N., Micheva, K.D., Mehalow, A.K., Huberman, A.D., Stafford, B.*, et al.* (2007). The Classical Complement Cascade Mediates CNS Synapse Elimination. Cell *131*, 1164-1178.

Stone, K.E., and Sakaguchi, D.S. (1996). Perturbation of the developing Xenopus retinotectal projection following injections of antibodies against beta1 integrin receptors and N-cadherin. Dev Biol *180*, 297-310.

Straub, V., and Campbell, K.P. (1997). Muscular dystrophies and the dystrophin-glycoprotein complex. Curr Opin Neurol *10*, 168-175.

Strittmatter, S.M., Fankhauser, C., Huang, P.L., Mashimo, H., and Fishman, M.C. (1995a). Neuronal pathfinding is abnormal in mice lacking the neuronal growth cone protein GAP-43. Cell *80*, 445-452.

Strittmatter, S.M., Fankhauser, C., Huang, P.L., Mashimo, H., and Fishman, M.C. (1995b). Neuronal pathfinding is abnormal in mice lacking the neuronal growth cone protein GAP-43. Cell *80*, 445-452.

Su, J., Haner, C.V., Imbery, T.E., Brooks, J.M., Morhardt, D.R., Gorse, K., Guido, W., and Fox, M.A. (2011). Reelin is required for class-specific retinogeniculate targeting. J Neurosci *31*, 575-586.

Sun, C., Speer, C.M., Wang, G.Y., Chapman, B., and Chalupa, L.M. (2008). Epibatidine application in vitro blocks retinal waves without silencing all retinal ganglion cell action potentials in developing retina of the mouse and ferret. J Neurophysiol *100*, 3253-3263.

Sun, L.O., Brady, C.M., Cahill, H., Al-Khindi, T., Sakuta, H., Dhande, O.S., Noda, M., Huberman, A.D., Nathans, J., and Kolodkin, A.L. (2015). Functional Assembly of Accessory Optic System Circuitry Critical for Compensatory Eye Movements. Neuron, 1-14.

Sun, L.O., Jiang, Z., Rivlin-Etzion, M., Hand, R., Brady, C.M., Matsuoka, R.L., Yau, K.-w., Feller, M.B., and Kolodkin, A.L. (2013). On and off retinal circuit assembly by divergent molecular mechanisms. Science (New York, NY) *342*, 1241974.

Sunada, Y., Bernier, S.M., Kozak, C.A., Yamada, Y., and Campbell, K.P. (1994). Deficiency of merosin in dystrophic dy mice and genetic linkage of laminin M chain gene to dy locus. J Biol Chem *269*, 13729-13732.

Tabata, H., and Nakajima, K. (2003). Multipolar migration: the third mode of radial neuronal migration in the developing cerebral cortex. J Neurosci *23*, 9996-10001.

Takahashi, H., Kanesaki, H., Igarashi, T., Kameya, S., Yamaki, K., Mizota, A., Kudo, A., Miyagoe-Suzuki, Y., Takeda, S., and Takahashi, H. (2011). Reactive gliosis of astrocytes and Muller glial cells in retina of POMGnT1-deficient mice. Mol Cell Neurosci *47*, 119-130.

Takeda, S., Kondo, M., Sasaki, J., Kurahashi, H., Kano, H., Arai, K., Misaki, K., Fukui, T., Kobayashi, K., Tachikawa, M.*, et al.* (2003). Fukutin is required for maintenance of muscle integrity, cortical histiogenesis and normal eye development. Hum Mol Genet *12*, 1449-1459.

Tamamaki, N., Nakamura, K., Okamoto, K., and Kaneko, T. (2001). Radial glia is a progenitor of neocortical neurons in the developing cerebral cortex. Neurosci Res *41*, 51-60.

Tanabe, K., Takahashi, Y., Sato, Y., Kawakami, K., Takeichi, M., and Nakagawa, S. (2006). Cadherin is required for dendritic morphogenesis and synaptic

terminal organization of retinal horizontal cells. Development *133*, 4085-4096.

Taniguchi-Ikeda, M., Morioka, I., Iijima, K., and Toda, T. (2016). Mechanistic aspects of the formation of alpha-dystroglycan and therapeutic research for the treatment of alpha-dystroglycanopathy: A review. Mol Aspects Med *51*, 115-124.

Tao, C., and Zhang, X. (2016). Retinal Proteoglycans Act as Cellular Receptors for Basement Membrane Assembly to Control Astrocyte Migration and Angiogenesis. Cell Rep *17*, 1832-1844.

Tau, G.Z., and Peterson, B.S. (2010). Normal development of brain circuits. Neuropsychopharmacology *35*, 147-168.

Taylor, L., Arner, K., Engelsberg, K., and Ghosh, F. (2015). Scaffolding the retina: the interstitial extracellular matrix during rat retinal development. Int J Dev Neurosci *42*, 46-58.

Thompson, H., Andrews, W., Parnavelas, J.G., and Erskine, L. (2009). Robo2 is required for Slit-mediated intraretinal axon guidance. Developmental biology *335*, 418-426.

Thompson, H., Barker, D., Camand, O., and Erskine, L. (2006a). Slits contribute to the guidance of retinal ganglion cell axons in the mammalian optic tract. Developmental biology *296*, 476-484.

Thompson, H., Camand, O., Barker, D., and Erskine, L. (2006b). Slit proteins regulate distinct aspects of retinal ganglion cell axon guidance within

dorsal and ventral retina. The Journal of neuroscience : the official journal of the Society for Neuroscience *26*, 8082-8091.

Timpl, R., and Brown, J.C. (1996). Supramolecular assembly of basement membranes. Bioessays *18*, 123-132.

Toda, T. (1999). Fukutin, a novel protein product responsible for Fukuyama-type congenital muscular dystrophy. Seikagaku *71*, 55-61.

Torborg, C.L., and Feller, M.B. (2004). Unbiased analysis of bulk axonal segregation patterns. J Neurosci Methods *135*, 17-26.

Tronche, F., Kellendonk, C., Kretz, O., Gass, P., Anlag, K., Orban, P.C., Bock, R., Klein, R., and Schutz, G. (1999). Disruption of the glucocorticoid receptor gene in the nervous system results in reduced anxiety. Nat Genet *23*, 99-103.

Usrey, W.M., Reppas, J.B., and Reid, R.C. (1999). Specificity and strength of retinogeniculate connections. J Neurophysiol *82*, 3527-3540.

van Reeuwijk, J., Grewal, P.K., Salih, M.A., Beltran-Valero de Bernabe, D., McLaughlan, J.M., Michielse, C.B., Herrmann, R., Hewitt, J.E., Steinbrecher, A., Seidahmed, M.Z.*, et al.* (2007). Intragenic deletion in the LARGE gene causes Walker-Warburg syndrome. Hum Genet *121*, 685-690.

van Reeuwijk, J., Janssen, M., van den Elzen, C., Beltran-Valero de Bernabe, D., Sabatelli, P., Merlini, L., Boon, M., Scheffer, H., Brockington, M., Muntoni, F.*, et al.* (2005). POMT2 mutations cause alpha-dystroglycan

hypoglycosylation and Walker-Warburg syndrome. J Med Genet *42*, 907-912.

Vaney, D.I., Sivyer, B., and Taylor, W.R. (2012). Direction selectivity in the retina: symmetry and asymmetry in structure and function. Nat Rev Neurosci *13*, 194-208.

Varshney, S., Hunter, D.D., and Brunken, W.J. (2015). Extracellular Matrix Components Regulate Cellular Polarity and Tissue Structure in the Developing and Mature Retina. J Ophthalmic Vis Res *10*, 329-339.

Wang, S.W., Kim, B.S., Ding, K., Wang, H., Sun, D., Johnson, R.L., Klein, W.H., and Gan, L. (2001). Requirement for math5 in the development of retinal ganglion cells. Genes Dev *15*, 24-29.

Wassle, H., and Boycott, B.B. (1991). Functional architecture of the mammalian retina. Physiol Rev *71*, 447-480.

Wassle, H., Puller, C., Muller, F., and Haverkamp, S. (2009). Cone contacts, mosaics, and territories of bipolar cells in the mouse retina. J Neurosci *29*, 106-117.

Wassle, H., and Riemann, H.J. (1978). The mosaic of nerve cells in the mammalian retina. Proc R Soc Lond B Biol Sci *200*, 441-461.

Wiesel, T.N., and Hubel, D.H. (1963). SINGLE-CELL RESPONSES IN STRIATE CORTEX OF KITTENS DEPRIVED OF VISION IN ONE EYE. J Neurophysiol *26*, 1003-1017.

Williams, S.E., Grumet, M., Colman, D.R., Henkemeyer, M., Mason, C.A., and Sakurai, T. (2006). A role for Nr-CAM in the patterning of binocular visual pathways. Neuron *50*, 535-547.

Williams, S.E., Mann, F., Erskine, L., Sakurai, T., Wei, S., Rossi, D.J., Gale, N.W., Holt, C.E., Mason, C.A., and Henkemeyer, M. (2003). Ephrin-B2 and EphB1 mediate retinal axon divergence at the optic chiasm. Neuron *39*, 919-935.

Williamson, R.A., Henry, M.D., Daniels, K.J., Hrstka, R.F., Lee, J.C., Sunada, Y., Ibraghimov-Beskrovnaya, O., and Campbell, K.P. (1997). Dystroglycan is essential for early embryonic development: disruption of Reichert's membrane in Dag1-null mice. Hum Mol Genet *6*, 831-841.

Winder, S.J. (1997). The membrane-cytoskeleton interface: the role of dystrophin and utrophin. J Muscle Res Cell Motil *18*, 617-629.

Winder, S.J. (2001). The complexities of dystroglycan. Trends Biochem Sci *26*, 118-124.

Wright, K.M., Lyon, K.A., Leung, H., Leahy, D.J., Ma, L., and Ginty, D.D. (2012). Dystroglycan organizes axon guidance cue localization and axonal pathfinding. Neuron *76*, 931-944.

Xiao, T., Staub, W., Robles, E., Gosse, N.J., Cole, G.J., and Baier, H. (2011). Assembly of lamina-specific neuronal connections by slit bound to type IV collagen. Cell *146*, 164-176.

Xu, H.P., Burbridge, T.J., Ye, M., Chen, M., Ge, X., Zhou, Z.J., and Crair, M.C. (2016). Retinal Wave Patterns Are Governed by Mutual Excitation among

Starburst Amacrine Cells and Drive the Refinement and Maintenance of Visual Circuits. J Neurosci *36*, 3871-3886.

Yamada, H., Shimizu, T., Tanaka, T., Campbell, K.P., and Matsumura, K. (1994). Dystroglycan is a binding protein of laminin and merosin in peripheral nerve. FEBS Lett *352*, 49-53.

Yang, B., Jung, D., Motto, D., Meyer, J., Koretzky, G., and Campbell, K.P. (1995). SH3 domain-mediated interaction of dystroglycan and Grb2. J Biol Chem *270*, 11711-11714.

Yang, L., Cai, C.L., Lin, L., Qyang, Y., Chung, C., Monteiro, R.M., Mummery, C.L., Fishman, G.I., Cogen, A., and Evans, S. (2006). Isl1Cre reveals a common Bmp pathway in heart and limb development. Development *133*, 1575-1585.

Yonehara, K., Farrow, K., Ghanem, A., Hillier, D., Balint, K., Teixeira, M., Juttner, J., Noda, M., Neve, R.L., Conzelmann, K.K.*, et al.* (2013). The first stage of cardinal direction selectivity is localized to the dendrites of retinal ganglion cells. Neuron *79*, 1078-1085.

Yoshida, A., Kobayashi, K., Manya, H., Taniguchi, K., Kano, H., Mizuno, M., Inazu, T., Mitsuhashi, H., Takahashi, S., Takeuchi, M.*, et al.* (2001). Muscular dystrophy and neuronal migration disorder caused by mutations in a glycosyltransferase, POMGnT1. Dev Cell *1*, 717-724.

Yoshida, T., Pan, Y., Hanada, H., Iwata, Y., and Shigekawa, M. (1998). Bidirectional signaling between sarcoglycans and the integrin adhesion system in cultured L6 myocytes. J Biol Chem *273*, 1583-1590.

Young, R.W. (1984). Cell death during differentiation of the retina in the mouse. J Comp Neurol *229*, 362-373.

Young, R.W. (1985). Cell differentiation in the retina of the mouse. Anat Rec *212*, 199-205.

Yurchenco, P.D. (2011). Basement membranes: cell scaffoldings and signaling platforms. Cold Spring Harb Perspect Biol *3*.

Zaccaria, M.L., Di Tommaso, F., Brancaccio, A., Paggi, P., and Petrucci, T.C. (2001). Dystroglycan distribution in adult mouse brain: a light and electron microscopy study. Neuroscience *104*, 311-324.

Zenker, M., Aigner, T., Wendler, O., Tralau, T., Muntefering, H., Fenski, R., Pitz, S., Schumacher, V., Royer-Pokora, B., Wuhl, E.*, et al.* (2004). Human laminin beta2 deficiency causes congenital nephrosis with mesangial sclerosis and distinct eye abnormalities. Hum Mol Genet *13*, 2625-2632.

Zhang, C., Kolodkin, A.L., Wong, R.O., and James, R.E. (2017). Establishing Wiring Specificity in Visual System Circuits: From the Retina to the Brain. Annu Rev Neurosci *40*, 395-424.

Zhang, X.M., and Yang, X.J. (2001). Regulation of retinal ganglion cell production by Sonic hedgehog. Development *128*, 943-957.